

UCSF

UC San Francisco Electronic Theses and Dissertations

Title

Regulation of Candida albicans gastrointestinal colonization

Permalink

<https://escholarship.org/uc/item/6pk00323>

Author

Witchley, Jessica

Publication Date

2018

Peer reviewed|Thesis/dissertation

Regulation of *C. albicans* gastrointestinal commensal colonization

by

Jessica N. Witchley

DISSERTATION

Submitted in partial satisfaction of the requirements for the degree of

DOCTOR OF PHILOSOPHY

in

Genetics

in the

GRADUATE DIVISION

of the

UNIVERSITY OF CALIFORNIA, SAN FRANCISCO

To my little sister, Cami, whose love and support have always been a source of inspiration

Acknowledgments

Many people had a hand in training me over the years. To all of them, I would like to express my sincere gratitude. Kalyan Pande and Changbin Chen initiated the screen project that evolved into Chapter 2 of my thesis. Pallavi Penumetcha is a dedicated member of the lab who has successfully brought *in vivo* imaging to our work and contributed substantially to Chapter 2. Nina V. Abon helped with strain construction and mouse commensal competitions. Cedric A. Brimacombe was a great friend and collaborator on the white-opaque regulator project in Chapter 3. Mark Voorhies was instrumental in development of my bioinformatics approaches in Chapters 2, 3, 4 and 5. Dr. Robi Mitra and his lab provided reagents and *in silico* tools that allowed me to develop the Calling card-seq techniques. Dr. June Round and her student, Ty Chiaro, were essential collaborators in the gnotobiotic studies included in Chapter 5. Dr. Andrew Koh and his excellent technician, Laura Coughlin, performed the qPCR for bacterial abundance included in Chapter 5.

Of course, I would also like to thank my UCSF Tetrad cohort for their support and advice over the years. The fourth floor of Parnassus Health Science East and the rest of the Microbiology and Immunology Department have also been very friendly and supportive during my time in the Noble lab. My thesis committee members, Drs. Anita Sil and Susan Lynch, have given tremendously helpful advice that has improved my projects greatly.

My thesis adviser, Dr. Suzanne Noble, has given me both the freedom as well as the structure I needed to succeed in my projects. Without her encouragement and positivity, I may have given up on several of the techniques that proved most fruitful.

I would like to acknowledge the Center for Advanced Technology and the Diabetes Center at UCSF and the QB3 Vincent J. Coates Genomics Sequencing Laboratory at UC Berkeley for the use of their equipment. Specifically, I would like to thank the directors, Drs. Eric Chow and

Shana McDevitt, of the sequencing cores for helpful advice when developing several of the novel sequencing techniques.

To my family, though you may not have understood my academic drive, you still encouraged me to pursue my passions. Through all the years, you have still supported me even when my career took me far away.

Over the last four years, the Sharp family has been a wonderful West Coast surrogate for my own East Coast family. From welcoming me into their home on holidays to inviting me on family vacations, I have always felt like part of your family and hope we have many more years together. In particular, my partner, Andrew, has been a constant source of encouragement and love who I credit for making me take the necessary breaks I needed.

Thank you all,
Jessica N. Witchley

Scientific Acknowledgments

Large parts of the Introduction (Chapter 1) were taken from the published review Noble, Gianetti, and Witchley Nature Review Microbiology 2017.

Abstract

Candida albicans is both a fungal commensal as well as an opportunistic pathogen of humans. This fungus does not have a known environmental niche and exists primarily as a commensal of the human skin, gastrointestinal tract and genitourinary tract. It has been established that the same strains that are found in commensal niches are the ones that cause diseases. This suggests a model of infection whereby the commensal strains are triggered to become pathogenic by the host environment. *C. albicans* can adopt many different cell morphologies and each is accompanied by a distinct expression profile. Through a series of genetic screens and candidate based approaches, I explore the role for regulators of fungal morphology in the commensal fitness of *C. albicans* in the gastrointestinal tract. First, I developed a method for screening large numbers of *C. albicans* mutants in a single infection that led to the role of transcription factors that are activators of the yeast-to-hyphal transition as inhibitors of commensal fitness. RNA expression profiling of a mutant of one of these hypha-activating transcription factors, Ume6, led to the establishment of a role for a secreted effector, Sap6, in modulating the commensal fitness of *C. albicans*, likely through a host-mediated response to the fungus. Next, I established a role for regulators of the white-opaque switch in commensal fitness. Interestingly, the direction of commensal regulation did not always line up with the predicted role for these transcription factors based on their role in regulation of the white-to-opaque switch. To explore how these transcription factors control the commensal program, I developed a method, Calling Card-seq, for determining *in vivo* binding events of these regulators in the mammalian GI tract. Together with mRNA-seq, this technique shows promise for defining the regulatory targets of transcription factors *in vivo* that modulate the commensal and virulent properties of this important human pathogen.

Table of Contents

Chapter 1. Introduction: <i>C. albicans</i> morphological plasticity in health and disease	1
1.1. Yeasts, hyphae, pseudohyphae and chlamyospores	2
1.1.1. Characteristics of yeasts, hyphae, pseudohyphae and chlamyospores ...	2
1.1.2. Roles of a/ α yeasts, pseudohyphae and hyphae in biofilm formation.....	4
1.1.3. Virulence of yeasts, hyphae and pseudohyphae	5
1.1.4. Commensalism of yeasts and hyphae	6
1.2. Yeast-like morphotypes: White, opaque, gray, and GUT	7
1.2.1. Characteristics of white ^a and opaque ^a cells	7
1.2.2. Comparison of white ^{a/α} and white ^a to opaque ^a cell filamentation	9
1.2.3. White-to-opaque switching, mating locus, and sexual competency.....	9
1.2.4. Characteristics of opaque ^{a/α} and gray cells.....	11
1.2.5. Virulence and commensalism of opaque ^{a/α} and gray cells	12
1.2.6. Characteristics of GUT cells	12
1.2.7. Commensalism and virulence of GUT cells	13
1.2.8. Fitness and metabolism of yeast morphotypes.....	15
1.3. Regulation of morphogenesis	15
1.3.1. Environmental cues and their signaling pathways	16
1.3.2. Transcriptional regulation of morphogenesis.....	17
1.3.2.1. Efg1.....	17
1.3.2.2. Transcriptional regulation of yeast-to-hypha transition and biofilms	18

1.3.2.3. Transcriptional regulation of white ^a - opaque ^a switch	20
1.4. Thesis outline	23
1.5. References	24
Chapter 2. Regulation of yeast-to-hypha switch is an important determinant of <i>C. albicans</i> commensal fitness	39
2.1. Introduction.....	39
2.2. Results.....	41
2.2.1. Screens for <i>C. albicans</i> commensalism factors identify activators of filamentation	41
2.2.2. Transcriptional activators of filamentation inhibit commensal fitness	45
2.2.3. <i>C. albicans</i> colonizes the GI tract as a mixed population of yeasts and filaments	47
2.2.4. NanoString profiling of <i>C. albicans</i> gene expression in the GI tract reveals a strong hypha-specific response	51
2.2.5. RNA-seq reveals that Ume6 controls a subset of hypha-specific genes during gut colonization	54
2.2.6. A pro-inflammatory factor is detrimental to <i>C. albicans</i> commensal fitness	57
2.3. Discussion.....	59
2.4. Materials and Methods	61
2.4.1. Strains.....	61
2.4.2. <i>in vivo</i> studies	62
2.4.3. Preparation of sequencing libraries from <i>in vivo</i> screen for GI commensalism factors.....	62
2.4.4. Quantification of mutant abundances in screens.....	63
2.4.5. <i>in vivo</i> imaging of <i>C. albicans</i>	64
2.4.6. NanoString transcriptional profiling.....	65

2.4.7. RNA-seq library preparation and sequencing	66
2.4.8. Transcriptome analysis	67
2.5. References	67
Chapter 3. Chapter 3. Dual role for white-opaque regulators in <i>C. albicans</i> GI commensalism	72
3.1. Introduction	72
3.2. Results.....	73
3.2.1. Regulators of sexual switching also control commensal fitness	73
3.2.2. Overexpression of transcription factors leads to commensal phenotypes in some cases	76
3.2.3. Genetic epistasis reveals rewiring between the transcriptional circuits controlling sex and commensal fitness.....	78
3.2.4. White-opaque regulators are also regulators of filamentation <i>in vitro</i>	80
3.2.5. Gene expression changes by mRNA-seq.....	84
3.2.6. Transcription factors bind upstream of filamentation regulators <i>in vivo</i>	89
3.3. Discussion.....	91
3.4. Materials and Methods.....	92
3.4.1. Strains.....	92
3.4.2. <i>in vivo</i> mouse studies.....	93
3.4.3. <i>in vivo</i> imaging of <i>Candida albicans</i>	93
3.4.4. mRNA-seq library preparation and sequencing	94
3.4.5. Calling card-seq	95
3.5. References	96

Chapter 4. A new method for studying transcription factor dynamics, Calling-card seq in	
<i>C. albicans</i>	99
4.1. Introduction	99
4.2. Results	100
4.2.1. Codon optimized PiggyBac transposase is active in <i>Candida albicans</i> ..	100
4.2.2. Iron transcription factors	101
4.2.3. White-opaque regulators	105
4.3. Discussion	108
4.4. Materials and Methods	109
4.4.1. <i>C. albicans</i> PiggyBac transposon construction.....	109
4.4.2. PiggyBac transposase fusion construct generation.....	110
4.4.3. Strain growth conditions.....	111
4.4.4. Sequencing library preparation	113
4.4.5. Data analysis	113
4.5. References	114
Chapter 5. Host mouse background as well as microbiota can influence white-to-GUT	
switch and fitness phenotype	117
5.1. Introduction	117
5.2. Results	118
5.2.1. Bacteria are not required for the white-GUT switch.....	119
5.2.2. Host background influences timing and fitness of GUT cells	120
5.2.3. The co-colonizing bacterial microbiota influences the competitive fitness of	
GUT cells.....	122

5.2.4. Increased abundance of <i>Lactobacillus</i> species is coincident with decreased GUT cell fitness	125
5.3. Discussion.....	125
5.4. Materials and Methods.....	127
5.4.1. Yeast strains	127
5.4.2. Mouse lines.....	127
5.4.3. <i>in vivo</i> competitions.....	128
5.4.1. Bacteria abundance analysis	128
5.5. References	128
Chapter 6. Hgc1	130
6.1. Introduction	130
6.2. Results.....	131
6.2.1. Loss of Hgc1 confers increased commensal fitness.....	132
6.2.2. Hgc1 mutant does not form hyphae in the mammalian GI tract.....	133
6.2.3. Hgc1 contributes to gene expression in different environments	133
6.3. Discussion.....	135
6.4. Materials and Methods.....	137
6.4.1. Yeast strains	137
6.4.2. Gastrointestinal mouse competitions	137
6.4.3. Fluorescent <i>in situ</i> hybridization (FISH).....	137
6.4.4. Gene expression analysis.....	138
6.5. References	138
Appendix.....	139

A.1. File locations 139

List of tables

Table 3.1. Efg1-PBase only Calling Card-seq binding events compared to previous ChIP and mRNA-seq data sets	90
Table A.1. Screen details.....	139

List of Figures

Figure 1.1. Simplified regulation of yeast-to-hypha transition	3
Figure 1.2. Simplified regulation of white ^a -to-opaque ^a switch	8
Figure 1.3. GUT, opaque ^{a/α} and grey ^{a/α} regulation	14
Figure 2.1. Filamentation defective mutants confer fitness advantage in GI commensal model	43
Figure 2.2. One-to-one competitions between wild-type and filamentation mutants confirms screen results	44
Figure 2.3. Relative abundance of competitive strains in GI compartments at end of time course	46
Figure 2.4. Fluorescent <i>in situ</i> hybridization (FISH) reveals similar morphological abundances between wild type and <i>ume6</i>	47
Figure 2.5. Representative FISH of GI compartments for wild type and <i>ume6</i> monotypic colonizations quantified in Figure 2.4.B	48
Figure 2.6. Alternative imaging of <i>C. albicans</i> in the large intestine using a polyclonal pan-fungal antibody used in previous studies	49
Figure 2.7. Gastrointestinal colonization of the feces in monotypic infections with wild type and <i>ume6</i>	50
Figure 2.8. Pilot NanoString with tissue and contents separated	52
Figure 2.9. NanoString time course over 10 days	53
Figure 2.10. Pilot RNA-seq of the mouse GI compartments.....	55
Figure 2.11. Overlap between published data sets and mRNA-seq of wild type under hypha- inducing conditions.	56
Figure 2.12. mRNA-seq reveals differences between wild type and <i>ume6</i> strains	58
Figure 2.13. <i>sap6</i> and <i>hyr1</i> mutants are hyperfit compared to wild type.....	59

Figure 3.1. One-to-one competitions reveal role for white-opaque regulators in commensalism	74
Figure 3.2. Newly made <i>wor1</i> isolates are not as hypofit as previous strains	76
Figure 3.3. Overexpression competitions	77
Figure 3.4. Epigenetic analysis during commensal colonization reveals hierarchy of transcription factors (part 1)	79
Figure 3.5. Epigenetic analysis during commensal colonization reveals hierarchy of transcription factors (part 2)	81
Figure 3.6. Filamentation phenotypes of white-opaque regulators	82
Figure 3.7. GUT cells in the GI tract are hypofilamentous	83
Figure 3.8. Loss of <i>efg1</i> or overexpression of <i>WOR1</i> confers an early growth advantage in the gut.....	84
Figure 3.9. Volcano plots of mRNA-seq comparisons in the large intestine.....	85
Figure 3.10. Expression of a core set of hypha-coregulated genes is dampened in the strains that are hyperfit.....	86
Figure 3.11. Enhanced expression of secreted chitinase may increase fitness of hyperfit strains	89
Figure 3.12. Calling card-seq overlap for Efg1-PBase, Czf1-PBase, and Wor1-PBase.....	90
Figure 4.1. PiggyBac transposase validation	102
Figure 4.2. Comparison of Calling card-seq results with ChIP-seq for white-opaque transcription factors	104
Figure 4.3. Comparison of Calling card-seq results with ChIP-chip for iron regulated transcription factors	107
Figure 4.4. Schematic of PiggyBac transposase tagging constructs	111
Figure 5.1. GUT phenotype can be observed from gnotobiotic BALB/c mice	119
Figure 5.2. Passage through Swiss Webster mice results in intermediate phenotype	120

Figure 5.3. Repeat of wild type versus *WOR1^{OE}* competition in gnotobiotic BALB/c animals confirms host-specific role in GUT cell formation121

Figure 5.4. Facility-specific microbiota in BALB/c mice can modulate GUT phenotype123

Figure 5.5. Post cohousing animals, GUT cell phenotype is lost124

Figure 5.6. *Lactobacillus spp.* abundance is higher in Kingston animal126

Figure 6.1. Loss of Hgc1 enhances gastrointestinal commensal fitness132

Figure 6.2. *hgc1* mutant does not form hyphae *in vivo*133

Figure 6.3. Volcano plots of RNA expression data from large intestine and under *in vitro* conditions136

List of abbreviations

bp	base pair
GUT	Gastrointestinally indUced Transition
ORF	open reading frame
PBase	PiggyBac transposase
TF	transcription factor
WT	wild type

Chapter 1. Introduction: *C. albicans* morphological plasticity in health and disease

First described ~150 years ago, *Candida albicans* is now recognized as the most prominent fungal commensal and pathogen of humans. As a commensal, *C. albicans* colonizes the gastrointestinal tract (1,2), mouth (3), skin (4,5), and female reproductive tract (6,7) of at least 70% of healthy adults (8). Human hosts are usually colonized in infancy (9) and longitudinal molecular typing studies indicate that strains persist clonally for many years, with little evidence for strain replacement (10). These observations, coupled with the failure to identify an environmental reservoir, suggest that *C. albicans* is exquisitely adapted to healthy mammalian hosts. However, benign commensal colonization can become pathogenic if hosts develop immune deficits, epithelial damage, or microbial dysbiosis (11). Ironically, the pool of vulnerable patients has increased with the availability of modern medical treatments such as antibiotics, cancer chemotherapy, and solid organ transplantation, and *Candida* species now rank as the 3rd or 4th most common cause of invasive bloodstream infections in hospitals in the United States (12-14). In this context, it is notable that fundamental questions regarding the mechanisms by which *C. albicans* thrives during its commensal and pathogenic lifestyles remain to be answered. For example, how is commensal colonization first established, and how does *C. albicans* persist for extended periods despite host immunity and bacterial competition? What controls the transition from commensalism to pathogenesis in vulnerable hosts? How does *C. albicans* succeed in the wide diversity of niches it encounters as a commensal and a pathogen? Some insights into these questions have been provided by a series of reports that link newly described *C. albicans* cell types to niche-specific functional adaptations (15-17).

The fungal kingdom is characterized by vast morphological plasticity. Fungi range in scale from the micron-sized microsporidia family of obligate intracellular pathogens (18) to *Armillaria ostoyae*, a tree pathogen whose 9.6 km² mycelial clone in Northern Oregon is considered the world's largest living organism (19). Furthermore, many species undergo morphological transformations in response to specific environmental cues. For example, 'thermally dimorphic'

fungal pathogens propagate as multicellular, branching, filamentous structures known as mycelia in environmental niches such as soil, and transition into unicellular, budding yeasts (or spherules, in the case of *Coccidioides immitis*) within warm-blooded hosts (20-22). Given that the entire known lifecycle of *C. albicans* occurs in mammalian hosts, one might expect less morphological plasticity from these species; however, the opposite is true, and nine distinct cell shapes have already been described. The characteristics of the classic cell types yeasts, hyphae, pseudohyphae and chlamyospores as well as yeast-like morphotypes, including opaque^{a/α}, gray and GUT cells are discussed. At each stage, cell characteristics, commensal and virulent properties, are discussed. Finally, environmental cues and transcriptional regulatory circuits that control morphology are discussed.

1.1. Yeasts, hyphae, pseudohyphae and chlamyospores

Yeasts, hyphae, pseudohyphae and chlamyospores were the first *C. albicans* cell types to be described. They differ in morphology, mode of division, occurrence and virulence potential.

1.1.1. Characteristics of yeasts, hyphae, pseudohyphae and chlamyospores

Among the four classic *C. albicans* cells types, yeasts and hyphae are the best characterized (reviewed in (23-25)), whereas pseudohyphae and chlamyospores are less well understood (reviewed in (23-26)). Standard yeasts, also known as ‘white’ cells, have a round-to-oval cell morphology, similar to that of *Saccharomyces cerevisiae*. Yeasts reproduce by budding, and nuclear division occurs at the junction between mother and daughter cells. Because progeny cells detach completely from their mothers after cytokinesis, yeasts are considered to be unicellular (reviewed in (23); see also (27)). By contrast, hyphal cells are thin, tube-shaped cells that resemble segments of a garden hose (depicted in **Figure 1.1**). Nuclear division occurs within hyphal daughter cells, followed by migration of one progeny nucleus back into the mother cells. Hyphal cells remain firmly attached end-to-end following cytokinesis, such that iterative rounds of

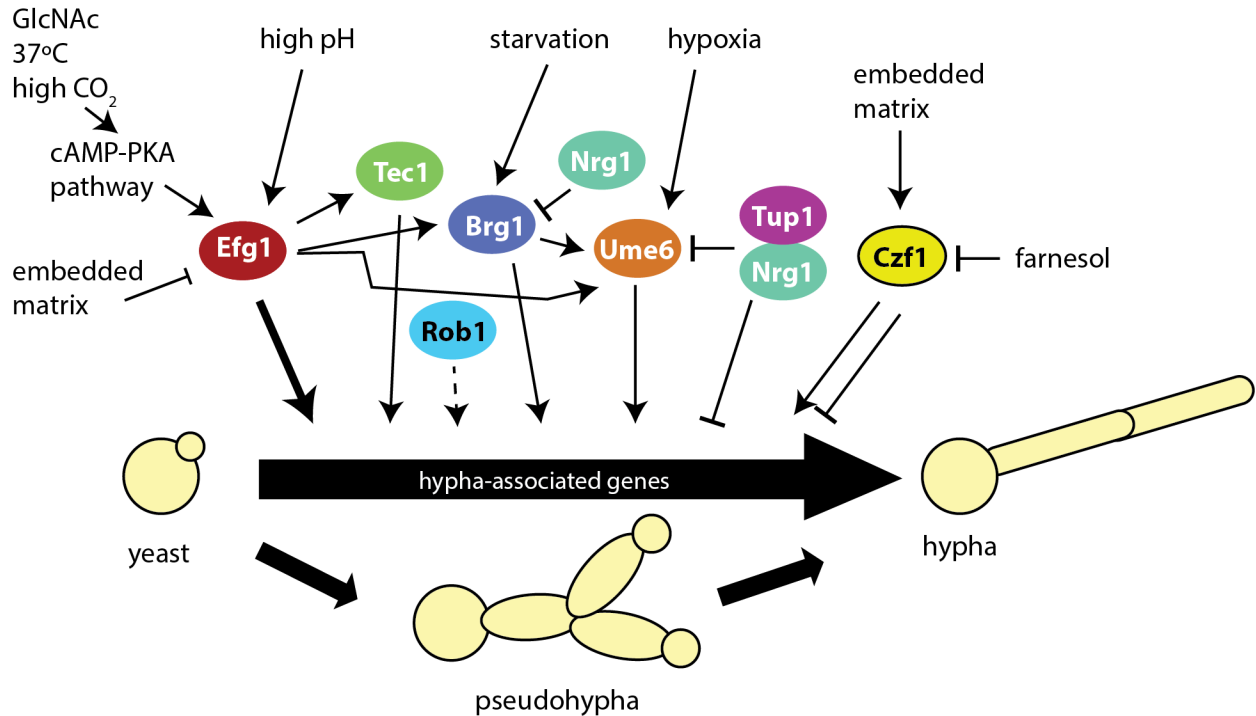


Figure 1.1. Simplified regulation of yeast-to-hypha transition. Arrowhead indicates activating effect. T-end indicates inhibiting effect. References supporting relationships between transcription factors are described in section 1.3.2.2.

cell division produce multicellular, sparsely branched, filamentous structures called mycelia. Ellipsoid-shaped pseudohyphal cells share features of both yeasts and hyphae, and there remains some controversy over whether they represent a *bona fide* terminal cell type or an intermediate between these other, better characterized cell types (28). Unlike for yeasts and hyphae, there are no known *in vitro* conditions to induce pure, stable populations of pseudohyphae. Instead, modulation of transcription factor levels that favor hyphal formation can allow for propagation of pseudohyphal populations to study gene dynamics (28). Like hyphae, pseudohyphal cells remain attached following cytokinesis and generate mycelia after multiple rounds of cell division. As in yeasts, nuclear division in pseudohyphae occurs at mother-daughter junctions; in contrast to hyphae, these junctions are demarcated by visible indentations. Finally, chlamydospores are large, spherical, thick-walled cells observed *in vitro* under certain harsh conditions, such as starvation and hypoxia ((29), reviewed in (30)). Chlamydospores are

generated by suspensor cells, which are cells at the distal ends of mycelial filaments. Nuclear division occurs within the suspensor cell parent, followed by migration of a progeny nucleus to the nascent chlamydospore, which remains attached to its mother (31).

1.1.2. Roles of *a/α* yeasts, pseudohyphae and hyphae in biofilm formation

Yeasts, pseudohyphae and hyphae are also required for biofilm formation (reviewed in (32,33)), a *C. albicans* attribute of substantial clinical importance. Biofilms are communities of microorganisms that often form on solid surfaces in the environment or within mammalian hosts. Medical device-associated biofilms are of enormous clinical importance because of their high prevalence and intrinsic resistance to antibiotics and the mammalian immune system. *C. albicans* *MTLa/MTLα* white^{a/α} cells form conventional biofilms in a stereotyped fashion (reviewed in (34,35)). Biofilms are initiated when white^{a/α} phase yeasts attach to a solid substrate. Yeasts proliferate to form microcolonies, followed by the appearance and proliferation of hyphae and pseudohyphae, which constitute the bulk of the mature biofilm, together with an extracellular matrix composed of proteins, polysaccharides, and nucleic acids. Biofilm dispersion is thought to occur when white^{a/α} yeasts detach from a mature biofilm only to reattach at a second site. Multispecies biofilms, in which *C. albicans* coordinates with bacteria such as *Streptococcus oralis*, have also been shown to cooperate to increase tissue invasion, which have clinical relevance when treating for invasive disease (reviewed in (36)). *MTLa* and *MTLα* white^a cells have recently been shown to form sexual biofilms (see Section 1.2. for description of white^a cells). These biofilms differ from conventional biofilms by multiple criteria, including increased permeability, decreased resistance to antibiotics and host immune cells, and promotion of chemotropism between opaque^a *MTLa* and *MTLα* cells (37,38). It has been proposed that a primary function of white^a cell biofilms is to facilitate mating between sexually competent *MTLa* and *MTLα* opaque^a cells (38).

1.1.3. Virulence of yeasts, hyphae and pseudohyphae

Yeasts, hyphae, and pseudohyphae can either propagate stably as the same cell type or give rise to other cell types in a process known as morphogenesis (**Figure 1.1**), depending on cues from the local environment (described in section 1.3.1.). Morphogenesis has long been a central focus of *C. albicans* research because of links between each of these cell types and important host-fungal interactions. Traditionally, the filamentous forms (hyphae and pseudohyphae) were considered pathogenic, whereas yeasts were primarily viewed as commensals. Hyphae are intrinsically invasive on solid media and hyphal tip cells exhibit thigmotropism, or the unusual ability to ‘track’ along substrate surface irregularities (39) (reviewed in (40)). Moreover, pseudohyphae and hyphae express numerous cell type-specific virulence factors such as adhesins (for example, Hwp1, Hyr1, Als3, Als10, Fav2 and Pga55), tissue-degrading enzymes (for example, Sap4, Sap5 and Sap6), antioxidant defense proteins (for example, Sod5), and even a recently described cytolytic peptide toxin (Ece1) (28,41-45). The increased virulence potential of hyphae compared to other cell types has been conclusively shown in superficial candidiasis models, such as models of oropharyngeal (46,47) and vulvovaginal (48) infection. For example, hyphae, but not yeasts, induce their endocytic uptake by cultured human oral epithelial cells via a specific interaction between the hyphal adhesin, Als3, and host E-cadherin; internalized hyphae then proceed to damage the host cells (47). Hyphae can also actively penetrate into oral epithelial cells, possibly via physical pressure and secreted enzymes (49,50). Thus, in a reconstituted model of human oral epithelial tissue, invading hyphae trigger multiple pro-inflammatory host signaling pathways, whereas yeasts, which merely colonize the surface of the tissue without causing damage, produce a more muted inflammatory response (46).

However, the simple dichotomy between virulent hyphae versus commensal yeasts does not account for observations of disseminated candidiasis, where both cell types seem to contribute to disease. For example, yeasts, hyphae and pseudohyphae are all present in infected

tissues that were recovered from human patients and animals with disseminated candidiasis (51-53). Moreover, *C. albicans* mutants trapped as either yeasts or filaments are both defective in bloodstream infection models, suggesting that the ability to interconvert among different cell types is required for virulence (see, for example, (54-57)). Traditionally, yeasts, being smaller and unicellular, were hypothesized to disseminate through the bloodstream, whereas hyphae, being naturally invasive, were thought to escape the vasculature, penetrate into internal organs, and damage the host. Therefore, it came as a surprise when a study using a tetracycline-regulatable strain that can be propagated indefinitely as either yeasts or hyphae showed that yeast-locked *C. albicans* is as capable of egress from blood vessels, penetration into internal organs, and propagation within host tissues as a wild-type strain that can transition into hyphae (57). Nevertheless, unlike wild-type *C. albicans*, the yeast-locked strain failed to kill its host, supporting previous observations that the yeast-to-hypha transition is required for virulence in disseminated infections. Together, these observations in localized versus disseminated infection models support a central role for yeast-hypha-pseudohypha morphogenesis in *C. albicans*-host interactions, but also suggest that yeasts may have different roles in different host niches. In contrast to the other cell types, chlamydo spores, which are readily induced *in vitro* (58,59), have rarely been observed in clinical specimens (60) or animal models of disease (61), and their biological role remains undefined (26).

1.1.4. Commensalism of yeasts and hyphae

Much less is known of the commensal properties of yeasts and hyphae compared to their role in virulence, while the role of pseudohyphae and chlamydo spores in commensal fitness has not been investigated. Several previous reports of yeasts as the primary colonizers of the healthy gastrointestinal tract, along with the role for hyphae in virulence (see section 1.1.3), has led to the conclusion that yeasts, and not hyphae, are the commensally propagated morphology of *C. albicans* in the gut (62,63). In addition, a specialized yeast cell type, GUT (discussed in section

1.2.6), exhibits a hyperfit phenotype in competition in a murine gastrointestinal colonization model compared to white^{a/α} cells. The yeast form is considered to be the commensal cell type of the skin as well, based on a previous report that the yeast form is not recognized by epithelial cells *in vitro* (46). *Candida* species are a normal part of a healthy oral microbiome (64) but oral thrush, essentially a biofilm in the mouth, is a common manifestation in immunocompromised people (65).

1.2. Yeast-like morphotypes: White, opaque, gray, and GUT

In addition to standard 'white', round-to-oval yeast morphology, described above, *C. albicans* transitions into several more elongated yeast-like cell types (opaque, gray, and GUT) that exhibit distinct *in vitro* properties and interactions with the host. Moreover, a minority of white and opaque cells that have lost genetic material at the Mating Type-Like Locus (*MTL*) exhibit further alterations in their propensities for mating, filamentation, virulence, commensalism, and/or biofilm formation. The different types of white and opaque cells are not generally distinguished by genotype in the *C. albicans* literature. To clarify cell identity, we will introduce the convention of appending a superscript 'a/α' to white or opaque cells with the standard genotype of *MTLa/MTLα*. A superscript 'α' will designate cells containing only the *MTLα* allele, whereas a superscript 'a' will be used either as a general term for cells containing a single allele of the *MTL* (*MTLa* or *MTLα*) or as a specific term for ones containing only the *MTLa* allele.

1.2.1. Characteristics of white^a and opaque^a cells

White^a and opaque^a cells were first described in a particular *C. albicans* clinical isolate, WO-1, based on *in vitro* observations of rare but heritable changes in cell and colony morphology (**Figure 1.2**) (66). White^a WO-1 yeasts have an identical appearance to standard white^{a/α} yeasts, described above, and form similar, creamy white, shiny, domed colonies on solid media. On

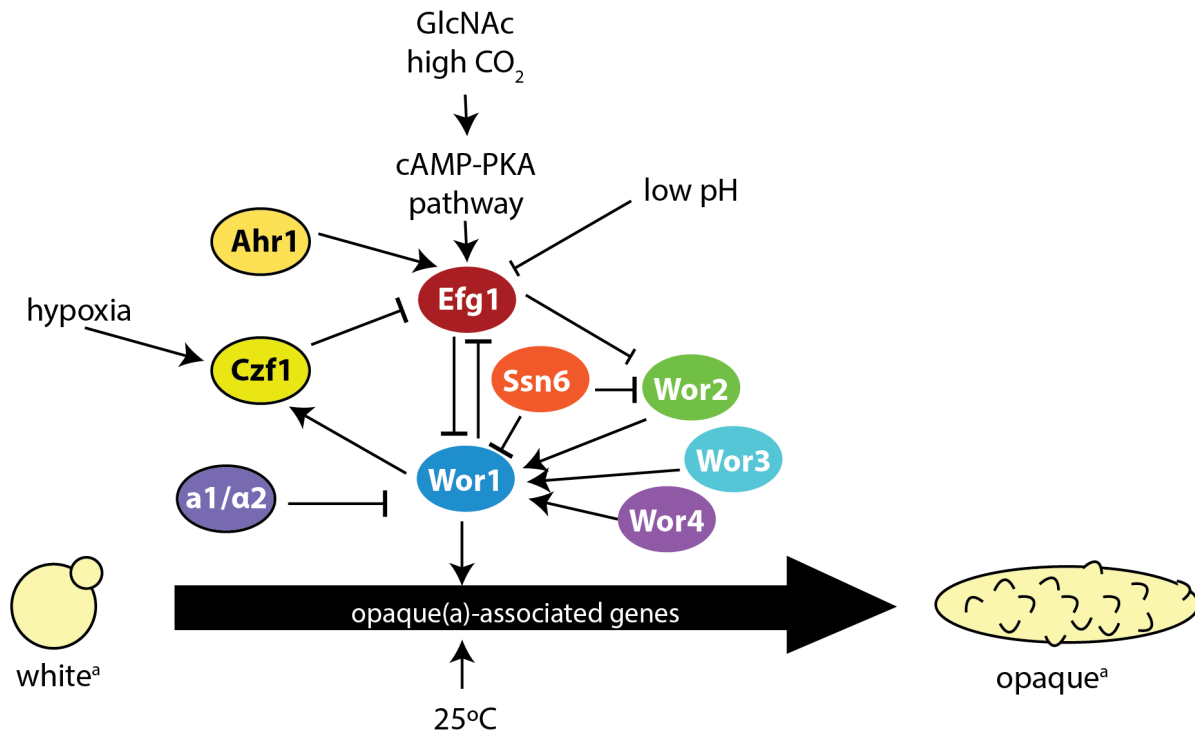


Figure 1.2. Simplified regulation of white^a-to-opaque^a switch. Arrowhead indicates activating effect. T-end indicates inhibiting effect. References supporting relationships between transcription factors are described in section 1.3.2.3.

glucose-containing media maintained at room temperature, however, white^a colonies occasionally give rise to slower growing sectors of opaque^a cells. Opaque^a colony sectors appear slightly darker, matte and flattened compared to white^a colonies. For undetermined reasons, opaque^a cells also take up a dye, phloxine B, which allows for rapid visualization of opaque^a colonies and colony sectors that are stained bright pink on media containing this dye. Microscopically, opaque^a cells are elongated compared to white^a cells and ~3 times larger (by volume), with more pronounced vacuoles (66). Additional opaque^a-specific features include cell surface 'pimples' (that is, protuberances with an unknown biological role that are detected by scanning electron microscopy) (67), relative resistance to phagocytosis by host macrophages and neutrophils (68,69), sensitivity to distinct filamentation-inducing cues (70,71), and changes in the expression of >1000 genes, including genes important for mating and respiration (72-74). Similarly to yeast-hypha-pseudohypha morphogenesis, switching between the white^a and opaque^a phenotypes is

highly sensitive to environmental conditions: N-acetylglucosamine, $\geq 5\%$ CO₂, and acidic pH all favor switching to the opaque^a state (75-77), whereas glucose, low CO₂ levels, alkaline pH, and mammalian body temperature promote the reverse switch back to the white^a state (66).

1.2.2. Comparison of white^{a/α} and white^a to opaque^a cell filamentation

Until recently, it was not widely appreciated that opaque^a cells could switch from yeasts to hyphae, though it was reported as long ago as 1989 that opaque^a cells had the capacity to form filaments (78). In several recent studies, opaque^a cells were observed to respond to environmental signals distinct from those of white cells (70,71). Traditional *C. albicans* hypha-inducing stimuli include serum, high temperature (37°C), neutral pH, and nutrient starvation which were shown not to stimulate opaque^a filamentation (70). Instead opaque^a filamentation was optimal at room temperature. Higher temperatures were observed to inhibit opaque^a cell filamentation. Sorbitol and low phosphate conditions in particular were shown to stimulate opaque^a cell filamentation but not white cell filamentation. Despite these differences, white and opaque^a filamentation programs share several common signaling pathways and transcriptional regulators (discussed below). The differences in required hyphal-inducing conditions hints at the specialization of different yeast forms for distinct host niches during commensalism and pathogenesis.

1.2.3. White^a-to-opaque^a switching, mating locus, and sexual competency

The functional significance of the white^a-to-opaque^a switch was revealed with the discovery that *C. albicans* opaque^a cells are specialized for mating (79). Fungal mating has been well described in the model yeast, *S. cerevisiae*, in which haploid cells are the sexually-competent cell type (reviewed in (80)). Haploid 'a' cells express the *MATa* allele of the Mating Type Locus, whereas haploid 'α' cells express the *MATα* allele. *MATa* and *MATα* encode different transcription

factors that activate key mating genes in the respective haploid cell types. When **a** and α cells occur in proximity, pheromones secreted by mating partners of opposite mating type induce mutual cell cycle arrest, production of polarized mating projections, and cell and nuclear fusion to produce diploid **a**/ α cells. Wild *S. cerevisiae* exists in the diploid form except under nutrient starvation conditions, which triggers meiosis and the formation of hardy haploid spores. These spores germinate when nutrients become available, and the mating cycle resumes.

In contrast to *S. cerevisiae*, *C. albicans* has never been observed to undergo meiosis or sporulation and was long considered to be an asexual species. However, in 2000, two groups reported low frequency mating between *C. albicans* **a** and α cells (81,82). Most *C. albicans* strains carry single copies of two different alleles of the Mating Type-Like Locus, *MTL_a* and *MTL _{α}* , one apiece on two copies of Chromosome 5; these *MTL* alleles are orthologous to *S. cerevisiae* *MAT_a* and *MAT _{α}* (83). Researchers generated 'a' and ' α ' cells by deleting *MTL_a* or *MTL _{α}* from **a**/ α strains via targeted gene disruption (81) or selection for loss of one copy of Chromosome 5 (82). Remarkably, mixtures of these engineered **a** and α cells *in vitro* (82) or in a mouse bloodstream infection model (81) produced a small number of tetraploid cells containing markers of both parental strains. One group subsequently determined the relationship between allelism at *MTL*, opaque^a or opaque ^{α} cell formation, and mating: unlike typical **a**/ α cells, **a** and α cells (including the natural α strain, WO-1) can switch to the opaque^a or opaque ^{α} states, respectively, and opaque^a and opaque ^{α} cells are the mating-competent cell types in *C. albicans* (79). The molecular mechanism preventing the white^a-to-opaque^a switch in **a**/ α cells is mediated by direct transcriptional repression of genes required for the switch by a1/ α 2, which is a heterodimeric transcription factor encoded by the combination of *MTL_a* with *MTL _{α}* (73,84-86). More recently, another study reported that white^a and white ^{α} cells may also play a role in mating via formation of specialized 'sexual' biofilms that constrain mating-competent opaque^a and opaque ^{α} cells in space (37,38).

Despite these advancements in our understanding of the relationship between *MTL* genotype, white^a-to-opaque^a switching and mating competency, the larger contribution of sex to *C. albicans* biology remains uncertain. Analysis of *C. albicans* population structures has revealed a primarily clonal mode of reproduction, with little evidence for sexual recombination among naturally circulating strains (87,88). The rarity of sexual recombination is consistent with the observation that more than 90% of clinical isolates are heterozygous at the *MTL* locus and therefore incapable of switching or mating (89,90). Similarly, it remains unknown why *C. albicans*, along with its close relatives, *C. dubliniensis* and *C. tropicalis*, introduced a baroque requirement for a white^a-to-opaque^a phenotypic switch into its mating program, given that *S. cerevisiae* and the vast majority of fungi mate efficiently without such a system. Some insights into the latter question are suggested by the recent discovery of three additional cell morphologies with some features of opaque^a cells in the *MTLa/α* genetic background, discussed below.

1.2.4. Characteristics of opaque^{a/α} and gray cells

A recent study discovered opaque^{a/α} cells in a screen of 94 *C. albicans* clinical isolates for morphological responses to opaque^a-inducing signals (15). This group had previously shown that exposure of white^a cells to 1% N-acetylglucosamine (as a sole carbon source) and 5% CO₂ induces 100% full-colony switching to the opaque^a phenotype (76). Using the same conditions, they found that ~1/3 of their *a/α* isolates developed opaque^a-like (that is, bright pink-staining with phloxine B) colony sectors. Moreover, opaque^{a/α} cells recovered from pink sectors were elongated, contained cell surface pimples, and expressed several opaque^a-specific genes, like traditional opaque^a cells. However, unlike opaque^a cells, opaque^{a/α} cells were incapable of mating (15). The same group subsequently discovered additional *a/α* isolates that switch among white^{a/α}, opaque^{a/α}, and a novel 'gray' phenotype (16). Gray cells are elongated but smaller than conventional yeasts, lack pimples, stain only moderately with phloxine B and mate with very low

efficiency (16). In strains that are capable of white^{al}_α-opaque^{al}_α-gray switching, the transition to gray cell morphology is induced by exposure to nutrient-rich growth medium (YEPD), whereas exposure to nutrient-poor medium (Lee's), N-acetylglucosamine, and elevated CO₂ favor the opaque^{al}_α phenotype (16).

1.2.5. Virulence and commensalism of opaque^a, opaque^{al}_α and gray cells

Interestingly, initial studies in mammalian infection models suggest that opaque^{al}_α, gray, and opaque^a cells may have increased fitness on host epithelial surfaces (15,16,91). For example, opaque^{al}_α and opaque^a cells have each been reported to colonize skin more effectively than isogenic white^{al}_α or white^a strains in a neonatal mouse skin infection model (15,91). Likewise, in an *ex vivo* tongue infection model, gray cells have the fastest doubling time, followed by opaque^{al}_α cells, with white^{al}_α cells proliferating most slowly (16). By contrast, white^{al}_α cells are consistently most virulent in mouse bloodstream infection models (15,16,91,92). The mechanisms underlying these functional differences have not yet been defined but cell type-specific differences in metabolism and/or enzyme secretion appear likely to play a role (15,16,73,74,93). WO-1, a naturally white^α *C. albicans* clinical isolate, was shown to switch en masse to opaque^α cells upon passage through the mouse gastrointestinal tract (94). The role for these yeast cell types in commensalism is currently being investigated but the ability of these cell types to transition between yeasts and hyphae in response to signals that differ from white^{al}_α also suggests a role for these cell types in modulating host interactions that would favor one cell type over another (70,71).

1.2.6. Characteristics of GUT cells

C. albicans "GUT" (gastrointestinally induced transition) cells were discovered by means of a genetic screen for fungal mediators of commensalism within the mammalian digestive tract

(17). Pools of a/α gene deletion mutants were competed in a mouse model of persistent gastrointestinal colonization, in which the host remains healthy despite high levels of commensally growing *C. albicans*, and the fitness of each fungal strain was calculated as a ratio of the relative abundance in mouse feces to that in the infecting inoculum. Two mutants affecting a pair of mutually inhibitory transcription factors emerged because of their striking and opposite effects on commensal fitness: the *efg1* knockout mutant was hyperfit, outcompeting all other mutants and wild-type *C. albicans*, whereas *wor1* was strongly attenuated in this model. Consistent with a positive role for Wor1 in promoting commensal fitness, it was shown that expression of the *WOR1* gene was induced 10,000-fold when wild-type yeasts were propagated within the host digestive tract compared to standard laboratory conditions. Furthermore, forced expression of *WOR1* (*WOR1*^{OE}) via a strong, heterologous promoter (*WOR1*^{OE}) induced a hypercompetitive phenotype. Unexpectedly, after ~10 days of exposure to the mammalian model, a subset of the *WOR1*^{OE} yeasts recovered from animals exhibited altered cell and colony morphology. Moreover, these GUT cells rapidly dominated the recovered yeast population for the remainder of the 25-day time course. Similar to opaque^a cells (and opaque^a/ α cells), GUT cells are elongated relative to isogenic white^a/ α cells and generate darker, flattened colonies that stain (weakly) with phloxine B (**Figure 1.3**, (17) and Gianetti and Noble, unpublished data). Intriguingly, the initial appearance of the GUT phenotype coincided with a sharp gain in fitness of the *WOR1*^{OE} strain, suggesting that the two phenotypes might be linked. Indeed, when GUT cells are introduced into naive animals, they are immediately hypercompetitive, unlike white^a/ α isolates of the same strain.

1.2.7. Commensalism and virulence of GUT cells

After demonstrating that GUT cells lack the classic features of white^a/ α and opaque^a cells, it was hypothesized that this novel cell type might be specialized for commensalism within the mammalian digestive tract. In support of this hypothesis, it was shown that GUT cells are

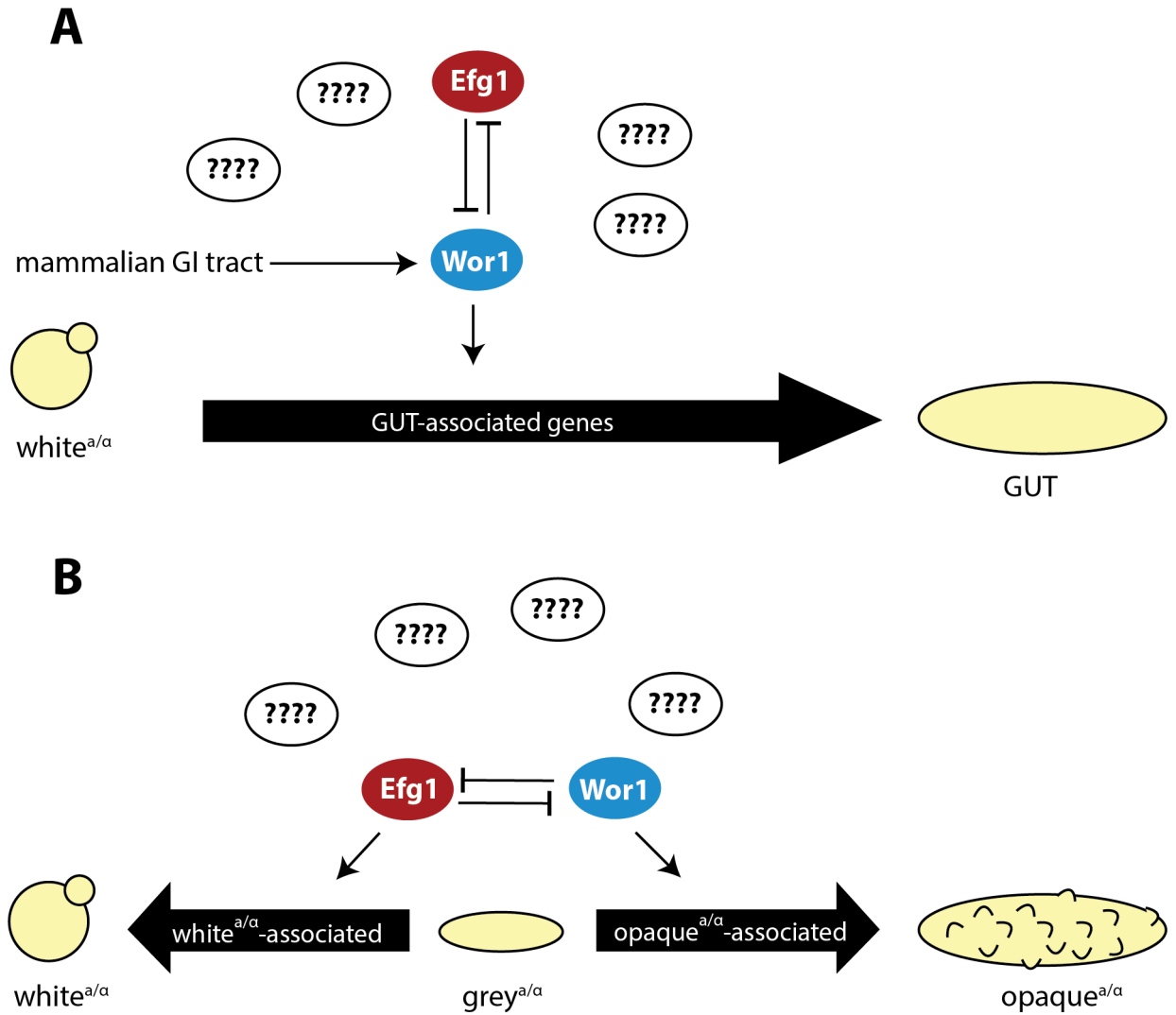


Figure 1.3. GUT, opaque^{a/α} and grey^{a/α} regulation. With the exception of the contributions of Efg1 and Wor1 to GUT, opaque^{a/α} and grey^{a/α} switches, the other regulatory players have not yet been defined in the literature.

substantially more fit than both white^{a/α} and opaque^a cells in the gastrointestinal commensalism model, with a relative fitness of GUT >> white^{a/α} >> opaque^a (17). This fitness advantage seems to be specific to gastrointestinal commensalism, as GUT cells proliferate more slowly than white^{a/α} cells under standard laboratory conditions and are less virulent in a mouse bloodstream infection model. Furthermore, unlike opaque^a cells, GUT cells lack surface pimples and are unable to mate. Taken together, these data support a model in which signals from the mammalian gastrointestinal tract induce *C. albicans* yeasts to express *WOR1* and switch from white^{a/α} to GUT. Whereas GUT

cells thrive within the digestive tract, wild-type *C. albicans* strains rapidly revert to the white^{al α} phenotype upon exit from animals, when signals required to maintain the GUT phenotype are removed. Thus, the detection of GUT cells outside of the host reflected the serendipitous use of a *WOR1*^{OE} strain, as continuous expression of *Wor1* presumably stabilizes the phenotype. Future investigations will be required to define the host signals and fungal machinery that affect the white^{al α} -to-GUT switch.

1.2.8. Fitness and metabolism of yeast morphotypes

Comparative transcriptomics of white^{al α} (16,17), opaque^{al α} (16), gray (16), GUT (17), white^a (73,74,95) and opaque^a (73,74,95) yeasts has revealed metabolic differences that may help to account for the functional differences among these cell types. The clearest case can be made for GUT cells, which, compared to white cells, exhibit general downregulation of pathways for utilization of glucose and iron uptake, with concomitant upregulation of pathways for utilization of N-acetylglucosamine and short chain fatty acids (17). Thus, GUT cell metabolism seems to be optimized for nutrients available in the distal mammalian digestive tract, the niche in which it thrives as a commensal (17). By contrast, opaque^{al α} and opaque^a cells upregulate pathways involved in oxidative respiration (for example, the Krebs's cycle) (73,74,95), whereas white^{al α} and white^a cells upregulate fermentation pathways (for example, glucose uptake and, to varying degrees, glycolysis) (73,74,95). The transcriptome of gray cells shows differences in metabolic gene expression that are harder to categorize (16). The functional importance of these cell type-specific metabolic signatures will hopefully be rationalized once the natural host niches of each cell type are identified.

1.3 Regulation of morphogenesis

Morphogenesis depends on environmental cues such as temperature and nutrient availability that signal through multiple pathways and activate a variety of transcriptional regulatory circuits. Most

of these pathways were initially characterized with respect to the yeast-to-hypha transition by white^{al} cells; however, several of these same signaling pathways also control discrete behaviors by additional cell types. The evolution of such elaborate systems to regulate morphogenesis speaks to the central importance of morphogenesis in *C. albicans* biology.

1.3.1. Environmental cues and their signaling pathways

On the basis of *in vitro* studies, various signals (mammalian body temperature, serum, N-acetylglucosamine (GlcNAc), low nitrogen, CO₂, peptidoglycan, and amino acids) have been shown to activate the fungal cAMP-PKA signaling pathway (96-112). In white^{al} cells, cAMP-mediated signaling through the protein kinase A (PKA) complex activates transcription factors that promote the expression of hypha-specific genes and filamentation (109). Alternatively, in white^a cells, PKA activation by GlcNAc or CO₂ promotes a switch to the opaque^a phenotype (75,76,98,100). Similarly, the Cek1 MAP kinase pathway can promote either filamentation or mating in different cell types (113,114). In white^{al} cells, nitrogen starvation or growth in an embedded matrix such as agar activates Cek1 to promote filamentation (97,114-119). In *MTL* homozygous opaque^a cells, Cek1 activation by mating pheromones triggers the expression of genes required for mating (120-124). In addition, various forms of cell stress (oxidative, osmotic, cell wall damage) affect filamentation indirectly via the Hog1 signaling pathway, which inhibits Cek1 and activates a transcriptional inhibitor of filamentation (125-135). In white^{al} cells exposed to alkaline pH, the RIM101 pH sensing pathway proteolytically activates the Rim101 transcription factor, leading to activation of hypha-specific genes and filamentation (136-139). Additional, less well-described pathways negatively regulate filamentation in response to low oxygen levels and starvation, respectively (140,141). Notably, the depicted pathways fail to account for certain observations in the host, such as the finding that white^{al} yeasts appear to predominate in the mammalian GI tract (62), despite relatively high concentrations of GlcNAc and CO₂ in this niche,

which would be expected to trigger filamentation or the white^a-to-opaque^a switch based on *in vitro* evidence. Such discrepancies suggest that additional signaling pathways and/or crosstalk among existing pathways remain to be discovered. The multiplicity and complexity of the known signaling pathways suggest a model in which *C. albicans* continuously surveils the mammalian host, integrating a variety of signaling inputs to generate adaptive responses to the local environment.

1.3.2. Transcriptional regulation of morphogenesis

1.3.2.1. Efg1

Remarkably, every morphological transition described here is regulated to some extent by the transcription factor, Efg1 (15-17,142-144). The roles of Efg1 in *C. albicans* morphogenesis were deduced from phenotypes of *EFG1* mutants, with different cell shapes correlating with high or low levels of *EFG1* expression. Efg1 is a basic helix-loop-helix transcription factor of the fungal-specific APSES (Asm1p, Phd1p, Sok2p, Efg1p and StuAp) family whose orthologs regulate diverse morphological transitions in different fungal species ((145,146), reviewed in (147)). Upon exposure to host serum, N-acetylglucosamine, high CO₂, nutrient depletion, and/or iron depletion, Efg1 promotes white^{a/α} cells to undergo the yeast-to-hypha transition (142); however, under agar-embedded conditions, Efg1 promotes the *reverse* transition from hypha-to-yeast (145). In another case, under low oxygen, nutrient-depleted conditions, Efg1 promotes **a/α** hyphae and pseudohyphae to generate chlamydo spores (144). In contrast, upon exposure to glucose and low CO₂, Efg1 promotes **a** and **α** opaque^a cells to switch to the white^a state (75) and certain **a/α** clinical isolates to undergo opaque-to-white^{a/α} or gray-to-white^{a/α} switches (15,16). Finally, Efg1 inhibits **a/α** GUT-to-white^{a/α} cells from switching to the white^{a/α} state in all tested environments *other than* the mammalian intestinal tract (17). Strains lacking *EFG1* have reduced virulence in a mouse model of systemic infection (55). The role for *EFG1* in commensalism is less clear as

different labs have reported different levels of GI commensal fitness but our lab consistently sees a hyperfit phenotype (17,62,148-150).

1.3.2.2. Transcriptional regulation of yeast-to-hypha transition and biofilms

A large number of transcription factors have been implicated in promoting or repressing hypha formation (151). While I will not be exhaustive, I will highlight the most well characterized transcription factors that appear in **Figure 1.1** as well as a few that are less well known but that will be referred to in my thesis. The TEA/ATTS transcription factor family is conserved throughout eukaryotes (152-154). The zinc finger, Cys₂His₂ (C₂H₂), family of transcription factors is conserved across eukaryotes (reviewed in (155)). The GATA family of transcription factors which binds the DNA sequence “GATA” is conserved from yeasts to humans (reviewed in (156,157)). The zinc cluster, Zn(II)₂Cys₆, family of transcription factors is restricted to fungi (reviewed in (157)).

Tec1 is a member of the TEA/ATTS family of transcription factors and has been shown to be required for the yeast-to-hypha transition *in vitro* as well as biofilm formation (158,159). Macrophage evasion is also diminished by knockout of *TEC1* (158). In a mouse model of systemic infection, a *tec1* strain was able to form hyphae but was unable to kill the host (158).

Brg1, formerly known as Gat2, is a member of the GATA family of transcription factors and plays a positive role in both the yeast-to-hyphal transition and biofilm formation (160-163). Deletion of *BRG1* leads to attenuated virulence in a mouse model of systemic infection (162). Brg1 is a key component of a negative feedback loop with the yeast-to-hypha inhibitor Nrg1 in initiation of hyphal formation (160). In response to nutrient starvation, Brg1 acts downstream of Tor1 signaling to promote starvation induced filamentation (161). Brg1 has also been implicated in a screen for white-opaque regulators as an inhibitor though follow-up is warranted to place it in the regulatory diagram (164). All core white-opaque regulators bind upstream of *BRG1* (95).

Rob1 is the least characterized of the transcription factors presented here, not being the sole focus of a single paper, but has appeared in several large scale screens for transcription

factors involved in morphology and biofilm formation (151,163). Rob1, named for regulator of biofilm, is a member of the $Zn(II)_2Cys_6$ family of regulators and the *rob1* mutant appears to have the strongest correlation with *brg1* in its filamentation defects (151,165). Chromatin immunoprecipitation followed by microarray hybridization (ChIP-chip) of Rob1 and Brg1 in biofilms revealed distinct but overlapping DNA binding profiles in that context (163).

Ume6 is a transcription factor in the $Zn(II)_2Cys_6$ family that acts as an important positive regulator of filamentation in multiple yeast cell types (70,166,167). The *Candida* homologue was named for *S. cerevisiae* Ume6, which regulates meiosis in that fungus (168). Deletion of *UME6*, which results in a complete defect in hyphal formation was used to highlight the importance of the ability to form hyphae in a mouse model of disseminated infection (166). In white cells, ectopic overexpression of *UME6* in an *efg1cph1* mutant was used to show that Ume6 acts downstream of Efg1 and Cph1 in hyphal formation (167). In opaque^a cells, Ume6 also positively regulates hyphal formation though it is unclear if this is through Efg1 (70). Ume6 has a positive role in biofilm formation as overexpression results in thicker biofilms (167). During biofilm formation, which relies on the successful formation and maintenance of hyphae, 5 of 6 (Efg1, Brg1, Ndt80, Bcr1, Tec1 but not Rob1) core biofilm transcription factors are enriched at the *UME6* promoter (163).

Czf1 is a $Zn(II)_2Cys_6$ family member that is unique to the *Candida* genus but most similar to Ume6 (169). It is a regulator of filamentous growth best known for its roles in mediating the response of *C. albicans* to the quorum sensing molecule, farnesol, and requirement for embedded filamentous growth (169,170). Farnesol inhibits filamentous growth and a *czf1* mutant was found to be filamentous in the presence of farnesol under hypha-inducing conditions (169). Czf1 is additionally a positive regulator of white-opaque switching (see section 1.4.3).

Nrg1, Mig1, Rfg1 and Tup1 act as negative regulators of hypha-formation (56,171-173). Tup1 does not have a DNA binding domain and relies on cofactors for its role in repression (42,172). The regulatory heterodimers Nrg1-Tup1 and Nrg1-Rfg1 have been shown to prevent Ume6 expression and hyphal formation (174).

1.3.2.3. Transcriptional regulation of white-opaque switch

In similar studies to Efg1, Wor1, a transcriptional regulator with a newly identified DNA binding domain called WOPR that is present across fungi, was shown to oppose Efg1 in the control of the white^a-opaque^a, white^{a/α}-gray-opaque^{a/α}, and white^{a/α}-GUT transitions (15-17,84-86,175,176). Wor1 is part of a family of proteins that are fungal-specific transcription factors whose orthologues regulate diverse morphological transitions in different fungal species (175,177-180). In *C. albicans*, Efg1 and Wor1 have been demonstrated to bind to each other's promoters, where they are thought to mediate mutual transcriptional repression (181,182). Regulation of *C. albicans* cell shape is more than a simple function of Efg1 and Wor1 levels, however, because each factor's activity is influenced by genotype at *MTL* and local environmental cues. A key unanswered question is how the genotype of the *MTL* locus and signals associated with different host niches contribute to discrete morphological outcomes. This challenge is compounded by the fact that cues such as N-acetylglucosamine and CO₂ promote distinct morphological switches in different contexts, as described above. Arguably the best characterized switch, in terms of its core transcriptional regulation, is the white^a- opaque^a switch of *MTL a* and α cells (**Figure 1.2**) (84-86,95,164,181,183-186). Under conditions in which pro-white^a and pro-opaque^a environmental cues are balanced (for example, glucose-containing medium maintained at 25°C), switching between white^a and opaque^a cell types occurs infrequently and stochastically in single cells, and both white^a-to-opaque^a and opaque^a-to-white^a switching occurs (66). In this setting, cell morphology is thought to be programmed by the predominance of either Efg1 or Wor1 protein, such that switching might be triggered by events such as unequal distribution of Efg1 or Wor1 protein between a mother and daughter cell (86,181). In contrast, under environmental conditions that heavily favor the white^a (glucose-containing medium maintained in room air at 37°C) or opaque^a (N-acetylglucosamine-containing medium in ≥5% CO₂) state, switching occurs in a concerted fashion across the entire cell population (66,75-77). In these settings, it seems

likely that potent environmental cues reinforce or inhibit transcriptional regulatory components in addition to Efg1 and Wor1 to produce a specific outcome. This switch is controlled by numerous transcription factors in addition to the 'master regulators' Efg1 and Wor1, which together form an interlocking circuit of positive and negative feedback loops (simplified in Figure 1.2, (84-86,95,164,181,183-186)).

Czf1, in addition to its roles in filamentation described above, was identified as a core member of the white-opaque regulatory network (see Figure 1.2 (187)). Czf1, Wor1 and Efg1 were shown to bind their own promoters as well as the promoters of the other two (181,182,187,188). Epistasis analysis was used to determine the genetic relationships between Wor1, Efg1 and Czf1 (181). This revealed that under non-inducing conditions white^a cells could be driven to form opaque^a cells with 100% frequency (compared to empty vector at <1% switching) when *WOR1* or *CZF1* were ectopically expressed in otherwise wild-type white^a cells (181). However, *WOR1* was required for the Czf1 phenotype as ectopic overexpression of *CZF1* in a *wor1* mutant mimicked the switching defect in the *wor1* parent strain (181). Additional testing of double deletion mutants determined that Czf1 is responsible for inhibiting Efg1, which promotes the white^a state (181). Czf1 was determined to be required for opaque^a cell formation in a study of hypoxia induced white^a-to-opaque^a switching in the *C. albicans* WO-1 strain (94).

Ahr1, originally designated Zcf37, is a member of the Zn(II)₂Cys₆ transcription factor family whose deletion enhances white^a-to-opaque^a switching (165,183). Ectopic expression of *AHR1* in an *efg1* mutant abolished the ability of opaque^a cells to switch to white^a suggesting that Ahr1 acts through Efg1 (183). In white^a cells, *AHR1* is bound only by Ahr1 (95). In opaque^a cells, *AHR1* is a target of Wor1, Wor2, Wor3, Wor4 and Ssn6 but not Efg1 or Czf1 (95). In *a/α* cells, Ahr1 can act as both a repressor as well as activator of filamentation (151). An *ahr1* white^{a/α} strain was not defective in mouse kidney colonization in a disseminated infection model (189). Recently, it has

been shown that Ahr1 is required for growth on amino acids and pH neutralization both *in vitro* as well as in macrophage phagosomes (190).

Wor2 belongs to the Zn(II)₂Cys₆ transcription factor family described above. It was first identified as an activator of the white-to-opaque switch under conditions where *C. albicans* stochastically switches, hence the name, but has subsequently been shown to inhibit filamentous growth at high temperatures as a *wor2* mutant in an *a/α* is hyperfilamentous at 42°C (151,181). The *WOR2* transcript was upregulated by the Hap43 CCAAT-binding complex under low-iron conditions (191). By ChIP-chip, Wor2 binds and is bound by all core white-opaque regulators in opaque^a cells (95). Ectopic expression of Wor2 does not lead to greatly enhanced switching of white^a cells to opaque^a cells and the deletion of *WOR2*, which leads to a decrease in switching frequency, can be bypassed by the ectopic expression of *WOR1* which suggests Wor2 acts upstream of Wor1 to promote switching and is inhibited by Efg1 in white cells (181). Under opaque^a-inducing conditions (on N-acetylglucosamine-containing medium), Wor2 is dispensable for the white-to-opaque switch (192).

Wor3 belongs to a previously undescribed family of DNA binding proteins that is present in a very small clade of eukaryotes, which includes *C. albicans* and other fungal pathogens, and has thus been characterized in a limited fashion (184). As the name suggests, Wor3 was originally identified by its role in the white^a-opaque^a switch (184). Unique among the white^a-opaque^a regulators, both ectopic expression as well as deletion in white^a cells promotes switching to the opaque^a state (184). Interestingly, it was also recently reported that overexpression of *WOR3* promotes filamentous growth and leads to a decrease in gastrointestinal commensal fitness in gnotobiotic mice (193).

Wor4 was also recently identified as an activator of the white^a-to-opaque^a switch and is predicted to be a member of the C₂H₂ zinc finger transcription factor family (186). The deletion and ectopic expression phenotypes of *WOR4* are similar to those of *CZF1*, in that deletion ablates stochastic white-to-opaque switching and ectopic expression results in a more modest increase

in switching from white-to-opaque (~30%) (186). Wor4 is present in both white^a and opaque^a cells and has similar localization (72,95,186). Wor4 was determined to only bind upstream of *WOR1* in white^a cells but upstream of all core white^a-opaque^a regulators in opaque^a cells (186). There is a large overlap between the DNA binding targets of Wor4 and those of Wor1 and Wor2 in opaque^a cells as determined by ChIP-seq (186).

Recently, Ssn6 was characterized as an inhibitor in white^a-to-opaque^a switching (185). Ssn6 is the *C. albicans* homologue of the Cyc8 corepressor in *S. cerevisiae* and does not have a DNA binding domain (194,195). Instead it appears to colocalize with DNA binding proteins to repress transcription of opaque^a specific genes in white^a cells and white^a specific genes in opaque^a cells (185). The pattern of localization in opaque^a cells correlates strongly with Wor1 and Wor2 (185). In *a/α* cells, Ssn6 works with Tup1 as well as independently to suppress filamentous growth (151,194,196,197).

1.4. Thesis Outline

The role of different yeast morphotypes and hyphae in colonizing healthy individuals are not well defined. Most healthy humans are colonized by *C. albicans*, and it is thought that the same strains that cause pathogenesis are those that initially colonize the healthy host.

Here, I will present data accumulated for the commensal roles of transcription factors involved in the yeast-to-hypha transition as well as the white-opaque switch that suggest colonization by yeasts is favored over hyphae. In Chapter 2, I characterize the role for the yeast-to-hypha transcriptional regulatory network in negative regulation of commensal fitness and the role of a hypha-coregulated gene that is a secreted effector in modulating commensal fitness. In Chapter 3, I systematically define the roles for white-opaque regulators in commensal fitness. Also, in Chapter 3, I examine the coordination of white-opaque regulators as additional regulators of filamentation. In Chapter 4, I present validation of a new method in *C. albicans* for profiling transcription factor binding events. In Chapter 5, I examine the role of host background and

microbiota contributions to the commensal fitness of the GUT cell type. In Chapter 6, I characterize the inhibitory role of Hgc1, a hypha-specific G1 cyclin-like protein required for hyphal formation, in commensal fitness.

Throughout, I highlight important techniques that we have developed during my years in the Noble lab that contribute substantially to our ability to characterize cell morphologies as well as transcriptional regulation in the mammalian gut. In particular, I have developed a method (Calling card-seq) for profiling *C. albicans* transcription factor binding events in the mammalian host. The ultimate goal will be to use our RNA expression profiling data of transcription factor mutants colonizing the gut in combination with Calling card-seq *in vivo* to identify direct regulatory targets of these transcription factors that are specific to gastrointestinal colonization. Because of the complex nature of the transcription factor regulatory networks in *C. albicans*, advances in the ability to study *C. albicans* in the context of different host niches should advance our knowledge of the effectors that are important in different host contexts.

1.5. References

1. Hoffmann, C., Dollive, S., Grunberg, S., Chen, J., Li, H., Wu, G. D., Lewis, J. D., and Bushman, F. D. (2013) Archaea and fungi of the human gut microbiome: correlations with diet and bacterial residents. *PLoS one* **8**, e66019
2. Nash, A. K., Auchtung, T. A., Wong, M. C., Smith, D. P., Gesell, J. R., Ross, M. C., Stewart, C. J., Metcalf, G. A., Muzny, D. M., Gibbs, R. A., Ajami, N. J., and Petrosino, J. F. (2017) The gut mycobiome of the Human Microbiome Project healthy cohort. *Microbiome* **5**, 153
3. Ghannoum, M. A., Jurevic, R. J., Mukherjee, P. K., Cui, F., Sikaroodi, M., Naqvi, A., and Gillevet, P. M. (2010) Characterization of the oral fungal microbiome (mycobiome) in healthy individuals. *PLoS pathogens* **6**, e1000713
4. Findley, K., Oh, J., Yang, J., Conlan, S., Deming, C., Meyer, J. A., Schoenfeld, D., Nomicos, E., Park, M., Program, N. I. H. I. S. C. C. S., Kong, H. H., and Segre, J. A. (2013) Topographic diversity of fungal and bacterial communities in human skin. *Nature* **498**, 367-370
5. Oyeka, C. A., and Ugwu, L. O. (2002) Fungal flora of human toe webs. *Mycoses* **45**, 488-491
6. Drell, T., Lillsaar, T., Tummeleht, L., Simm, J., Aaspollu, A., Vain, E., Saarma, I., Salumets, A., Donders, G. G., and Metsis, M. (2013) Characterization of the vaginal micro- and mycobiome in asymptomatic reproductive-age Estonian women. *PLoS one* **8**, e54379

7. Merenstein, D., Hu, H., Wang, C., Hamilton, P., Blackmon, M., Chen, H., Calderone, R., and Li, D. (2013) Colonization by *Candida* species of the oral and vaginal mucosa in HIV-infected and noninfected women. *AIDS Res Hum Retroviruses* **29**, 30-34
8. Odds, F. C. (1987) *Candida* infections: an overview. *Critical reviews in microbiology* **15**, 1-5
9. Russell, C., and Lay, K. M. (1973) Natural history of *Candida* species and yeasts in the oral cavities of infants. *Arch Oral Biol* **18**, 957-962
10. Odds, F. C., Davidson, A. D., Jacobsen, M. D., Tavanti, A., Whyte, J. A., Kibbler, C. C., Ellis, D. H., Maiden, M. C., Shaw, D. J., and Gow, N. A. (2006) *Candida albicans* strain maintenance, replacement, and microvariation demonstrated by multilocus sequence typing. *Journal of clinical microbiology* **44**, 3647-3658
11. Perleth, J., Choi, B., and Spellberg, B. (2007) Nosocomial fungal infections: epidemiology, diagnosis, and treatment. *Med Mycol* **45**, 321-346
12. Edmond, M. B., Wallace, S. E., McClish, D. K., Pfaller, M. A., Jones, R. N., and Wenzel, R. P. (1999) Nosocomial bloodstream infections in United States hospitals: a three-year analysis. *Clinical infectious diseases : an official publication of the Infectious Diseases Society of America* **29**, 239-244
13. Pfaller, M. A., and Diekema, D. J. (2007) Epidemiology of invasive candidiasis: a persistent public health problem. *Clinical microbiology reviews* **20**, 133-163
14. Wisplinghoff, H., Bischoff, T., Tallent, S. M., Seifert, H., Wenzel, R. P., and Edmond, M. B. (2004) Nosocomial bloodstream infections in US hospitals: analysis of 24,179 cases from a prospective nationwide surveillance study. *Clinical infectious diseases : an official publication of the Infectious Diseases Society of America* **39**, 309-317
15. Xie, J., Tao, L., Nobile, C. J., Tong, Y., Guan, G., Sun, Y., Cao, C., Hernday, A. D., Johnson, A. D., Zhang, L., Bai, F. Y., and Huang, G. (2013) White-opaque switching in natural MTL α isolates of *Candida albicans*: evolutionary implications for roles in host adaptation, pathogenesis, and sex. *PLoS biology* **11**, e1001525
16. Tao, L., Du, H., Guan, G., Dai, Y., Nobile, C. J., Liang, W., Cao, C., Zhang, Q., Zhong, J., and Huang, G. (2014) Discovery of a "white-gray-opaque" tristable phenotypic switching system in *Candida albicans*: roles of non-genetic diversity in host adaptation. *PLoS biology* **12**, e1001830
17. Pande, K., Chen, C., and Noble, S. M. Passage through the mammalian gut triggers a phenotypic switch that promotes *Candida albicans* commensalism. *Nat Genet* **45**, 1088-1091
18. Didier, E. S. (2005) Microsporidiosis: an emerging and opportunistic infection in humans and animals. *Acta Trop* **94**, 61-76
19. Ferguson, B. A. D., T. A.; Parks, C. G.; Filip, G. M.; Schmitt, C. L. (2003) Coarse-scale population structure of pathogenic *Armillaria* species in a mixed-conifer forest in the Blue Mountains of northeast Oregon. *Canadian Journal of Forest Research* **33**, 612-623
20. Edwards, J. A., Chen, C., Kemski, M. M., Hu, J., Mitchell, T. K., and Rappleye, C. A. (2013) *Histoplasma* yeast and mycelial transcriptomes reveal pathogenic-phase and lineage-specific gene expression profiles. *BMC Genomics* **14**, 695
21. Nemecek, J. C., Wuthrich, M., and Klein, B. S. (2006) Global control of dimorphism and virulence in fungi. *Science* **312**, 583-588

22. Beyhan, S., Gutierrez, M., Voorhies, M., and Sil, A. (2013) A temperature-responsive network links cell shape and virulence traits in a primary fungal pathogen. *PLoS biology* **11**, e1001614
23. Sudbery, P., Gow, N., and Berman, J. (2004) The distinct morphogenic states of *Candida albicans*. *Trends Microbiol* **12**, 317-324
24. Thompson, D. S., Carlisle, P. L., and Kadosh, D. (2011) Coevolution of morphology and virulence in *Candida* species. *Eukaryotic cell* **10**, 1173-1182
25. Sudbery, P. E. (2011) Growth of *Candida albicans* hyphae. *Nat Rev Microbiol* **9**, 737-748
26. Staib, P., and Morschhauser, J. (2007) Chlamyospore formation in *Candida albicans* and *Candida dubliniensis*--an enigmatic developmental programme. *Mycoses* **50**, 1-12
27. Warena, A. J., and Konopka, J. B. (2002) Septin function in *Candida albicans* morphogenesis. *Molecular biology of the cell* **13**, 2732-2746
28. Carlisle, P. L., Banerjee, M., Lazzell, A., Monteagudo, C., Lopez-Ribot, J. L., and Kadosh, D. (2009) Expression levels of a filament-specific transcriptional regulator are sufficient to determine *Candida albicans* morphology and virulence. *Proceedings of the National Academy of Sciences of the United States of America* **106**, 599-604
29. Jansons, V. K., and Nickerson, W. J. (1970) Induction, morphogenesis, and germination of the chlamyospore of *Candida albicans*. *Journal of bacteriology* **104**, 910-921
30. Whiteway, M., and Bachewich, C. (2007) Morphogenesis in *Candida albicans*. *Annu Rev Microbiol* **61**, 529-553
31. Martin, S. W., Douglas, L. M., and Konopka, J. B. (2005) Cell cycle dynamics and quorum sensing in *Candida albicans* chlamyospores are distinct from budding and hyphal growth. *Eukaryotic cell* **4**, 1191-1202
32. Desai, J. V., and Mitchell, A. P. (2015) *Candida albicans* Biofilm Development and Its Genetic Control. *Microbiol Spectr* **3**
33. Ramage, G., Mowat, E., Jones, B., Williams, C., and Lopez-Ribot, J. (2009) Our current understanding of fungal biofilms. *Critical reviews in microbiology* **35**, 340-355
34. Nobile, C. J., and Johnson, A. D. (2015) *Candida albicans* Biofilms and Human Disease. *Annu Rev Microbiol* **69**, 71-92
35. Soll, D. R., and Daniels, K. J. (2016) Plasticity of *Candida albicans* Biofilms. *Microbiol Mol Biol Rev* **80**, 565-595
36. Lohse, M. B., Gulati, M., Johnson, A. D., and Nobile, C. J. (2018) Development and regulation of single- and multi-species *Candida albicans* biofilms. *Nat Rev Microbiol* **16**, 19-31
37. Daniels, K. J., Park, Y. N., Srikantha, T., Pujol, C., and Soll, D. R. (2013) Impact of environmental conditions on the form and function of *Candida albicans* biofilms. *Eukaryotic cell* **12**, 1389-1402
38. Park, Y. N., Daniels, K. J., Pujol, C., Srikantha, T., and Soll, D. R. (2013) *Candida albicans* forms a specialized "sexual" as well as "pathogenic" biofilm. *Eukaryotic cell* **12**, 1120-1131
39. Thomson, D. D., Wehmeier, S., Byfield, F. J., Janmey, P. A., Caballero-Lima, D., Crossley, A., and Brand, A. C. (2015) Contact-induced apical asymmetry drives the thigmotropic responses of *Candida albicans* hyphae. *Cellular microbiology* **17**, 342-354
40. Brand, A., and Gow, N. A. (2009) Mechanisms of hypha orientation of fungi. *Curr Opin Microbiol* **12**, 350-357

41. Carlisle, P. L., and Kadosh, D. (2013) A genome-wide transcriptional analysis of morphology determination in *Candida albicans*. *Molecular biology of the cell* **24**, 246-260
42. Kadosh, D., and Johnson, A. D. (2005) Induction of the *Candida albicans* filamentous growth program by relief of transcriptional repression: a genome-wide analysis. *Molecular biology of the cell* **16**, 2903-2912
43. Lane, S., Birse, C., Zhou, S., Matson, R., and Liu, H. (2001) DNA array studies demonstrate convergent regulation of virulence factors by Cph1, Cph2, and Efg1 in *Candida albicans*. *J Biol Chem* **276**, 48988-48996
44. Nantel, A., Dignard, D., Bachewich, C., Harcus, D., Marcil, A., Bouin, A. P., Sensen, C. W., Hogues, H., van het Hoog, M., Gordon, P., Rigby, T., Benoit, F., Tessier, D. C., Thomas, D. Y., and Whiteway, M. (2002) Transcription profiling of *Candida albicans* cells undergoing the yeast-to-hyphal transition. *Molecular biology of the cell* **13**, 3452-3465
45. Moyes, D. L., Wilson, D., Richardson, J. P., Mogavero, S., Tang, S. X., Wernecke, J., Hofs, S., Gratacap, R. L., Robbins, J., Runglall, M., Murciano, C., Blagojevic, M., Thavaraj, S., Forster, T. M., Hebecker, B., Kasper, L., Vizcay, G., Iancu, S. I., Kichik, N., Hader, A., Kurzai, O., Luo, T., Kruger, T., Kniemeyer, O., Cota, E., Bader, O., Wheeler, R. T., Gutschmann, T., Hube, B., and Naglik, J. R. (2016) Candidalysin is a fungal peptide toxin critical for mucosal infection. *Nature* **532**, 64-68
46. Moyes, D. L., Runglall, M., Murciano, C., Shen, C., Nayar, D., Thavaraj, S., Kohli, A., Islam, A., Mora-Montes, H., Challacombe, S. J., and Naglik, J. R. (2010) A biphasic innate immune MAPK response discriminates between the yeast and hyphal forms of *Candida albicans* in epithelial cells. *Cell host & microbe* **8**, 225-235
47. Phan, Q. T., Myers, C. L., Fu, Y., Sheppard, D. C., Yeaman, M. R., Welch, W. H., Ibrahim, A. S., Edwards, J. E., Jr., and Filler, S. G. (2007) Als3 is a *Candida albicans* invasin that binds to cadherins and induces endocytosis by host cells. *PLoS biology* **5**, e64
48. Peters, B. M., Palmer, G. E., Nash, A. K., Lilly, E. A., Fidel, P. L., Jr., and Noverr, M. C. (2014) Fungal morphogenetic pathways are required for the hallmark inflammatory response during *Candida albicans* vaginitis. *Infection and immunity* **82**, 532-543
49. Dalle, F., Wachtler, B., L'Ollivier, C., Holland, G., Bannert, N., Wilson, D., Labruere, C., Bonnin, A., and Hube, B. (2010) Cellular interactions of *Candida albicans* with human oral epithelial cells and enterocytes. *Cellular microbiology* **12**, 248-271
50. Wachtler, B., Citiulo, F., Jablonowski, N., Forster, S., Dalle, F., Schaller, M., Wilson, D., and Hube, B. (2012) *Candida albicans*-epithelial interactions: dissecting the roles of active penetration, induced endocytosis and host factors on the infection process. *PloS one* **7**, e36952
51. Di Carlo, P., Di Vita, G., Guadagnino, G., Cocorullo, G., D'Arpa, F., Salamone, G., Salvatore, B., Gulotta, G., and Cabibi, D. (2013) Surgical pathology and the diagnosis of invasive visceral yeast infection: two case reports and literature review. *World Journal of Emergency Surgery* **8**, 38
52. Chin, V. K., Foong, K. J., Maha, A., Rusliza, B., Norhafizah, M., and Chong, P. P. (2014) Multi-step pathogenesis and induction of local immune response by systemic *Candida albicans* infection in an intravenous challenge mouse model. *Int J Mol Sci* **15**, 14848-14867
53. Gupta, K. L. (2001) Fungal infections and the kidney. *Indian Journal of Nephrology* **11**, 147-154

54. Braun, B. R., van Het Hoog, M., d'Enfert, C., Martchenko, M., Dungan, J., Kuo, A., Inglis, D. O., Uhl, M. A., Hogues, H., Berriman, M., Lorenz, M., Levitin, A., Oberholzer, U., Bachewich, C., Marcus, D., Marcil, A., Dignard, D., Iouk, T., Zito, R., Frangeul, L., Tekaia, F., Rutherford, K., Wang, E., Munro, C. A., Bates, S., Gow, N. A., Hoyer, L. L., Kohler, G., Morschhauser, J., Newport, G., Znaidi, S., Raymond, M., Turcotte, B., Sherlock, G., Costanzo, M., Ihmels, J., Berman, J., Sanglard, D., Agabian, N., Mitchell, A. P., Johnson, A. D., Whiteway, M., and Nantel, A. (2005) A human-curated annotation of the *Candida albicans* genome. *PLoS genetics* **1**, 36-57
55. Lo, H. J., Kohler, J. R., DiDomenico, B., Loebenberg, D., Cacciapuoti, A., and Fink, G. R. (1997) Nonfilamentous *C. albicans* mutants are avirulent. *Cell* **90**, 939-949
56. Murad, A. M., Leng, P., Straffon, M., Wishart, J., Macaskill, S., MacCallum, D., Schnell, N., Talibi, D., Marechal, D., Tekaia, F., d'Enfert, C., Gaillardin, C., Odds, F. C., and Brown, A. J. (2001) NRG1 represses yeast-hypha morphogenesis and hypha-specific gene expression in *Candida albicans*. *The EMBO journal* **20**, 4742-4752
57. Saville, S. P., Lazzell, A. L., Monteagudo, C., and Lopez-Ribot, J. L. (2003) Engineered control of cell morphology in vivo reveals distinct roles for yeast and filamentous forms of *Candida albicans* during infection. *Eukaryotic cell* **2**, 1053-1060
58. Alicia, Z. S., Blanca, O. S., Mariana, G. H., Magdalena, C. C., and Alexandro, B. (2006) Rapid production of *Candida albicans* chlamydospores in liquid media under various incubation conditions. *Nihon Ishinkin Gakkai Zasshi* **47**, 231-234
59. Citiulo, F., Moran, G. P., Coleman, D. C., and Sullivan, D. J. (2009) Purification and germination of *Candida albicans* and *Candida dubliniensis* chlamydospores cultured in liquid media. *FEMS yeast research* **9**, 1051-1060
60. Chabasse, D., Bouchara, J. P., de Gentile, L., and Chennebault, J. M. (1988) [*Candida albicans* chlamydospores observed in vivo in a patient with AIDS]. *Ann Biol Clin (Paris)* **46**, 817-818
61. Cole, G. T., Seshan, K. R., Phaneuf, M., and Lynn, K. T. (1991) Chlamydospore-like cells of *Candida albicans* in the gastrointestinal tract of infected, immunocompromised mice. *Can J Microbiol* **37**, 637-646
62. White, S. J., Rosenbach, A., Lephart, P., Nguyen, D., Benjamin, A., Tzipori, S., Whiteway, M., Meccas, J., and Kumamoto, C. A. (2007) Self-regulation of *Candida albicans* population size during GI colonization. *PLoS pathogens* **3**, e184
63. Vautier, S., Drummond, R. A., Chen, K., Murray, G. I., Kadosh, D., Brown, A. J., Gow, N. A., MacCallum, D. M., Kolls, J. K., and Brown, G. D. (2015) *Candida albicans* colonization and dissemination from the murine gastrointestinal tract: the influence of morphology and Th17 immunity. *Cellular microbiology* **17**, 445-450
64. Krom, B. P., Kidwai, S., and Ten Cate, J. M. (2014) *Candida* and other fungal species: forgotten players of healthy oral microbiota. *J Dent Res* **93**, 445-451
65. Thompson, G. R., 3rd, Patel, P. K., Kirkpatrick, W. R., Westbrook, S. D., Berg, D., Erlandsen, J., Redding, S. W., and Patterson, T. F. (2010) Oropharyngeal candidiasis in the era of antiretroviral therapy. *Oral Surg Oral Med Oral Pathol Oral Radiol Endod* **109**, 488-495
66. Slutsky, B., Staebell, M., Anderson, J., Risen, L., Pfaller, M., and Soll, D. R. (1987) "White-opaque transition": a second high-frequency switching system in *Candida albicans*. *Journal of bacteriology* **169**, 189-197

67. Anderson, J., Mihalik, R., and Soll, D. R. (1990) Ultrastructure and antigenicity of the unique cell wall pimple of the *Candida* opaque phenotype. *Journal of bacteriology* **172**, 224-235
68. Lohse, M. B., and Johnson, A. D. (2008) Differential phagocytosis of white versus opaque *Candida albicans* by *Drosophila* and mouse phagocytes. *PLoS one* **3**, e1473
69. Sasse, C., Hasenberg, M., Weyler, M., Gunzer, M., and Morschhauser, J. (2013) White-opaque switching of *Candida albicans* allows immune evasion in an environment-dependent fashion. *Eukaryotic cell* **12**, 50-58
70. Si, H., Hernday, A. D., Hirakawa, M. P., Johnson, A. D., and Bennett, R. J. (2013) *Candida albicans* white and opaque cells undergo distinct programs of filamentous growth. *PLoS pathogens* **9**, e1003210
71. Guan, G., Xie, J., Tao, L., Nobile, C. J., Sun, Y., Cao, C., Tong, Y., and Huang, G. (2013) Bcr1 plays a central role in the regulation of opaque cell filamentation in *Candida albicans*. *Molecular microbiology* **89**, 732-750
72. Tuch, B. B., Mitrovich, Q. M., Homann, O. R., Hernday, A. D., Monighetti, C. K., De La Vega, F. M., and Johnson, A. D. (2010) The transcriptomes of two heritable cell types illuminate the circuit governing their differentiation. *PLoS genetics* **6**, e1001070
73. Tsong, A. E., Miller, M. G., Raisner, R. M., and Johnson, A. D. (2003) Evolution of a combinatorial transcriptional circuit: a case study in yeasts. *Cell* **115**, 389-399
74. Lan, C. Y., Newport, G., Murillo, L. A., Jones, T., Scherer, S., Davis, R. W., and Agabian, N. (2002) Metabolic specialization associated with phenotypic switching in *Candida albicans*. *Proceedings of the National Academy of Sciences of the United States of America* **99**, 14907-14912
75. Huang, G., Srikantha, T., Sahni, N., Yi, S., and Soll, D. R. (2009) CO(2) regulates white-to-opaque switching in *Candida albicans*. *Current biology : CB* **19**, 330-334
76. Huang, G., Yi, S., Sahni, N., Daniels, K. J., Srikantha, T., and Soll, D. R. (2010) N-acetylglucosamine induces white to opaque switching, a mating prerequisite in *Candida albicans*. *PLoS pathogens* **6**, e1000806
77. Sun, Y., Cao, C., Jia, W., Tao, L., Guan, G., and Huang, G. (2015) pH Regulates White-Opaque Switching and Sexual Mating in *Candida albicans*. *Eukaryotic cell* **14**, 1127-1134
78. Anderson, J., Cundiff, L., Schnars, B., Gao, M. X., Mackenzie, I., and Soll, D. R. (1989) Hypha formation in the white-opaque transition of *Candida albicans*. *Infection and immunity* **57**, 458-467
79. Miller, M. G., and Johnson, A. D. (2002) White-opaque switching in *Candida albicans* is controlled by mating-type locus homeodomain proteins and allows efficient mating. *Cell* **110**, 293-302
80. Madhani, H. (2007) From a to alpha: Yeast as a Model for Cellular Differentiation. *Cold Spring Harbor Laboratory Press*
81. Hull, C. M., Raisner, R. M., and Johnson, A. D. (2000) Evidence for mating of the "asexual" yeast *Candida albicans* in a mammalian host. *Science* **289**, 307-310
82. Magee, B. B., and Magee, P. T. (2000) Induction of mating in *Candida albicans* by construction of MTL α and MTL α strains. *Science* **289**, 310-313
83. Hull, C. M., and Johnson, A. D. (1999) Identification of a mating type-like locus in the asexual pathogenic yeast *Candida albicans*. *Science* **285**, 1271-1275

84. Huang, G., Wang, H., Chou, S., Nie, X., Chen, J., and Liu, H. (2006) Bistable expression of WOR1, a master regulator of white-opaque switching in *Candida albicans*. *Proceedings of the National Academy of Sciences of the United States of America* **103**, 12813-12818
85. Srikantha, T., Borneman, A. R., Daniels, K. J., Pujol, C., Wu, W., Seringhaus, M. R., Gerstein, M., Yi, S., Snyder, M., and Soll, D. R. (2006) TOS9 regulates white-opaque switching in *Candida albicans*. *Eukaryotic cell* **5**, 1674-1687
86. Zordan, R. E., Galgoczy, D. J., and Johnson, A. D. (2006) Epigenetic properties of white-opaque switching in *Candida albicans* are based on a self-sustaining transcriptional feedback loop. *Proceedings of the National Academy of Sciences of the United States of America* **103**, 12807-12812
87. Bougnoux, M. E., Pujol, C., Diogo, D., Bouchier, C., Soll, D. R., and d'Enfert, C. (2008) Mating is rare within as well as between clades of the human pathogen *Candida albicans*. *Fungal genetics and biology : FG & B* **45**, 221-231
88. Graser, Y., Volovsek, M., Arrington, J., Schonian, G., Presber, W., Mitchell, T. G., and Vilgalys, R. (1996) Molecular markers reveal that population structure of the human pathogen *Candida albicans* exhibits both clonality and recombination. *Proceedings of the National Academy of Sciences of the United States of America* **93**, 12473-12477
89. Legrand, M., Lephart, P., Forche, A., Mueller, F. M., Walsh, T., Magee, P. T., and Magee, B. B. (2004) Homozygosity at the MTL locus in clinical strains of *Candida albicans*: karyotypic rearrangements and tetraploid formation. *Molecular microbiology* **52**, 1451-1462
90. Lockhart, S. R., Pujol, C., Daniels, K. J., Miller, M. G., Johnson, A. D., Pfaller, M. A., and Soll, D. R. (2002) In *Candida albicans*, white-opaque switchers are homozygous for mating type. *Genetics* **162**, 737-745
91. Kvaal, C., Lachke, S. A., Srikantha, T., Daniels, K., McCoy, J., and Soll, D. R. (1999) Misexpression of the opaque-phase-specific gene PEP1 (SAP1) in the white phase of *Candida albicans* confers increased virulence in a mouse model of cutaneous infection. *Infection and immunity* **67**, 6652-6662
92. Lockhart, S. R., Wu, W., Radke, J. B., Zhao, R., and Soll, D. R. (2005) Increased virulence and competitive advantage of a/alpha over a/a or alpha/alpha offspring conserves the mating system of *Candida albicans*. *Genetics* **169**, 1883-1890
93. Ene, I. V., Lohse, M. B., Vladu, A. V., Morschhauser, J., Johnson, A. D., and Bennett, R. J. (2016) Phenotypic Profiling Reveals that *Candida albicans* Opaque Cells Represent a Metabolically Specialized Cell State Compared to Default White Cells. *mBio* **7**
94. Ramirez-Zavala, B., Reuss, O., Park, Y. N., Ohlsen, K., and Morschhauser, J. (2008) Environmental induction of white-opaque switching in *Candida albicans*. *PLoS pathogens* **4**, e1000089
95. Hernday, A. D., Lohse, M. B., Fordyce, P. M., Nobile, C. J., DeRisi, J. L., and Johnson, A. D. (2013) Structure of the transcriptional network controlling white-opaque switching in *Candida albicans*. *Molecular microbiology* **90**, 22-35
96. Shapiro, R. S., Uppuluri, P., Zaas, A. K., Collins, C., Senn, H., Perfect, J. R., Heitman, J., and Cowen, L. E. (2009) Hsp90 orchestrates temperature-dependent *Candida albicans* morphogenesis via Ras1-PKA signaling. *Current biology : CB* **19**, 621-629

97. Biswas, K., and Morschhauser, J. (2005) The Mep2p ammonium permease controls nitrogen starvation-induced filamentous growth in *Candida albicans*. *Molecular microbiology* **56**, 649-669
98. Castilla, R., Passeron, S., and Cantore, M. L. (1998) N-acetyl-D-glucosamine induces germination in *Candida albicans* through a mechanism sensitive to inhibitors of cAMP-dependent protein kinase. *Cell Signal* **10**, 713-719
99. Feng, Q., Summers, E., Guo, B., and Fink, G. (1999) Ras signaling is required for serum-induced hyphal differentiation in *Candida albicans*. *Journal of bacteriology* **181**, 6339-6346
100. Klengel, T., Liang, W. J., Chaloupka, J., Ruoff, C., Schroppel, K., Naglik, J. R., Eckert, S. E., Mogensen, E. G., Haynes, K., Tuite, M. F., Levin, L. R., Buck, J., and Muhlschlegel, F. A. (2005) Fungal adenylyl cyclase integrates CO₂ sensing with cAMP signaling and virulence. *Current biology : CB* **15**, 2021-2026
101. Xu, X. L., Lee, R. T., Fang, H. M., Wang, Y. M., Li, R., Zou, H., Zhu, Y., and Wang, Y. (2008) Bacterial peptidoglycan triggers *Candida albicans* hyphal growth by directly activating the adenylyl cyclase Cyr1p. *Cell host & microbe* **4**, 28-39
102. Maidan, M. M., De Rop, L., Serneels, J., Exler, S., Rupp, S., Tourneu, H., Thevelein, J. M., and Van Dijck, P. (2005) The G protein-coupled receptor Gpr1 and the Galpha protein Gpa2 act through the cAMP-protein kinase A pathway to induce morphogenesis in *Candida albicans*. *Molecular biology of the cell* **16**, 1971-1986
103. Hall, R. A., Turner, K. J., Chaloupka, J., Cottier, F., De Sordi, L., Sanglard, D., Levin, L. R., Buck, J., and Muhlschlegel, F. A. (2011) The quorum-sensing molecules farnesol/homoserine lactone and dodecanol operate via distinct modes of action in *Candida albicans*. *Eukaryotic cell* **10**, 1034-1042
104. Leberer, E., Harcus, D., Dignard, D., Johnson, L., Ushinsky, S., Thomas, D. Y., and Schroppel, K. (2001) Ras links cellular morphogenesis to virulence by regulation of the MAP kinase and cAMP signalling pathways in the pathogenic fungus *Candida albicans*. *Molecular microbiology* **42**, 673-687
105. Fang, H. M., and Wang, Y. (2006) RA domain-mediated interaction of Cdc35 with Ras1 is essential for increasing cellular cAMP level for *Candida albicans* hyphal development. *Molecular microbiology* **61**, 484-496
106. Rocha, C. R., Schroppel, K., Harcus, D., Marcil, A., Dignard, D., Taylor, B. N., Thomas, D. Y., Whiteway, M., and Leberer, E. (2001) Signaling through adenylyl cyclase is essential for hyphal growth and virulence in the pathogenic fungus *Candida albicans*. *Molecular biology of the cell* **12**, 3631-3643
107. Zou, H., Fang, H. M., Zhu, Y., and Wang, Y. (2010) *Candida albicans* Cyr1, Cap1 and G-actin form a sensor/effector apparatus for activating cAMP synthesis in hyphal growth. *Molecular microbiology* **75**, 579-591
108. Hoyer, L. L., Cieslinski, L. B., McLaughlin, M. M., Torphy, T. J., Shatzman, A. R., and Livi, G. P. (1994) A *Candida albicans* cyclic nucleotide phosphodiesterase: cloning and expression in *Saccharomyces cerevisiae* and biochemical characterization of the recombinant enzyme. *Microbiology* **140 (Pt 7)**, 1533-1542

109. Bockmuhl, D. P., Krishnamurthy, S., Gerads, M., Sonneborn, A., and Ernst, J. F. (2001) Distinct and redundant roles of the two protein kinase A isoforms Tpk1p and Tpk2p in morphogenesis and growth of *Candida albicans*. *Molecular microbiology* **42**, 1243-1257
110. Sonneborn, A., Bockmuhl, D. P., Gerads, M., Kurpanek, K., Sanglard, D., and Ernst, J. F. (2000) Protein kinase A encoded by TPK2 regulates dimorphism of *Candida albicans*. *Molecular microbiology* **35**, 386-396
111. Goldberg, D., Marbach, I., Gross, E., Levitzki, A., and Simchen, G. (1993) A *Candida albicans* homolog of CDC25 is functional in *Saccharomyces cerevisiae*. *Eur J Biochem* **213**, 195-204
112. Enloe, B., Diamond, A., and Mitchell, A. P. (2000) A single-transformation gene function test in diploid *Candida albicans*. *Journal of bacteriology* **182**, 5730-5736
113. Scaduto, C. M., Kabrawala, S., Thomson, G. J., Scheving, W., Ly, A., Anderson, M. Z., Whiteway, M., and Bennett, R. J. (2017) Epigenetic control of pheromone MAPK signaling determines sexual fecundity in *Candida albicans*. *Proceedings of the National Academy of Sciences of the United States of America* **114**, 13780-13785
114. Csank, C., Schroppel, K., Leberer, E., Harcus, D., Mohamed, O., Meloche, S., Thomas, D. Y., and Whiteway, M. (1998) Roles of the *Candida albicans* mitogen-activated protein kinase homolog, Cek1p, in hyphal development and systemic candidiasis. *Infection and immunity* **66**, 2713-2721
115. Hope, H., Schmauch, C., Arkowitz, R. A., and Bassilana, M. (2010) The *Candida albicans* ELMO homologue functions together with Rac1 and Dck1, upstream of the MAP Kinase Cek1, in invasive filamentous growth. *Molecular microbiology* **76**, 1572-1590
116. Leberer, E., Harcus, D., Broadbent, I. D., Clark, K. L., Dignard, D., Ziegelbauer, K., Schmidt, A., Gow, N. A., Brown, A. J., and Thomas, D. Y. (1996) Signal transduction through homologs of the Ste20p and Ste7p protein kinases can trigger hyphal formation in the pathogenic fungus *Candida albicans*. *Proceedings of the National Academy of Sciences of the United States of America* **93**, 13217-13222
117. Csank, C., Makris, C., Meloche, S., Schroppel, K., Rollinghoff, M., Dignard, D., Thomas, D. Y., and Whiteway, M. (1997) Derepressed hyphal growth and reduced virulence in a VH1 family-related protein phosphatase mutant of the human pathogen *Candida albicans*. *Molecular biology of the cell* **8**, 2539-2551
118. Kohler, J. R., and Fink, G. R. (1996) *Candida albicans* strains heterozygous and homozygous for mutations in mitogen-activated protein kinase signaling components have defects in hyphal development. *Proceedings of the National Academy of Sciences of the United States of America* **93**, 13223-13228
119. Shapiro, R. S., Robbins, N., and Cowen, L. E. (2011) Regulatory circuitry governing fungal development, drug resistance, and disease. *Microbiol Mol Biol Rev* **75**, 213-267
120. Magee, B. B., Legrand, M., Alarco, A. M., Raymond, M., and Magee, P. T. (2002) Many of the genes required for mating in *Saccharomyces cerevisiae* are also required for mating in *Candida albicans*. *Molecular microbiology* **46**, 1345-1351
121. Bennett, R. J., Uhl, M. A., Miller, M. G., and Johnson, A. D. (2003) Identification and characterization of a *Candida albicans* mating pheromone. *Mol Cell Biol* **23**, 8189-8201
122. Chen, J., Wang, Q., and Chen, J. Y. (2000) CEK2, a Novel MAPK from *Candida albicans* Complement the Mating Defect of *fus3/kss1* Mutant. *Sheng Wu Hua Xue Yu Sheng Wu Wu Li Xue Bao (Shanghai)* **32**, 299-304

123. Whiteway, M., Dignard, D., and Thomas, D. Y. (1992) Dominant negative selection of heterologous genes: isolation of *Candida albicans* genes that interfere with *Saccharomyces cerevisiae* mating factor-induced cell cycle arrest. *Proceedings of the National Academy of Sciences of the United States of America* **89**, 9410-9414
124. Chen, J., Chen, J., Lane, S., and Liu, H. (2002) A conserved mitogen-activated protein kinase pathway is required for mating in *Candida albicans*. *Molecular microbiology* **46**, 1335-1344
125. Herrero de Dios, C., Roman, E., Diez, C., Alonso-Monge, R., and Pla, J. (2013) The transmembrane protein Opy2 mediates activation of the Cek1 MAP kinase in *Candida albicans*. *Fungal genetics and biology : FG & B* **50**, 21-32
126. Roman, E., Cottier, F., Ernst, J. F., and Pla, J. (2009) Msb2 signaling mucin controls activation of Cek1 mitogen-activated protein kinase in *Candida albicans*. *Eukaryotic cell* **8**, 1235-1249
127. Monge, R. A., Roman, E., Nombela, C., and Pla, J. (2006) The MAP kinase signal transduction network in *Candida albicans*. *Microbiology* **152**, 905-912
128. Raitt, D. C., Posas, F., and Saito, H. (2000) Yeast Cdc42 GTPase and Ste20 PAK-like kinase regulate Sho1-dependent activation of the Hog1 MAPK pathway. *The EMBO journal* **19**, 4623-4631
129. Ushinsky, S. C., Harcus, D., Ash, J., Dignard, D., Marcil, A., Morchhauser, J., Thomas, D. Y., Whiteway, M., and Leberer, E. (2002) CDC42 is required for polarized growth in human pathogen *Candida albicans*. *Eukaryotic cell* **1**, 95-104
130. Roman, E., Nombela, C., and Pla, J. (2005) The Sho1 adaptor protein links oxidative stress to morphogenesis and cell wall biosynthesis in the fungal pathogen *Candida albicans*. *Mol Cell Biol* **25**, 10611-10627
131. Posas, F., and Saito, H. (1997) Osmotic activation of the HOG MAPK pathway via Ste11p MAPKKK: scaffold role of Pbs2p MAPKK. *Science* **276**, 1702-1705
132. Smith, D. A., Nicholls, S., Morgan, B. A., Brown, A. J., and Quinn, J. (2004) A conserved stress-activated protein kinase regulates a core stress response in the human pathogen *Candida albicans*. *Molecular biology of the cell* **15**, 4179-4190
133. Alonso-Monge, R., Navarro-Garcia, F., Molero, G., Diez-Orejas, R., Gustin, M., Pla, J., Sanchez, M., and Nombela, C. (1999) Role of the mitogen-activated protein kinase Hog1p in morphogenesis and virulence of *Candida albicans*. *Journal of bacteriology* **181**, 3058-3068
134. Arana, D. M., Nombela, C., Alonso-Monge, R., and Pla, J. (2005) The Pbs2 MAP kinase kinase is essential for the oxidative-stress response in the fungal pathogen *Candida albicans*. *Microbiology* **151**, 1033-1049
135. Calera, J. A., Zhao, X. J., and Calderone, R. (2000) Defective hyphal development and avirulence caused by a deletion of the SSK1 response regulator gene in *Candida albicans*. *Infection and immunity* **68**, 518-525
136. Gomez-Raja, J. D., D.A. (2012) The beta-arrestin-like protein Rim8 is hyperphosphorylated and complexes with Rim21 and Rim101 to promote adaptation to neutral-alkaline pH. *Eukaryotic cell*, 683-693

137. Wolf, J. M., Johnson, D. J., Chmielewski, D., and Davis, D. A. (2010) The Candida albicans ESCRT pathway makes Rim101-dependent and -independent contributions to pathogenesis. *Eukaryotic cell* **9**, 1203-1215
138. Li, M., Martin, S. J., Bruno, V. M., Mitchell, A. P., and Davis, D. A. (2004) Candida albicans Rim13p, a protease required for Rim101p processing at acidic and alkaline pHs. *Eukaryotic cell* **3**, 741-751
139. Davis, D., Wilson, R. B., and Mitchell, A. P. (2000) RIM101-dependent and-independent pathways govern pH responses in Candida albicans. *Mol Cell Biol* **20**, 971-978
140. Lu, Y., Su, C., Solis, N. V., Filler, S. G., and Liu, H. (2013) Synergistic regulation of hyphal elongation by hypoxia, CO₂, and nutrient conditions controls the virulence of Candida albicans. *Cell host & microbe* **14**, 499-509
141. Bastidas, R. J., Heitman, J., and Cardenas, M. E. (2009) The protein kinase Tor1 regulates adhesin gene expression in Candida albicans. *PLoS pathogens* **5**, e1000294
142. Stoldt, V. R., Sonneborn, A., Leuker, C. E., and Ernst, J. F. (1997) Efg1p, an essential regulator of morphogenesis of the human pathogen Candida albicans, is a member of a conserved class of bHLH proteins regulating morphogenetic processes in fungi. *The EMBO journal* **16**, 1982-1991
143. Sonneborn, A., Tebarth, B., and Ernst, J. F. (1999) Control of white-opaque phenotypic switching in Candida albicans by the Efg1p morphogenetic regulator. *Infection and immunity* **67**, 4655-4660
144. Sonneborn, A., Bockmuhl, D. P., and Ernst, J. F. (1999) Chlamydospore formation in Candida albicans requires the Efg1p morphogenetic regulator. *Infection and immunity* **67**, 5514-5517
145. Doedt, T., Krishnamurthy, S., Bockmuhl, D. P., Tebarth, B., Stempel, C., Russell, C. L., Brown, A. J., and Ernst, J. F. (2004) APSES proteins regulate morphogenesis and metabolism in Candida albicans. *Molecular biology of the cell* **15**, 3167-3180
146. Tebarth, B., Doedt, T., Krishnamurthy, S., Weide, M., Monterola, F., Dominguez, A., and Ernst, J. F. (2003) Adaptation of the Efg1p morphogenetic pathway in Candida albicans by negative autoregulation and PKA-dependent repression of the EFG1 gene. *Journal of molecular biology* **329**, 949-962
147. Zhao, Y., Su, H., Zhou, J., Feng, H., Zhang, K. Q., and Yang, J. (2015) The APSES family proteins in fungi: Characterizations, evolution and functions. *Fungal genetics and biology : FG & B* **81**, 271-280
148. Pierce, J. V., Dignard, D., Whiteway, M., and Kumamoto, C. A. Normal adaptation of Candida albicans to the murine gastrointestinal tract requires Efg1p-dependent regulation of metabolic and host defense genes. *Eukaryotic cell* **12**, 37-49
149. Pierce, J. V., and Kumamoto, C. A. Variation in Candida albicans EFG1 expression enables host-dependent changes in colonizing fungal populations. *mBio* **3**, e00117-00112
150. Rosenbach, A., Dignard, D., Pierce, J. V., Whiteway, M., and Kumamoto, C. A. (2010) Adaptations of Candida albicans for growth in the mammalian intestinal tract. *Eukaryotic cell* **9**, 1075-1086
151. Homann, O. R., Dea, J., Noble, S. M., and Johnson, A. D. (2009) A phenotypic profile of the Candida albicans regulatory network. *PLoS genetics* **5**, e1000783

152. Davidson, I., Xiao, J. H., Rosales, R., Staub, A., and Chambon, P. (1988) The HeLa cell protein TEF-1 binds specifically and cooperatively to two SV40 enhancer motifs of unrelated sequence. *Cell* **54**, 931-942
153. Jacquemin, P., Hwang, J. J., Martial, J. A., Dolle, P., and Davidson, I. (1996) A novel family of developmentally regulated mammalian transcription factors containing the TEA/ATTS DNA binding domain. *J Biol Chem* **271**, 21775-21785
154. Burglin, T. R. (1991) The TEA domain: a novel, highly conserved DNA-binding motif. *Cell* **66**, 11-12
155. Wolfe, S. A., Nekludova, L., and Pabo, C. O. (2000) DNA recognition by Cys2His2 zinc finger proteins. *Annu Rev Biophys Biomol Struct* **29**, 183-212
156. Scazzocchio, C. (2000) The fungal GATA factors. *Curr Opin Microbiol* **3**, 126-131
157. MacPherson, S., Larochelle, M., and Turcotte, B. (2006) A fungal family of transcriptional regulators: the zinc cluster proteins. *Microbiol Mol Biol Rev* **70**, 583-604
158. Schweizer, A., Rupp, S., Taylor, B. N., Rollinghoff, M., and Schroppel, K. (2000) The TEA/ATTS transcription factor CaTec1p regulates hyphal development and virulence in *Candida albicans*. *Molecular microbiology* **38**, 435-445
159. Nobile, C. J., and Mitchell, A. P. (2005) Regulation of cell-surface genes and biofilm formation by the *C. albicans* transcription factor Bcr1p. *Current biology : CB* **15**, 1150-1155
160. Cleary, I. A., Lazzell, A. L., Monteagudo, C., Thomas, D. P., and Saville, S. P. (2012) BRG1 and NRG1 form a novel feedback circuit regulating *Candida albicans* hypha formation and virulence. *Molecular microbiology* **85**, 557-573
161. Lu, Y., Su, C., and Liu, H. (2012) A GATA transcription factor recruits Hda1 in response to reduced Tor1 signaling to establish a hyphal chromatin state in *Candida albicans*. *PLoS pathogens* **8**, e1002663
162. Du, H., Guan, G., Xie, J., Sun, Y., Tong, Y., Zhang, L., and Huang, G. (2012) Roles of *Candida albicans* Gat2, a GATA-type zinc finger transcription factor, in biofilm formation, filamentous growth and virulence. *PLoS one* **7**, e29707
163. Nobile, C. J., Fox, E. P., Nett, J. E., Sorrells, T. R., Mitrovich, Q. M., Hernday, A. D., Tuch, B. B., Andes, D. R., and Johnson, A. D. (2012) A recently evolved transcriptional network controls biofilm development in *Candida albicans*. *Cell* **148**, 126-138
164. Lohse, M. B., Ene, I. V., Craik, V. B., Hernday, A. D., Mancera, E., Morschhäuser, J., Bennett, R. J., and Johnson, A. D. (2016) Systematic Genetic Screen for Transcriptional Regulators of the *Candida albicans* White-Opaque Switch. *Genetics* **203**, 1679-1692
165. Maicas, S., Moreno, I., Nieto, A., Gomez, M., Sentandreu, R., and Valentin, E. (2005) In silico analysis for transcription factors with Zn(II)(2)C(6) binuclear cluster DNA-binding domains in *Candida albicans*. *Comp Funct Genomics* **6**, 345-356
166. Zeidler, U., Lettner, T., Lassnig, C., Muller, M., Lajko, R., Hintner, H., Breitenbach, M., and Bito, A. (2009) UME6 is a crucial downstream target of other transcriptional regulators of true hyphal development in *Candida albicans*. *FEMS yeast research* **9**, 126-142
167. Banerjee, M., Uppuluri, P., Zhao, X. R., Carlisle, P. L., Vipulanandan, G., Villar, C. C., Lopez-Ribot, J. L., and Kadosh, D. (2013) Expression of UME6, a key regulator of *Candida albicans* hyphal development, enhances biofilm formation via Hgc1- and Sun41-dependent mechanisms. *Eukaryotic cell* **12**, 224-232

168. Rubin-Bejerano, I., Sagee, S., Friedman, O., Pnueli, L., and Kassir, Y. (2004) The in vivo activity of Ime1, the key transcriptional activator of meiosis-specific genes in *Saccharomyces cerevisiae*, is inhibited by the cyclic AMP/protein kinase A signal pathway through the glycogen synthase kinase 3-beta homolog Rim11. *Mol Cell Biol* **24**, 6967-6979
169. Langford, M. L., Hargarten, J. C., Patefield, K. D., Marta, E., Blankenship, J. R., Fanning, S., Nickerson, K. W., and Atkin, A. L. (2013) *Candida albicans* Czf1 and Efg1 coordinate the response to farnesol during quorum sensing, white-opaque thermal dimorphism, and cell death. *Eukaryotic cell* **12**, 1281-1292
170. Polke, M., Sprenger, M., Scherlach, K., Alban-Proano, M. C., Martin, R., Hertweck, C., Hube, B., and Jacobsen, I. D. (2017) A functional link between hyphal maintenance and quorum sensing in *Candida albicans*. *Molecular microbiology* **103**, 595-617
171. Kadosh, D., and Johnson, A. D. (2001) Rfg1, a protein related to the *Saccharomyces cerevisiae* hypoxic regulator Rox1, controls filamentous growth and virulence in *Candida albicans*. *Mol Cell Biol* **21**, 2496-2505
172. Braun, B. R., and Johnson, A. D. (1997) Control of filament formation in *Candida albicans* by the transcriptional repressor TUP1. *Science* **277**, 105-109
173. Murad, A. M., d'Enfert, C., Gaillardin, C., Tournu, H., Tekaiia, F., Talibi, D., Marechal, D., Marchais, V., Cottin, J., and Brown, A. J. (2001) Transcript profiling in *Candida albicans* reveals new cellular functions for the transcriptional repressors CaTup1, CaMig1 and CaNrg1. *Molecular microbiology* **42**, 981-993
174. Banerjee, M., Thompson, D. S., Lazzell, A., Carlisle, P. L., Pierce, C., Monteagudo, C., Lopez-Ribot, J. L., and Kadosh, D. (2008) UME6, a novel filament-specific regulator of *Candida albicans* hyphal extension and virulence. *Molecular biology of the cell* **19**, 1354-1365
175. Nguyen, V. Q., and Sil, A. (2008) Temperature-induced switch to the pathogenic yeast form of *Histoplasma capsulatum* requires Ryp1, a conserved transcriptional regulator. *Proceedings of the National Academy of Sciences of the United States of America* **105**, 4880-4885
176. Lohse, M. B., Zordan, R. E., Cain, C. W., and Johnson, A. D. (2010) Distinct class of DNA-binding domains is exemplified by a master regulator of phenotypic switching in *Candida albicans*. *Proceedings of the National Academy of Sciences of the United States of America* **107**, 14105-14110
177. Pan, X., and Heitman, J. (2000) Sok2 regulates yeast pseudohyphal differentiation via a transcription factor cascade that regulates cell-cell adhesion. *Mol Cell Biol* **20**, 8364-8372
178. Dutton, J. R., Johns, S., and Miller, B. L. (1997) StuAp is a sequence-specific transcription factor that regulates developmental complexity in *Aspergillus nidulans*. *The EMBO journal* **16**, 5710-5721
179. Aramayo, R., Peleg, Y., Addison, R., and Metzzenberg, R. (1996) Asm-1+, a *Neurospora crassa* gene related to transcriptional regulators of fungal development. *Genetics* **144**, 991-1003
180. Michielse, C. B., Becker, M., Heller, J., Moraga, J., Collado, I. G., and Tudzynski, P. (2011) The *Botrytis cinerea* Reg1 protein, a putative transcriptional regulator, is required for pathogenicity, conidiogenesis, and the production of secondary metabolites. *Mol Plant Microbe Interact* **24**, 1074-1085

181. Zordan, R. E., Miller, M. G., Galgoczy, D. J., Tuch, B. B., and Johnson, A. D. (2007) Interlocking transcriptional feedback loops control white-opaque switching in *Candida albicans*. *PLoS biology* **5**, e256
182. Lassak, T., Schneider, E., Bussmann, M., Kurtz, D., Manak, J. R., Srikantha, T., Soll, D. R., and Ernst, J. F. (2011) Target specificity of the *Candida albicans* Efg1 regulator. *Molecular microbiology* **82**, 602-618
183. Wang, H., Song, W., Huang, G., Zhou, Z., Ding, Y., and Chen, J. *Candida albicans* Zcf37, a zinc finger protein, is required for stabilization of the white state. *FEBS Lett* **585**, 797-802
184. Lohse, M. B., Hernday, A. D., Fordyce, P. M., Noiman, L., Sorrells, T. R., Hanson-Smith, V., Nobile, C. J., DeRisi, J. L., and Johnson, A. D. Identification and characterization of a previously undescribed family of sequence-specific DNA-binding domains. *Proceedings of the National Academy of Sciences of the United States of America* **110**, 7660-7665
185. Hernday, A. D., Lohse, M. B., Nobile, C. J., Noiman, L., Laksana, C. N., and Johnson, A. D. (2016) Ssn6 Defines a New Level of Regulation of White-Opaque Switching in *Candida albicans* and Is Required For the Stochasticity of the Switch. *mBio* **7**
186. Lohse, M. B., and Johnson, A. D. (2016) Identification and Characterization of Wor4, a New Transcriptional Regulator of White-Opaque Switching. *G3 (Bethesda)* **6**, 721-729
187. Vinces, M. D., and Kumamoto, C. A. (2007) The morphogenetic regulator Czf1p is a DNA-binding protein that regulates white opaque switching in *Candida albicans*. *Microbiology* **153**, 2877-2884
188. Petrovska, I., and Kumamoto, C. A. (2012) Functional importance of the DNA binding activity of *Candida albicans* Czf1p. *PloS one* **7**, e39624
189. Vandeputte, P., Ischer, F., Sanglard, D., and Coste, A. T. (2011) In vivo systematic analysis of *Candida albicans* Zn2-Cys6 transcription factors mutants for mice organ colonization. *PloS one* **6**, e26962
190. Vylkova, S., and Lorenz, M. C. (2017) Phagosomal Neutralization by the Fungal Pathogen *Candida albicans* Induces Macrophage Pyroptosis. *Infection and immunity* **85**
191. Singh, R. P., Prasad, H. K., Sinha, I., Agarwal, N., and Natarajan, K. (2011) Cap2-HAP complex is a critical transcriptional regulator that has dual but contrasting roles in regulation of iron homeostasis in *Candida albicans*. *J Biol Chem* **286**, 25154-25170
192. Tong, Y., Cao, C., Xie, J., Ni, J., Guan, G., Tao, L., Zhang, L., and Huang, G. (2014) N-acetylglucosamine-induced white-to-opaque switching in *Candida albicans* is independent of the Wor2 transcription factor. *Fungal genetics and biology : FG & B* **62**, 71-77
193. Bohm, L., Torsin, S., Tint, S. H., Eckstein, M. T., Ludwig, T., and Perez, J. C. (2017) The yeast form of the fungus *Candida albicans* promotes persistence in the gut of gnotobiotic mice. *PLoS pathogens* **13**, e1006699
194. Garcia-Sanchez, S., Mavor, A. L., Russell, C. L., Argimon, S., Dennison, P., Enjalbert, B., and Brown, A. J. (2005) Global roles of Ssn6 in Tup1- and Nrg1-dependent gene regulation in the fungal pathogen, *Candida albicans*. *Molecular biology of the cell* **16**, 2913-2925
195. Keleher, C. A., Redd, M. J., Schultz, J., Carlson, M., and Johnson, A. D. (1992) Ssn6-Tup1 is a general repressor of transcription in yeast. *Cell* **68**, 709-719

196. Lee, J. E., Oh, J. H., Ku, M., Kim, J., Lee, J. S., and Kang, S. O. (2015) Ssn6 has dual roles in *Candida albicans* filament development through the interaction with Rpd31. *FEBS Lett* **589**, 513-520
197. Hwang, C. S., Oh, J. H., Huh, W. K., Yim, H. S., and Kang, S. O. (2003) Ssn6, an important factor of morphological conversion and virulence in *Candida albicans*. *Molecular microbiology* **47**, 1029-1043

Chapter 2. Regulation of yeast-to-hypha switch is an important determinant of *C. albicans* commensal fitness

2.1. Introduction

Candida albicans is the most common fungal pathogen of humans, causing hundreds of millions of symptomatic infections each year across the globe (1,2). Disease syndromes range from superficial, treatable infections of skin, nails, and mucous membranes to highly morbid, invasive diseases involving blood and internal organs (1,3,4). More typically, however, this fungus resides as a benign component of mammalian gut, skin, and genitourinary microbiota. *C. albicans* is exquisitely adapted to mammals such that, unlike the vast majority of fungi, it appears to lack environmental niches outside these hosts. Humans are typically colonized in childhood, and infecting fungal clones persist for years or even the lifetime of the host (2). Importantly, fungal cells from the commensal reservoir are the primary source of symptomatic disease (2).

C. albicans's ability to switch between yeast and hypha morphologies is its best known virulence attribute (5). Under standard *in vitro* conditions, *C. albicans* propagates as round-to-oval, single-celled yeasts. However, exposure to host-associated cues can trigger profound changes in the fungal cell cycle, cell morphology, and gene expression that collectively constitute the yeast-to-hypha transition. Hyphal cells are highly elongated cells that remain joined together following cell division, with the capacity to form complex, filamentous structures. Unlike yeasts, hyphae are intrinsically invasive and penetrate agar-based media in the laboratory. Within the host, hyphae enter epithelial and endothelial cells by a receptor-mediated induced uptake mechanism (reviewed in (6)), as well as active penetration (7). Hypha-specific virulence factors include degradative enzymes (such as the Sap family of secreted aspartyl proteases (reviewed in (8)), cell surface adhesins (such as Als3, Hwp1, and Hyr1 (9-12)), and the pore-forming toxin, Candidalysin (Ece1, (13)). Further supporting the tight connection between yeast-to-hypha morphogenesis and virulence, the majority of *C. albicans* mutants that exhibit strong filamentation

defects *in vitro* are also defective in animal models of localized and systemic disease ((14,15), as reviewed in (16)).

Cues for *in vitro* induction of yeast-to-hypha morphogenesis include mammalian body temperature (37°C), mammalian serum, N-acetylglucosamine, nutrient starvation, elevated CO₂, hypoxia, and alkaline pH (17-20). These signals are transduced by a network of fungal signaling pathways that terminate on specific transcription factors. The transcription factors, in turn, activate or inhibit genes that control the cell cycle, cell morphology, and genes that are expressed preferentially in either yeasts or hyphae. Among the pro-filamentation transcription factors, Ume6 plays a prominent role as a common downstream target of multiple signaling pathways (21) that is both necessary and sufficient for hypha formation *in vitro* (22).

In contrast to the positive relationship between *C. albicans* filamentation and virulence, far less is known of the impact of filamentation on fungal commensalism. Certain data support a special role for yeasts (versus hyphae) in the mammalian digestive tract. For example, two groups reported that yeasts are the primary colonizers of this niche, based on direct visual inspection of organisms recovered from the intestines of colonized mice (23,24). Moreover, a strain that overexpresses *UME6* is attenuated in the GI colonization model (24), whereas deletion of *EFG1*, encoding a different pro-filamentation transcription factor, confers a strong gain-of-fitness phenotype (25-27). At odds with these results, however, is the strong induction of several hypha-associated genes, including ones for virulence factors such as Ece1 and Als3, in wild-type strains propagated in the mammalian GI tract (28). It remains unclear why virulence factors would be expressed in the primary niche of commensalism and why, if yeasts truly predominate in this space, this cell type would express factors that are normally associated with hyphae.

To further characterize *C. albicans* commensalism, we performed unbiased screens of libraries comprising ~750 fungal gene disruption mutants in a mouse model of stable gastrointestinal colonization of which ~650 were detectable in the inoculum sequencing library pool (see Methods for more details). Four mutants affecting transcription factors known to

activate filamentation (Efg1, Brg1, Rob1, and Tec1) exhibited significant gain-of-fitness phenotypes, as did a newly constructed *ume6* deletion mutant. To determine whether the competitive advantage of these mutants derives from altered cell morphology, we used fluorescence *in situ* hybridization (FISH) to visualize wild-type *C. albicans* and the *ume6* mutant in the host GI tract. Surprisingly, the two strains colonize the gut as virtually indistinguishable, mixed populations of yeasts and hyphae, with yeasts predominating in proximal compartments (stomach and small intestines), and hyphae outnumbering yeasts more distally (cecum and large intestines). These observations suggest that hyphae are not intrinsically defective in colonization of the gut, that Ume6 is not required for the yeast-to-hypha transition *in vivo*, and that mutants affecting pro-filamentation transcription factors likely thrive within this niche because of differences in gene expression rather than altered cell morphology. Transcriptomic analysis revealed reduced expression of 36 hypha-associated genes in commensally propagated *ume6*. Remarkably, disruption of the *SAP6* gene, encoding a hypha-specific secreted aspartyl protease, confers a fitness advantage in the mouse GI colonization model. Together, our results suggest communication between *C. albicans* and mammalian hosts, with the fungus undergoing morphological transformations in different compartments of the host digestive tract, and the host actively curating the fungal population via antifungal responses to hypha-specific markers.

2.2. Results

2.2.1. Screens for C. albicans commensalism factors identify activators of filamentation

In a previous screen for *C. albicans* commensalism factors, we identified *efg1* as a hypercompetitive mutant among 48 co-infected strains (25). In that screen, the maximum number of strains that could be assessed in a single animal by qPCR was 48, limited by the number of unique DNA barcodes used to construct our homozygous gene knockout collection (29,30). We have now developed a linear PCR/high throughput sequencing-based protocol that permits

quantitation of larger pools of mutants by counting genomic sequences adjacent to each disrupted gene (described in Chapter 2.4. Methods).

Using the new method, we were able to test the competitive fitness of ~650 *C. albicans* mutants in a single pool using a mouse model of persistent gastrointestinal commensalism. Wild-type BALB/c mice were pretreated with antibiotics (penicillin and streptomycin) to partially clear the bacterial microbiota prior to direct installation of *C. albicans* yeasts into the stomach. Commensally infected animals remained healthy while harboring $\sim 2\text{-}5 \times 10^7$ CFU *C. albicans* per gram of GI contents. After collecting at multiple time points (see Table 2.1 for details), the competitive fitness of individual strains was calculated as the ratio of each strain's relative abundance after recovery from mouse feces compared to that in the infecting inoculum. To control for potential additional mutations that may have been introduced at the time of strain construction, two independent isolates of most strains were tested in separate inocula. Each mutant pool was recovered and sequenced from two to three animals.

The results of the first screen ("Screen 1") are presented in **Figures 2.1A** and **2.1B**. In this simultaneous test of every mutant in our collection as well as wild type, *efg1* emerged as the dominant strain in every animal. **Figure 2.1A** depicts the relative fitness of every strain in a representative animal, and **Figure 2.1B** depicts the results for *efg1* and wild-type in three animals infected with the same inoculum. The primary sequencing data are presented in **Table A.1**. Because all strains other than *efg1* were depleted from the population recovered from animals, it was not possible to determine the fitness of these other strains compared to each other, and therefore no mutants with loss of fitness phenotypes were identified. We therefore repeated the screen ("Screen 2"), this time using inocula from which *efg1* had been omitted. As shown in **Figure 2.1B**, two other hypercompetitive mutants, *brg1* and *rob1*, now dominated the population recovered from animals. In a final attempt to identify commensal regulators and effectors with reduced fitness phenotypes, we repeated the screen a third time ("Screen 3"), this time using

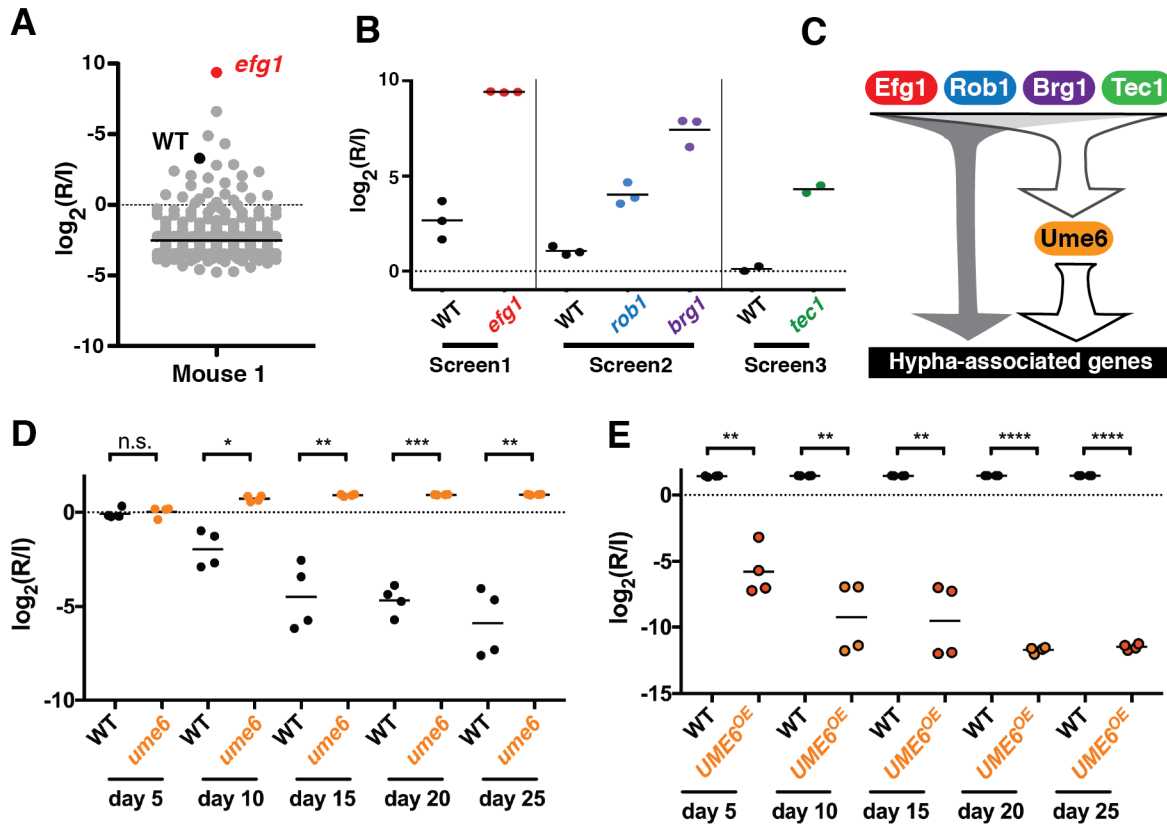


Figure 2.1. Filamentation defective mutants confer fitness advantage in GI commensal model. A. Relative abundance of all mutants in the feces from a single animal at day 10. R = recovered, I = inoculum. B. Relative abundances of selected mutants from screens compared to wild type. C. Model of transcriptional regulation of *C. albicans* yeast-to-hyphal transition. Regulatory model. Efg1 has been shown to act upstream of Ume6 via epistasis analysis and ChIP-seq (21,57). Brg1 and Tec1 binds upstream of Ume6 via ChIP-seq (33,58). Rob1 has not been shown to bind upstream of Ume6 (33). D. One-to-one commensal competition between wild type (WT, ySN250) and *ume6* (ySN1479). E. One-to-one competition between wild type (WT, ySN1555) and *UME6*-overexpression (*tetO-UME6*, ySN1557) strains. Paired student's t-test * $p < 0.05$, ** $p < 0.01$, *** $p < 0.001$, **** $p < 0.0001$.

inocula from which *efg1*, *brg1*, and *rob1* were omitted. As depicted in **Figure 2.1B**, a fourth hypercompetitive mutant, *tec1*, once again emerged from the screen.

The majority of mutants tested in this commensalism screen were previously assessed for virulence in a bloodstream infection model of disseminated disease. In that screen, in which mutants were competed in pools of 48, loss of fitness was the predominant mutant phenotype (29). To validate our results and to rule out the possibility that the hypercompetitive phenotypes exhibited by *efg1*, *brg1*, *rob1*, and *tec1* were an artifact of the large pool size, each mutant was

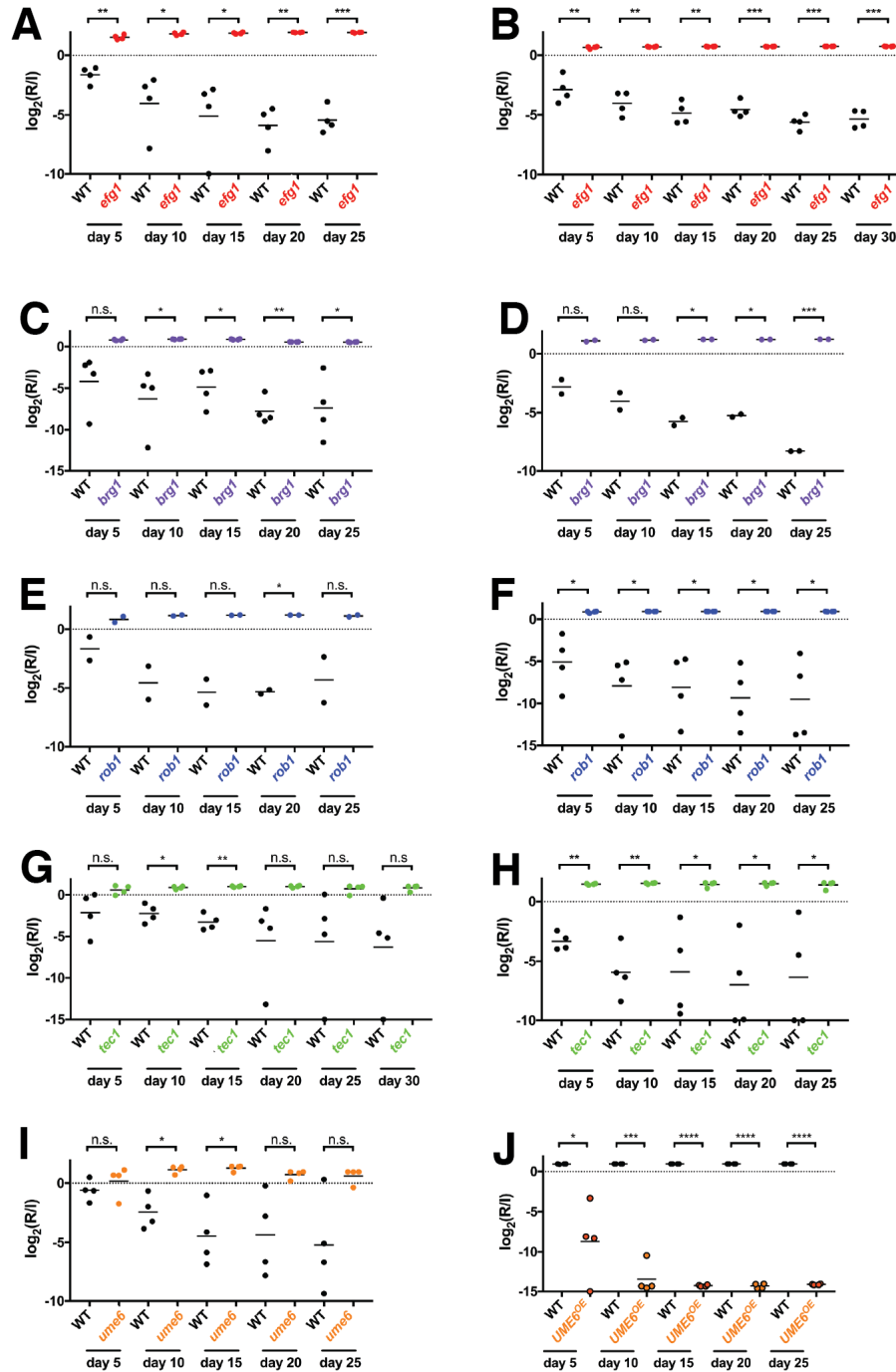


Figure 2.2. One-to-one competitions between wild-type and filamentation mutants confirms screen results. Relative abundances of strains recovered (R) from mouse feces compared to the inoculum (I) as determined by qPCR. A. Wild type (ySN250) versus *efg1* (ySN1011). B. Wild type (ySN226) versus *efg1* (ySN119). C. Wild type (ySN250) versus *brg1* (ySN1106). D. Wild type (ySN425) versus *brg1* (ySN1180). E. Wild type (ySN250) versus *rob1* (ySN1439). F. Wild type (ySN250) versus *rob1* (ySN1440). G. Wild type (ySN250) versus *tec1* (ySN1441). H. Wild type (ySN250) versus *tec1* (ySN1442). I. Wild type (ySN250) versus *ume6* (ySN1478). J. Wild type (ySN1556) versus *tetO-UME6* (ySN1558). Paired student's t-test * $p < 0.05$, ** $p < 0.01$, *** $p < 0.001$, **** $p < 0.0001$.

retested in a 1:1 competition with wild type, using qPCR and strain specific primers to determine the relative abundance of each strain. As shown in **Figure 2.2**, two independent isolates of all four mutants significantly outcompeted wild type in 1:1 competitions ($p < 0.05$ for most cases using the paired student's t-test), strongly validating the results of the genetic screens.

In our screens, fungal abundance in mouse feces was used to model abundance in the host GI tract. To verify the accuracy of this assumption, we determined the relative abundance of wild type and *brg1*, *rob1*, or *tec1* in the gut immediately after collecting the final specimens (from day 25) in the 1:1 competition experiments, above. Animals were humanely euthanized, and stomachs, small intestines, ceca, and large intestines were recovered using aseptic technique. Luminal contents were separated from tissues, and each sample was independently assessed to determine whether strains partition differentially in any compartment. As shown in **Figure 2.3**, the results in every specimen were largely identical to the results obtained with mouse feces, supporting the use of fecal specimens to monitor fungal colonization of the gut.

2.2.2. Transcriptional activators of filamentation inhibit commensal fitness

Remarkably, the four hyperfit mutants identified in our GI commensalism screen all affect transcription factors that are known to play important roles in *C. albicans* filamentation (described in 1.3.2., **Figure 2.1.C**; (5,30-34)). Numerous previous studies document substantial defects in the yeast-to-hypha transition of *efg1*, *brg1*, *rob1*, and *tec1* gene disruption mutants, and *efg1*, *brg1*, and *tec1* have also been shown to be defective for virulence in disseminated infection models (14,31,32). RNA expression and chromatin immunoprecipitation analyses indicate that all four transcription factors are required for normal activation of the genes associated with filamentation (33,35-37). Our independent identification of four components of the *C. albicans* filamentation program suggests that this program may play an additional role in the control of commensal fitness. To test this hypothesis, we created a *ume6* deletion strain, affecting a

transcription factor that has previously been reported to be necessary and sufficient for filamentation *in vitro* (**Figure 2.1C**; (21,22)). This mutant was not included in our original screens. As shown in **Figure 2.1.D**, the *ume6* mutant strongly outcompeted wild type in the GI commensalism model, like other deletion mutants affecting the pro-filamentation program. Conversely, as previously reported (24), a strain that overexpresses *UME6* in the absence of doxycycline (*UME6*^{OE}) exhibited a loss-of-fitness phenotype in the same model (**Figure 2.1E**). These results support a negative role for the *C. albicans* filamentation program in colonization of the mammalian gut.

2.2.3. *C. albicans* colonizes the GI tract as a mixed population of yeasts and filaments

Given previous reports that *C. albicans* colonizes the gut primarily in the yeast form (23,24), we hypothesized that yeasts might have a fitness advantage over hyphae and pseudohyphae in this niche, and that an increased ratio of yeasts to filaments might account for the hyperfit phenotype of the *efg1*, *brg1*, *rob1*, *tec1*, and *ume6* mutants. To test this idea, we developed a fluorescence *in situ* hybridization (FISH) protocol to visualize commensal *C. albicans* in the murine GI tract, based on a technique originally developed for the visualization of bacteria (38,39). Ten days after infection with a single *C. albicans* strain, a commensally infected mouse

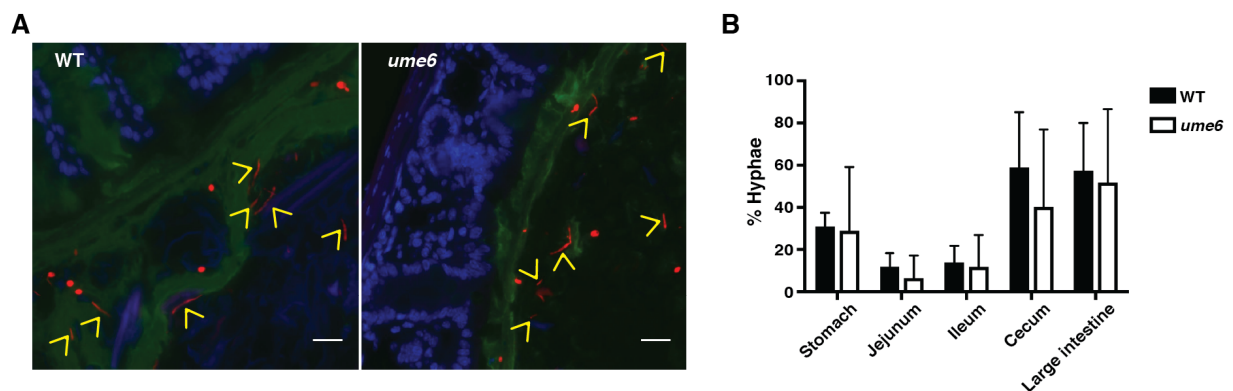


Figure 2.4. Fluorescent *in situ* hybridization (FISH) reveals similar morphological abundances between wild type and *ume6*. A. Fixed large intestine sections. WT = ySN250, *ume6* = ySN1479. Scale bar is 20 μ m. Yellow arrowheads highlight hyphae. Red = *C. albicans*, green = mucus, blue = nuclei. B. Quantification of *C. albicans* cell morphologies of 10 fields of each GI compartment from at least 5 animals each.

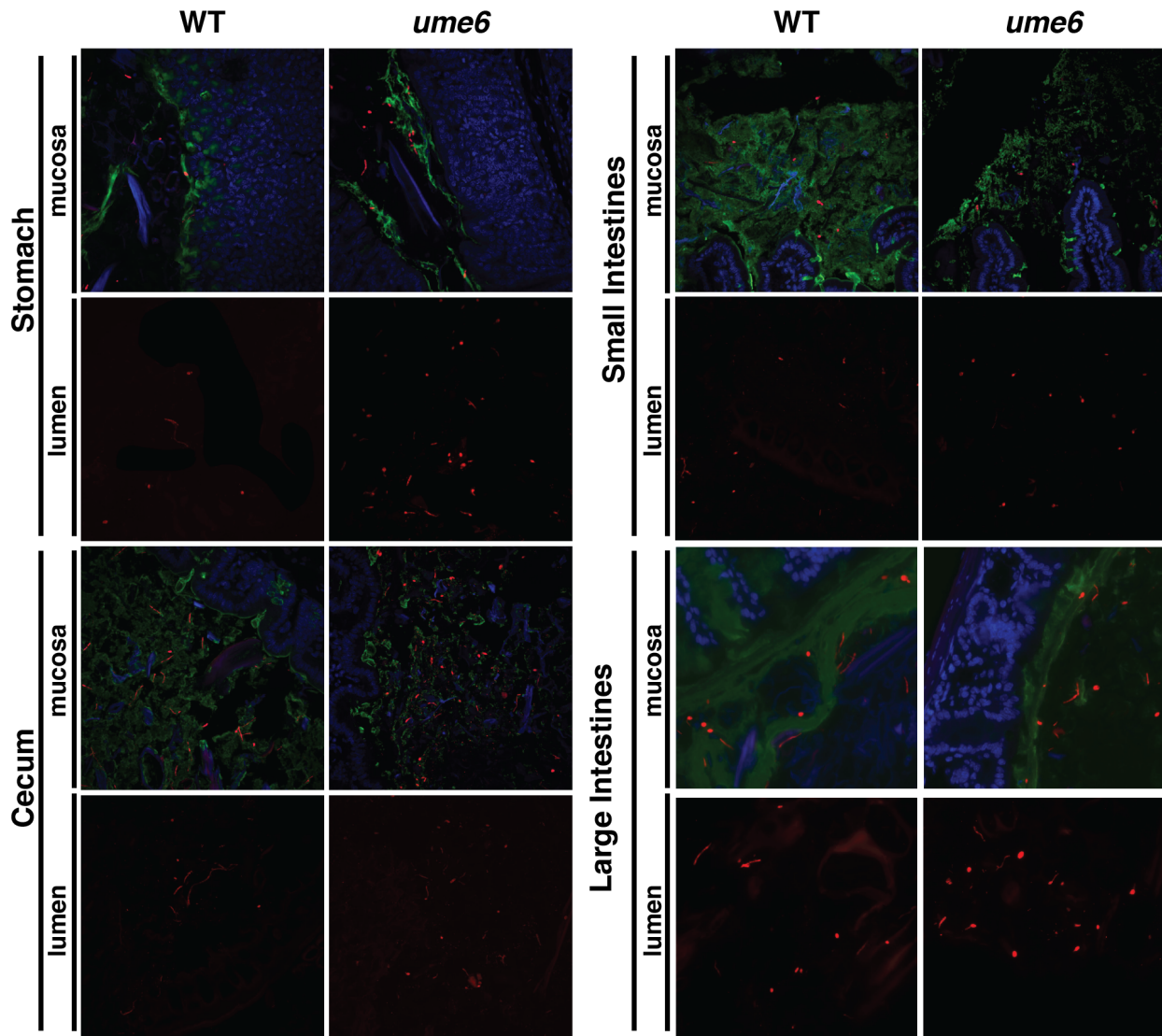


Figure 2.5. Representative FISH of GI compartments for wild type and *ume6* monotypic colonizations quantified in Figure 2.4.B. WT = ySN250, *ume6* = ySN1479. Scale bar is 20 μ m. Red = *C.albicans*, green = mucus, blue = nuclei.

is euthanized and the digestive tract fixed in methacarn, which preserves the architecture of luminal contents, including the mucus layer. Following embedding, sectioning, and dewaxing of the specimen, histological sections are hybridized to a fluorescein-coupled DNA oligonucleotide that hybridizes to fungal rRNA, which is distributed throughout the fungal cytoplasm.

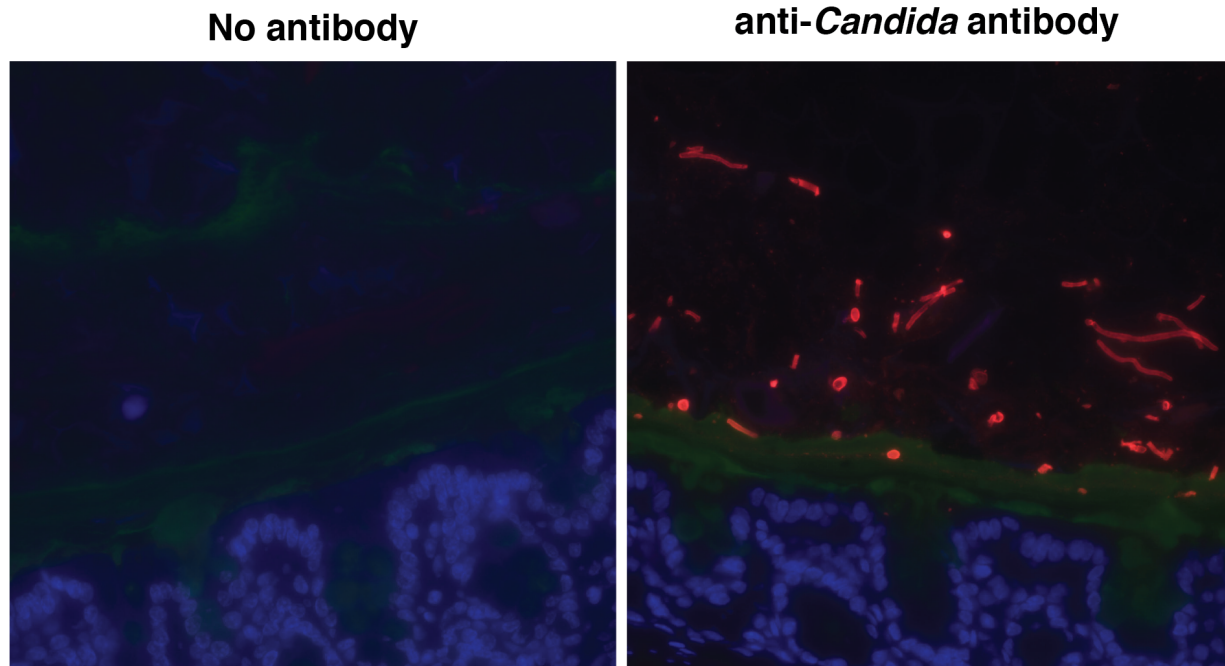


Figure 2.6. Alternative imaging of *C. albicans* in the large intestine using a polyclonal pan-fungal antibody used in previous studies (59,60). Left, *C. albicans*-infected without primary antibody. Right, *C. albicans*-infected with anti-*Candida* primary antibody.

Results for wild-type *C. albicans* are shown in **Figure 2.4.A,B** and **Figure 2.5**. Hyphae appeared thinner than expected, however, this is consistent with cytoplasmic staining when FISH staining is compared to staining using a previously described pan anti-fungal antibody to visualize fungi (**Figure 2.6**). As previously reported (23,24), we observed a preponderance of yeasts in the stomach, and jejunum and ileum of the small intestines, with filamentous forms making up only 30.8, and 11.8 and 13.8%, respectively, of the fungal population in these compartments (**Figure 2.4.B**). However, in the cecum and large intestines, filaments slightly outnumbered yeasts, making up 58.8 and 57.3% of the respective populations (**Figure 2.4.B**). Although previous researchers have not reported so many filamentous forms in the mammalian gut, most have focused on the ileum (the distal part of the small intestines) (23), where we also find that yeasts predominate. It is also possible that filaments were disproportionately lost during sample preparation in some previous studies, which examined *C. albicans* in extruded luminal contents,

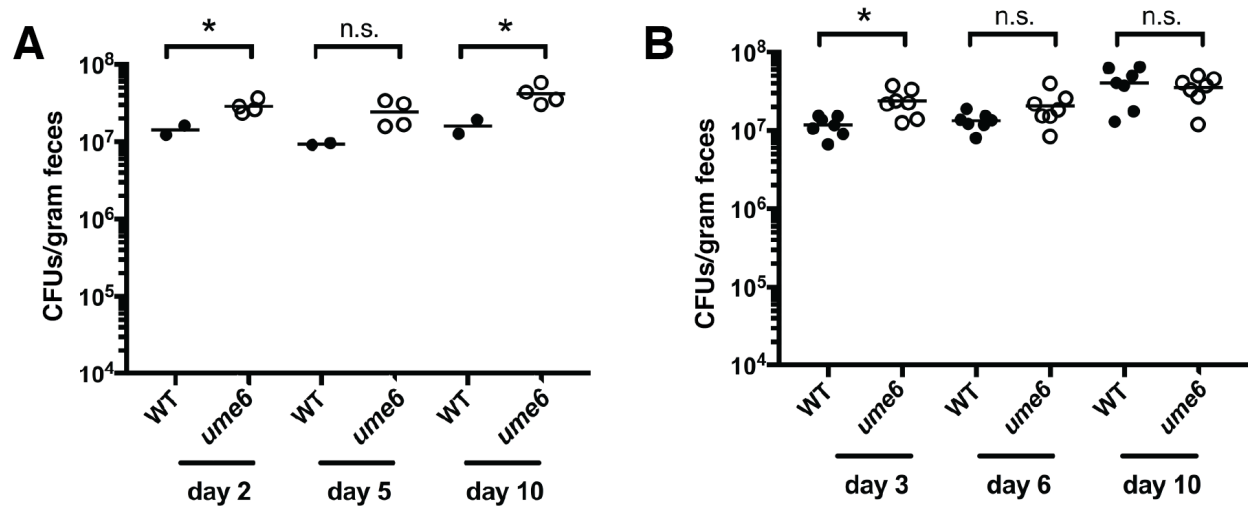


Figure 2.7. Gastrointestinal colonization of the feces in monotypic infections with wild type and *ume6*. Two different sets of monotypic infections of wild type or *ume6*. Unpaired student's t-test * $p < 0.05$.

after washing and filtering steps (23,24). Our results suggest that both yeasts and filaments colonize the mammalian gut, with the yeast form predominating in more proximal compartments and hyphae dominating more distally.

Results for the *ume6* mutant are shown in **Figure 2.4** and **Figure 2.5**. Remarkably, *ume6* colonizes the gut with virtually identical morphology to wild type. Although the absolute number of fungi is sometimes slightly higher in *ume6*-colonized animals (**Figure 2.7**), the proportion of yeasts and filaments is maintained, with hyphae in the minority in the stomach, jejunum, and ileum (28.8, 6.4 and 11.7%, respectively) but predominating in the cecum and large intestines (40.2 and 51.7%, respectively). The preserved ability of *ume6* to undergo the yeast-to-hypha transition within the host digestive tract contrasts sharply with its reported defect under *in vitro* hypha-inducing conditions (22), suggesting that hosts may contain hypha-inducing cues that are absent from the *in vitro* assay. Together, our FISH studies of wild-type *C. albicans* and *ume6* reveal that 1) both yeasts and hyphae are capable of colonizing the gut; 2) filamentation does not require Ume6 *in vivo*; and, therefore, 3) Ume6 suppresses *C. albicans* commensal fitness by a mechanism independent from morphology.

2.2.4. NanoString profiling of *C. albicans* gene expression in the GI tract reveals a strong hypha-specific response

If cell morphology *per se* does not determine *C. albicans* commensal fitness, we reasoned that cell type-specific genes expressed by yeasts vs. hyphae may influence their relative capacity to colonize the mammalian GI tract. We used NanoString to profile gene expression in wild-type *C. albicans* recovered from different regions of the murine gut colonization model over a 25-day time course. The method was selected because of its ability to accurately quantify small amounts of fungal RNA amid an excess of host and bacterial transcripts. In the initial experiment, we asked whether fungal RNA expression differed by GI compartment or by association with the gut lumen vs. the gut epithelium. Animals were colonized with wild-type *C. albicans* and euthanized after 10 days. Luminal contents were separated from tissues, and total RNA was prepared for each sample. NanoString was performed using 182 primer sets that detects transcripts for transcription factors as well as cell surface and secreted proteins whose expression is known to be triggered by environmental cues (40). The results are shown in **Figure 2.8**, expressed as a ratio of gene expression *in vivo* compared to log phase growth in rich laboratory medium. Overall, gene expression remained relatively stable throughout the gut, and there were no significant differences between transcripts expressed by fungi recovered from the lumen vs. those associated with host tissues. Based on these results, subsequent NanoString experiments were performed on whole compartments without separation.

We next wanted to know how *C. albicans* gene expression changed over time in the gut. Animals colonized with wild-type *C. albicans* were euthanized after 1, 4, 10, and 25 days (n=3 per

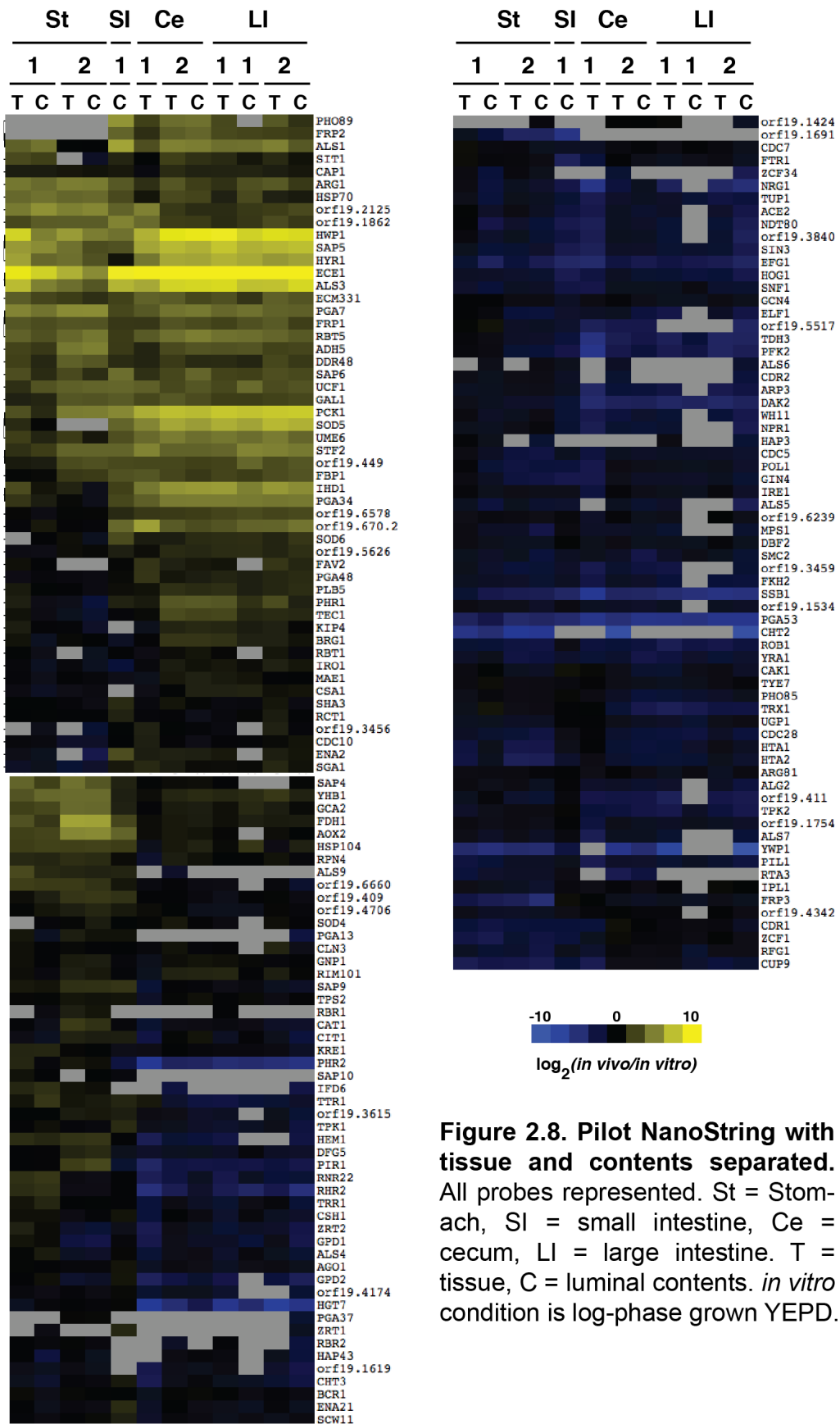


Figure 2.8. Pilot NanoString with tissue and contents separated. All probes represented. St = Stomach, SI = small intestine, Ce = cecum, LI = large intestine. T = tissue, C = luminal contents. *in vitro* condition is log-phase grown YEPD.

expression in both strains after recovery from the lumen of the large intestines (where *UME6* transcription is maximal in wild type, **Figure 2.9.A**). To our surprise, there were no significant differences in gene expression between the two strains in this niche, apart from *UME6* itself (data not shown).

2.2.5. RNA-seq reveals that *Ume6* controls a subset of hypha-specific genes during gut colonization

Whereas NanoString has the ability to detect very low abundance transcripts (such as those encoding transcription factors) in a complex mixture, a disadvantage is that a relatively expensive set of primers is required for each profiled gene, thereby limiting the number of genes that it is practical to evaluate. We hypothesized that *Ume6* might control the *in vivo* expression of genes that were not profiled in our NanoString analysis. To investigate global gene expression of wild type and *ume6* strains recovered from the murine large intestines, we turned to mRNA-seq, which quantifies all transcripts that are expressed to a threshold level. In a pilot experiment, we confirmed that we were able to detect *C. albicans* transcripts in the luminal contents of stomach, cecum and large intestine (**Figure 2.10**). Based on the expression in these compartments, *UME6* is highest in the cecum and large intestine. We hypothesized that *UME6* expression would have the largest effects in the large intestine and decided to focus on that compartment for the remainder of mRNA-seq experiments.

Experimental groups included wild-type and *ume6* strains propagated for 10 days in the murine commensal model (n=5 large intestine luminal contents per strain), as well as after *in vitro* propagation under standard conditions to an OD of 1 (YEPD liquid medium, 30°C, n=3 cultures) or hypha-inducing conditions for 5 hours (YEPD plus 10% bovine serum, 37°C, n=3 cultures).

Consistent with our hypothesis, global transcriptional profiling revealed multiple differences between wild type and *ume6* (**Figure 2.11**). In this setting, 116 genes are significantly downregulated in the *ume6* mutant compared to wild type (Table location described in Appendix).

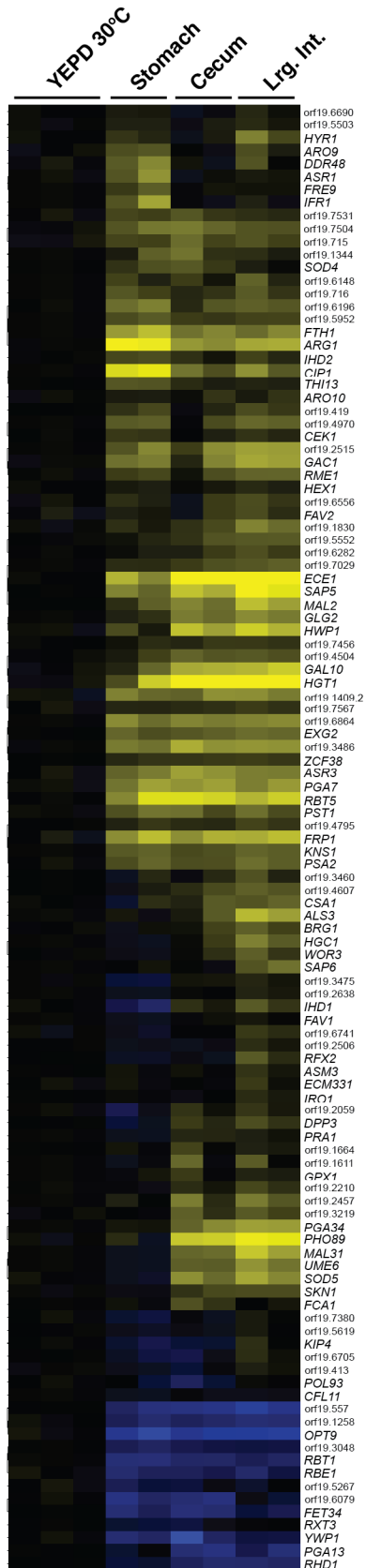


Figure 2.10. Pilot RNA-seq of the mouse GI compartments. mRNA-seq of stomach, cecum, and large intestine confirms NanoString results and use of RNA-seq as a viable method for studying *C. albicans* transcriptomes in the gut. Genes shown are those that are significantly changed under many different hyphal-inducing conditions as defined by Azadmanesh *et al.* (41) and mRNA-seq under hypha-inducing conditions (YEPD+10% serum at 37°C) from our lab.

Since all of the transcription factors we profiled affect the filamentation program, we hypothesized that filament-associated genes that do not impact morphology could be responsible for the commensal phenotype we observe. We defined hypha-induced transcripts as 131 transcripts that are upregulated or downregulated in wild-type *C. albicans* when propagated under hypha-inducing conditions compared to standard *in vitro* growth in our dataset that also showed substantial overlap with a recently published *in vitro* RNA-seq dataset comparing many different hypha-inducing conditions (all shown in **Figure 2.10**) (41). Within the *ume6* large intestine significantly downregulated set of genes, 32 were hypha-specific transcripts (**Figure 2.11.A**). Together with our finding that the *in vitro* filamentation defect of *ume6* is suppressed by propagation within the GI commensalism model, these results support the idea that redundant pathways are triggered within this niche that can at least partially compensate for the absence of Ume6.

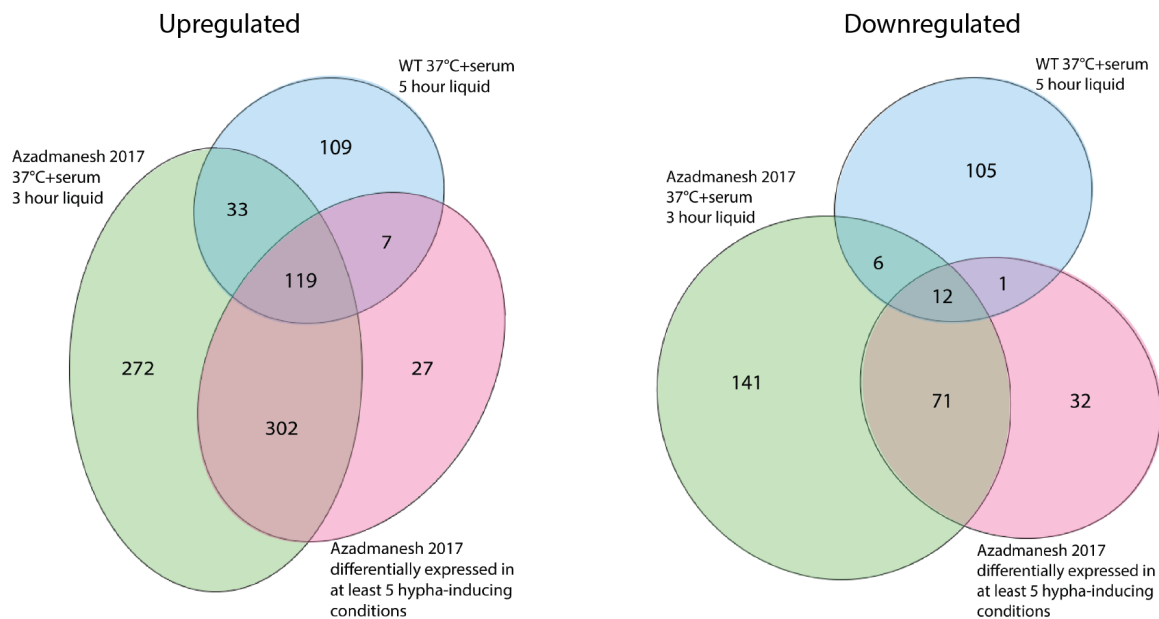


Figure 2.11. Overlap between published data sets (41) and mRNA-seq of wild type under hypha-inducing conditions. Genes filtered as significantly (adj. p-value < 0.05) upregulated or downregulated at least 2-fold. Hypha-specific gene filter defined as the overlap between all datasets.

2.2.6. A pro-inflammatory factor is detrimental to *C. albicans* commensal fitness

We hypothesized that some or all of the 32 filament-associated genes that are downregulated in *ume6* relative to wild-type in the GI commensal niche are responsible for the enhanced fitness phenotype of the former strain. To test this idea, we asked whether single gene knockouts of *SAP6*, encoding a secreted aspartyl protease, or *HYR1*, encoding a predicted GPI-anchored hypha cell wall protein, were also hypercompetitive in the GI commensalism model. Remarkably, both mutants—particularly *sap6*—exhibited enhanced fitness compared to wild type (**Figures 2.12.B and 2.13**). These results were reproduced with independent isolates of each mutant, and restoration of a single wild-type allele of the *SAP6* gene partially complemented the phenotype of *sap6* (**Figure 2.12.C**), supporting genetic linkage between the mutant phenotypes and the targeted gene disruptions. Overexpression of *SAP6* led to a loss of fitness consistent with the predicted effect (**Figure 2.12.D**).

To account for these results, we proposed a model in which *C. albicans* hyphae, which have well documented tissue invasive properties and are tightly associated with virulence, may be actively monitored by the host by means of hypha-specific gene products. That is, hypha-specific secreted factors such as Sap6 and hypha-specific cell wall proteins such as Hyr1 may be sensed by the host and may trigger local anti-fungal immune responses when they reach a certain threshold. In support of this concept, purified Sap6 has previously been shown to elicit pro-inflammatory immune responses from cultured murine macrophages and dendritic cells (42,43). These responses were independent of Sap6 protease activity and required host caspase-1 and caspase-11. To address the role for caspase-1/11 in modulating commensal fitness we will need to perform commensal competitions in caspase-1/11^{-/-} knockout animals. The microbiota of different mouse backgrounds or even from different facilities maintained by the same vendor has been shown to contribute to phenotypes seen for different microbes (see section 5.2.3). To limit these effects, we will first perform fecal transplants from our standard BALB/c animals into

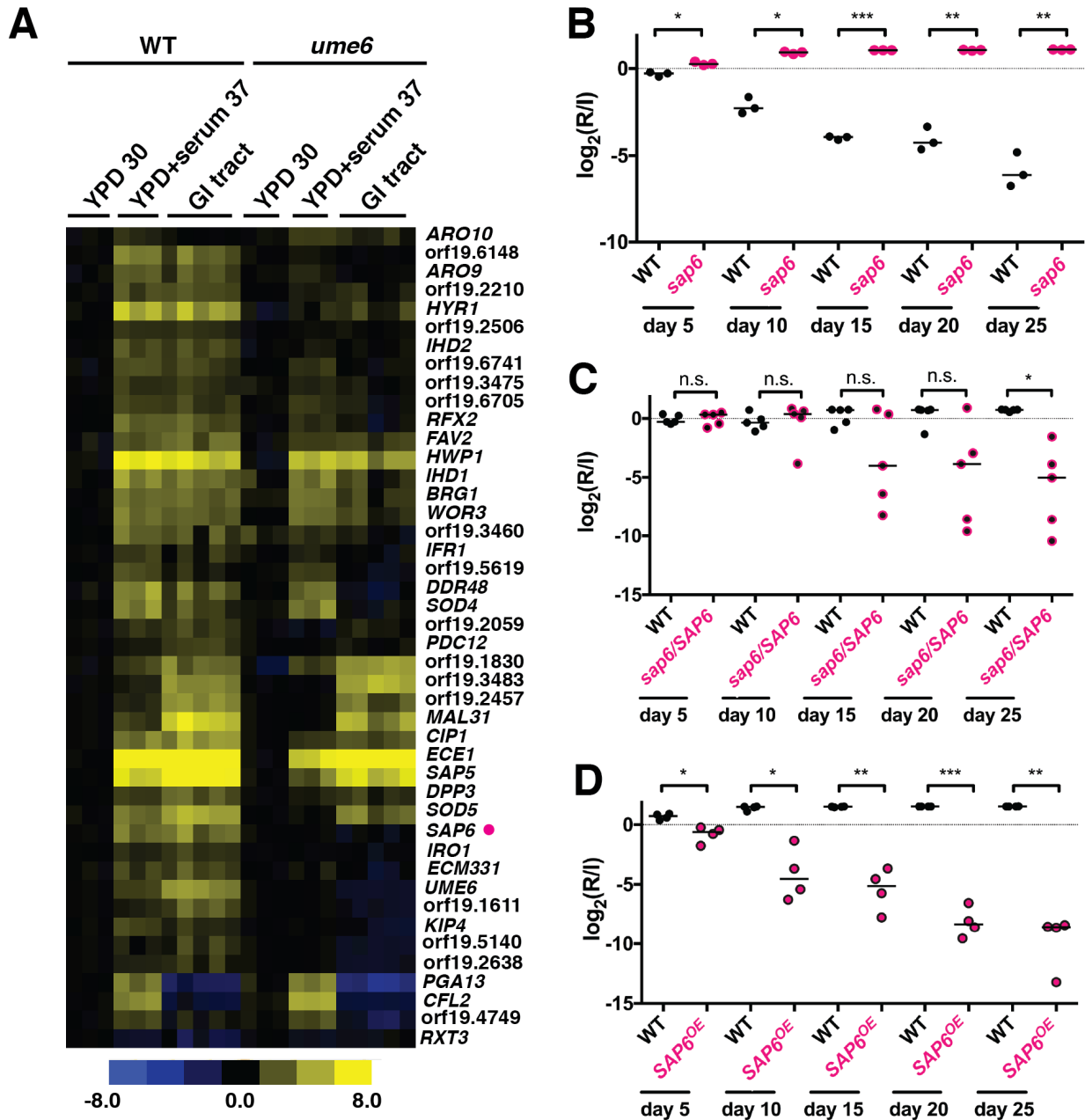


Figure 2.12. mRNA-seq reveals differences between wild type and *ume6* strains that implicate a secreted effector in modulating commensal fitness. A. Hypha-specific genes with expression greater than 2-fold upregulated or downregulated that are significantly different between wild type and *ume6* in the large intestine. B. WT (ySN250) v. *sap6* (ySN1664). C. WT (ySN234) v. *sap6/SAP6*-addback (ySN1796). C. WT (ySN235) v. *SAP6^{OE}* (ySN1798).

caspase-1/11^{-/-} animals and their wild-type controls. Then we will perform commensal competitions between wild type and the *sap6* strain.

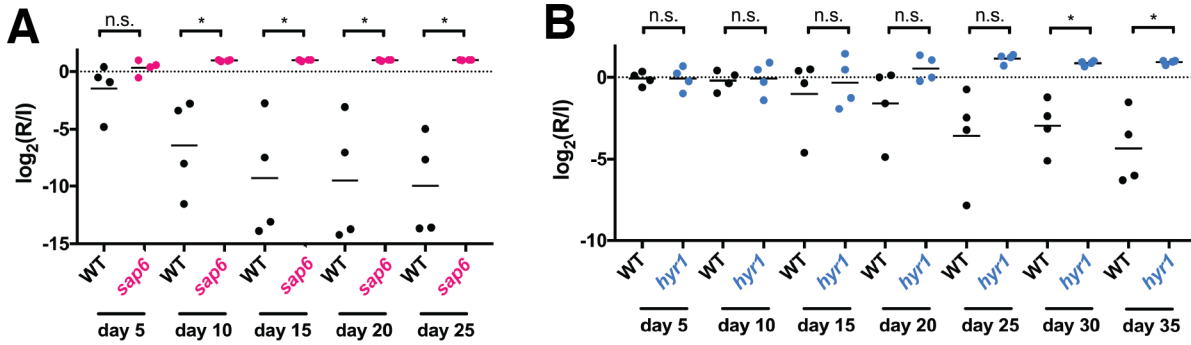


Figure 2.13. *sap6* and *hyr1* mutants are hyperfit compared to wild type. A. WT (ySN250) v. *sap6* (m886). B. WT (ySN250) v. *hyr1* (ySN511). Paired student's t-test * $p < 0.05$.

2.3. Discussion

The rules governing colonization of the mammalian gut are poorly understood for any microbial species, and particularly so for the fungal components of gut microbiota. In this study, our screens for *C. albicans* regulators and mediators of commensalism unexpectedly identified four pro-filamentation transcription factors as strong inhibitors of commensal fitness. Strains lacking *EFG1*, *BRG1*, *ROB1*, or *TEC1* are strongly hypercompetitive compared to wild type *C. albicans* and other mutants in our library of ~750 strains. Likewise, a newly constructed mutant lacking *UME6*, which encodes a transcription factor that is necessary and sufficient for filamentation under *in vitro* conditions, is also hypercompetitive in the mouse GI commensalism model, whereas a *UME6*^{OE} strain exhibits attenuated commensal fitness.

Prior to these studies, the roles played by *C. albicans* yeasts and hyphae in the host GI tract were unclear. In particular, two major observations have been difficult to reconcile: 1) *C. albicans* colonizes the mouse ileum primarily as yeasts; 2) Filament-specific genes are induced within the host GI tract. To clarify these observations, we performed detailed *in vivo* analysis on wild-type *C. albicans* as well as *ume6*, which affects a terminal regulator of filamentation. Our FISH data clearly indicate that wild-type *C. albicans* colonizes the mammalian gut as both yeasts and hyphae, with yeasts predominating in the stomach and small intestines while hyphae predominate more distally. The finding that fungal morphology differs in different compartments

of the GI tract makes sense in light of known features of these compartments, such as the low pH of the stomach, which favors yeast morphology, as well as hypoxia and hypercarbia in the distal GI tract, which favor hyphal morphology. Further, it suggests that hyphae are able to colonize at least some regions of the mammalian gut.

More surprising was the discovery that a *ume6* mutant exhibits normal filamentation in the gut, in striking contrast to its well-documented defects under a variety of hypha-inducing conditions *in vitro* (21,22). This observation suggests that signals present in the mammalian digestive tract but absent from *in vitro* hypha-induction assays activate at least one filamentation activator that is redundant with Ume6. Further, this result implies that the hypercommensal phenotype of the *ume6* mutant is independent of cell morphology.

Transcriptomic comparisons of wild-type and *ume6* strains propagated *in vitro* vs. in the mammalian gut dovetailed with the FISH experiments by exposing a larger Ume6-dependent regulon *in vitro* compared to *in vivo*. Whereas filamentation-specific genes require Ume6 for normal expression under standard *in vitro* hypha-inducing conditions, this number drops to 36 within the mammalian GI tract, again supporting redundant mechanisms for gene activation in this niche. Nevertheless, we demonstrated that differential expression of *SAP6* and *HYR1* genes has a dramatic effect on fitness within this niche, with knockouts of either filament-associated factor exhibiting enhanced competitive fitness.

Sap6 is part of a family of three *C. albicans* secreted aspartyl proteases that are highly conserved at the amino acid level, maintaining 90% identity overall ((44), reviewed in (8)). Despite their sequence conservation, the alleles are distinguished by features such as pattern of expression. For example, Sap4, Sap5, and Sap6 are expressed primarily by hyphae, whereas Sap1, Sap 2 and Sap3 are expressed primarily by yeasts (8). Different Saps have different pH optima of proteolytic activity (45,46). Sap2 and Sap6 are the only Saps with demonstrated activity in inducing a pro-inflammatory response from human monocytes, and cultured mouse macrophages and dendritic cells (42). This activity is independent of the proteolytic activity of the

Sap proteins, suggesting that the host has evolved to recognize these virulence effectors directly and not indirect damage caused by enzymatic activity (43). To determine whether host recognition of Sap6 influences *C. albicans* commensal fitness, we will compete wild type and *sap6* in wild-type C57Bl/6 animals vs. Caspase-1^{-/-}, Caspase-11^{-/-} animals. As we have demonstrated that the gut microbiota can influence *C. albicans* phenotypes, we will first perform fecal transplants from our standard BALB/c background to reduce confounding factors that may affect results.

To account for our observations, we propose a model in which *C. albicans* yeast cells are tolerated by the host, whether because they are inert or because they offer an as yet unidentified benefit. In contrast, hyphae—which are strongly associated with virulence—are monitored and maintained below a certain level. Specifically, when hypha-specific products such as secreted effectors (e.g. Sap6) and cell wall proteins (e.g. Hyr1) accumulate within the digestive tract, an antifungal immune response is triggered. Based on our observation that strains producing fewer hypha-specific antigens (e.g. *ume6*, *sap6*, *hyr1*) outcompete wild-type strain in competitive infections suggests that these responses are localized to areas of high antigen abundance, thereby sparing organisms in other regions of the gut. If true, our model implies that the composition of the gut microbiota is determined not only by microbial adaptations, but also by active host surveillance with selection for and against specific commensal microorganisms.

2.4. Materials and Methods

2.4.1. Strains

Genetic screens for *C. albicans* commensalism factors were performed with the Noble (29) and Homann (30) collections of isogenic, barcoded, homozygous deletion mutants. Both libraries are available from the Fungal Genetics Stock Center (<http://www.fgsc.net/>) (29,30). The *ume6*Δ/Δ and *hgc1*Δ/Δ were created for this study using a previously described fusion PCR technique (29,30,47). All mentioned strains are described in the Noble Lab Yeast Strains

database. All primers are described in the supplemental tables deposited on the Noble Lab server. Filenames are listed in the Appendix.

2.4.2. *in vivo studies*

All procedures involving animals were approved by the UCSF Institutional Animal Care and Use Committee. The mouse model of *C. albicans* commensalism was performed essentially as previously described (25,48) with minor modifications. Groups of 8–10-week (18-21 gram) female BALB/c mice were housed 2 per cage, unless otherwise specified, and treated with penicillin 1500 un/ml and streptomycin 2 mg/ml in their drinking water for 7-8 days prior to gavage, and continually throughout the experiment.

For competitions between isogenic wild-type *C. albicans* and mutants of interest, 2-6 mice were gavaged with 10^8 CFUs of a 1:1 mix of wild type and *efg1*, *brg1*, *rob1*, *tec1*, *ume6*, *tetO-UME6* or *hgc1* in 0.9% saline. Antibiotics were continued, and fecal pellets were collected at specified intervals. *C. albicans* recovery and quantification were performed as described previously (29). For screens, the Noble and Homann deletion collections (29,30) were individually inoculated into 1 mL of YEPD in 96 well plates, grown overnight and diluted 1:20 into 1 mL of fresh YEPD in 96 well plates. After 4 hours of growth at 30 C (mid log), strains were pooled, mice were gavaged with 10^8 CFUs and feces collected at described time points. Between 4 and 6 animals housed 2 per cage received each inoculum. Inoculum and fecal pellets from commensal assays were plated on Sabouraud/2% agar (BD) containing ampicillin (50 μ g/mL) and gentamicin (10 μ g/mL).

For some monotypic infection experiments, end organ plating was performed after removing the GI tract. The spleen, kidneys and liver were homogenized and a portion plated to determine CFUs.

2.4.3. *Preparation of sequencing libraries from in vivo screen for GI commensalism factors*

Genomic DNA from plated inoculum and fecal pellets was isolated as previously described (25,48). Feces from one animal per cage was prepared for sequencing. A linear-amplification based deep-sequencing method modified from (49) was used to selectively amplify the genomic DNA region flanking the gene disruption created by the *Candida dubliniensis* *HIS1* selectable marker (29). Briefly, 5-20 µg of genomic DNA was separately digested overnight using restriction enzymes AluI, BfaI, DpnII, RsaI, or TaqI (New England Biolabs). The restriction enzymes were heat inactivated, digests pooled and precipitated to concentrate the DNA, and gel-free size selection performed using SeraMag bead mix (as prepared in (50)) to capture DNA at 200-1000 bp. 1 µg of DNA was used for linear amplification by AccuPrime Taq (Invitrogen) with biotinylated primer SNO1774 for 100 cycles. Single-stranded biotinylated DNA was captured using streptavidin-coated beads overnight and second adapter ligation performed with CircLigase II (Epicentre) using primer SNO1775 the next day. PCR using AccuPrime Taq and Illumina primers 1 (SNO1777) and 2 (barcoded; SNO1776, SNO1819-1829 or SNO1949-1960) was performed for 15 cycles. Clean-up of PCR products to remove primers was performed using SeraMag bead mix. 2100 Bioanalyzer (Agilent) traces were used to quantify library abundances and size distribution. Multiplexed libraries for sequencing were pooled based on Bioanalyzer traces. For some libraries, additional size exclusion was achieved using the Sage Science BluePippin available in the UCSF Center for Advanced Technology. Sequencing of libraries (50 base pair-single end) was performed using custom sequencing primer SNO1830 at the University of California Berkeley QB3 Vincent J. Coates Genomics Sequencing Laboratory (GSL) on an Illumina HiSeq2000 or HiSeq4000.

2.4.4. Quantification of mutant abundances in screens

Reads from individual libraries were mapped to the *Candida albicans* genome (candidagenome.org, Assembly 21) using bowtie (51) and assigned to mutants based on the proximity (within 200 bp) of the start or end of a gene present in the Noble and Homann *Candida*

albicans deletion collections (30,47). Abundances of each strain in a library were determined as the ratio of the number of reads for an individual mutant to the total number of reads for all strains present in that library. If strain abundance in the inoculum was less than 100 reads, the mutant was removed from further analysis. Finally, fold changes for an individual strain were defined as the log₂ transformed ratio of the abundance of the strain in the fecal time point (recovered, R) over the abundance in the inoculum (I). All data files are deposited on the Noble Lab server and file paths are listed in the Appendix.

2.4.5. *in vivo* imaging of *Candida albicans*

For FISH experiments, mice were dissected at day 10 post infection, and stomach, small intestine (proximal, medial and distal), cecum and large intestine were placed in tissue cassettes and fixed in methacarn (60% methanol, 30% chloroform, 10% glacial acetic acid) at room temperature from a range of three hours and up to two weeks.

Tissue cassettes were processed post-fixation in the following washes: twice for 35 minutes in 100% methanol, twice for 25 minutes in 100% ethanol, twice for 20 minutes in xylenes (histological grade, Sigma-Aldrich) and then placed in melted paraffin wax for two hours at 70°C. Following processing, sections were embedded by UCSF Cancer Center Immunohistochemistry and Molecular Pathology Core, then sent to Nationwide Histology (Veradale, WA) to be cut into either 4 µm or 8 µm sections.

Fluorescence *in situ* hybridization (FISH) was performed as previously described (39) with the following modifications: hybridization was performed with a pan-fungal DNA probe conjugated to Cy3 (5'-Cy3-CTCTGGCTTCACCCTATTC-3'; Integrated DNA Technologies) (52,53), for three hours at 50°C and, instead of anti-Muc2 staining, sections were counterstained with DAPI, and either FITC conjugated UEA-1 (Sigma) for stomach and large intestine sections, or FITC conjugated UEA-1 and FITC-conjugated WGA-1 (Sigma) for small intestine and cecum sections,

at 4°C for 45 minutes. Sections were mounted with Vectashield (Vector Laboratories) and imaged on Keyence microscope model BZ-X700. Yeast and hyphal structures were quantified manually using the cell counter plug-in for Fiji (ImageJ) (54).

For immunohistochemistry, paraffin-embedded sections were rehydrated with the following washes: twice at 60°C in xylenes for 10 minutes, twice at room temperature in 100% ethanol for 5 minutes, once at room temperature in 70% ethanol for 5 minutes, once at room temperature in 50% ethanol for 5 minutes, and twice at room temperature in distilled water for 3 minutes. Slides were blocked with 10% normal goat serum (Santa Cruz Biotechnology) in PBS for 30 minutes. Then, slides were incubated with anti-*C. albicans* primary antibody (Meridian Life Sciences; 1:500 in PBS) for 2 hours followed by AlexaFluor594-goat anti-rabbit (Thermo-Fisher; 1:500 in PBS) for 1 hour. Finally, slides were counterstained with DAPI, and FITC-conjugated UEA-1, and mounted as described for FISH. All blocking and staining steps were performed at 4°C.

2.4.6. NanoString transcriptional profiling

For NanoString experiments, BALB/c mice, singly housed, were monotypically infected by oral gavage with either wild-type *C. albicans*, or the mutants of interest (*hgc1* or *ume6*). Remaining inoculum was spun down and pellet was flash frozen in liquid nitrogen and stored at -80 C prior to further processing. At each time point, each mouse GI tract was dissected and divided into four compartments: stomach, small intestine, cecum and large intestine. When tissue versus contents association was assessed, contents were squeezed out of the tissue using forceps. GI sections were flash frozen in liquid nitrogen and stored at -80C.

RNA extraction for NanoString was performed as previously described (55), with the following modifications. Frozen pellets of cells from the inocula were resuspended in 650 µL of buffer RLT (Qiagen) with 1% β-mercaptoethanol (β-ME), and then added to 650 µl phenol-chloroform-isoamyl alcohol (25:24:1), plus 250 µl of zirconia beads. 1.8 mL of buffer RLT with 1%

β -ME was added to each GI section. 650 μ l of homogenate was mixed with phenol-chloroform-isoamyl alcohol plus zirconia beads as described above.

The NanoString nCounter Analysis System was used with a previously described set of fluorescent probes for hybridization and detection (55). NanoString analysis was performed as previously described (55). Briefly, all samples were normalized to the average counts across all samples.

2.4.7. RNA-seq library preparation and sequencing

For mRNA-seq, animals were treated the same way as NanoString with the exception that the contents from all compartments were extruded using forceps, snap frozen in liquid nitrogen and processed in house.

RNA extraction for mRNA-seq was performed as previously described in (56), with modifications. Dow Corning vacuum grease was used for phase separation, instead of phase-lock tubes. Three to five additional acid phenol-chloroform (Ambion) and phenol-chloroform-isoamyl alcohol (Ambion) extractions were added to eliminate endogenous RNases. Following precipitation and resuspension of pellets in RNase-free water, RNA was further cleaned up using the MEGAclean transcription clean-up kit (Ambion). DNase I (NEB) treatment was performed on 10 μ g RNA for 10 minutes at 37 C, then 0.5 M EDTA was used to inactivate DNase I at 75 C for 10 min. Following DNase treatment, a final acid phenol-chloroform extraction was performed. RNA was then precipitated and resuspended in RNase-free water. *In vitro* and *in vivo* samples were treated identically.

NEBNext Ultra Directional RNA Library Prep Kit for Illumina in combination with NEBNext Poly(A) mRNA Magnetic Isolation Module and NEBNext Multiplex Oligos for Illumina was used to generate mRNA-seq libraries. The protocol provided by NEB was followed precisely using 1 μ g total RNA and 13-14 cycles in the final PCR, with the exception that Ampure XP bead mix was replaced with Sera-Mag Speed Beads (Thermo-Fisher) (50). Library fragment size was

determined using High Sensitivity DNA chips on a 2100 Bioanalyzer (Agilent). Library quantification was performed by qPCR with a library quantification kit from KAPA Biosystems (KK4824). Sequencing was performed on the UCSF Center for Advanced Technology HiSeq4000. All raw sequencing files and have been deposited on the Noble Lab. Filepaths are listed in the Appendix.

2.4.8. Transcriptome analysis

To determine significant changes in RNA expression, reads were mapped to the current haploid *C. albicans* transcriptome (Assembly 21, candidagenome.org) and transcript abundances were then evaluated using kallisto (57). Statistical comparisons of transcript abundances between different conditions were performed on estimated counts using *limma* as previously described (58). Data in heat maps where individual biological replicates are shown were made using transcript per Million mapped reads (tpm) values generated by kallisto. All data files are deposited on the Noble Lab server. File paths are listed in the Appendix.

2.5. References

1. Pfaller, M. A., and Diekema, D. J. (2007) Epidemiology of invasive candidiasis: a persistent public health problem. *Clinical microbiology reviews* **20**, 133-163
2. Odds, F. C., Davidson, A. D., Jacobsen, M. D., Tavanti, A., Whyte, J. A., Kibbler, C. C., Ellis, D. H., Maiden, M. C., Shaw, D. J., and Gow, N. A. (2006) *Candida albicans* strain maintenance, replacement, and microvariation demonstrated by multilocus sequence typing. *Journal of clinical microbiology* **44**, 3647-3658
3. Odds, F. C. (1987) *Candida* infections: an overview. *Critical reviews in microbiology* **15**, 1-5
4. Brown, G. D., Denning, D. W., Gow, N. A., Levitz, S. M., Netea, M. G., and White, T. C. (2012) Hidden killers: human fungal infections. *Science translational medicine* **4**, 165rv113
5. Noble, S. M., Gianetti, B. A., and Witchley, J. N. (2017) *Candida albicans* cell-type switching and functional plasticity in the mammalian host. *Nat Rev Microbiol* **15**, 96-108
6. Netea, M. G., Brown, G. D., Kullberg, B. J., and Gow, N. A. (2008) An integrated model of the recognition of *Candida albicans* by the innate immune system. *Nat Rev Microbiol* **6**, 67-78

7. Wachtler, B., Citiulo, F., Jablonowski, N., Forster, S., Dalle, F., Schaller, M., Wilson, D., and Hube, B. (2012) Candida albicans-epithelial interactions: dissecting the roles of active penetration, induced endocytosis and host factors on the infection process. *PloS one* **7**, e36952
8. Naglik, J. R., Challacombe, S. J., and Hube, B. (2003) Candida albicans secreted aspartyl proteinases in virulence and pathogenesis. *Microbiol Mol Biol Rev* **67**, 400-428, table of contents
9. Liu, Y., and Filler, S. G. (2011) Candida albicans Als3, a multifunctional adhesin and invasin. *Eukaryotic cell* **10**, 168-173
10. Nobile, C. J., Nett, J. E., Andes, D. R., and Mitchell, A. P. (2006) Function of Candida albicans adhesin Hwp1 in biofilm formation. *Eukaryotic cell* **5**, 1604-1610
11. Staab, J. F., Bradway, S. D., Fidel, P. L., and Sundstrom, P. (1999) Adhesive and mammalian transglutaminase substrate properties of Candida albicans Hwp1. *Science* **283**, 1535-1538
12. Bailey, D. A., Feldmann, P. J., Bovey, M., Gow, N. A., and Brown, A. J. (1996) The Candida albicans HYR1 gene, which is activated in response to hyphal development, belongs to a gene family encoding yeast cell wall proteins. *Journal of bacteriology* **178**, 5353-5360
13. Moyes, D. L., Wilson, D., Richardson, J. P., Mogavero, S., Tang, S. X., Wernecke, J., Hofs, S., Gratacap, R. L., Robbins, J., Runglall, M., Murciano, C., Blagojevic, M., Thavaraj, S., Forster, T. M., Hebecker, B., Kasper, L., Vizcay, G., Iancu, S. I., Kichik, N., Hader, A., Kurzai, O., Luo, T., Kruger, T., Kniemeyer, O., Cota, E., Bader, O., Wheeler, R. T., Gutschmann, T., Hube, B., and Naglik, J. R. (2016) Candidalysin is a fungal peptide toxin critical for mucosal infection. *Nature* **532**, 64-68
14. Lo, H. J., Kohler, J. R., DiDomenico, B., Loebenberg, D., Cacciapuoti, A., and Fink, G. R. (1997) Nonfilamentous C. albicans mutants are avirulent. *Cell* **90**, 939-949
15. Lu, Y., Su, C., Solis, N. V., Filler, S. G., and Liu, H. (2013) Synergistic regulation of hyphal elongation by hypoxia, CO₂, and nutrient conditions controls the virulence of Candida albicans. *Cell host & microbe* **14**, 499-509
16. Mayer, F. L., Wilson, D., and Hube, B. (2013) Candida albicans pathogenicity mechanisms. *Virulence* **4**, 119-128
17. Simonetti, N., Strippoli, V., and Cassone, A. (1974) Yeast-mycelial conversion induced by N-acetyl-D-glucosamine in Candida albicans. *Nature* **250**, 344-346
18. Mitchell, A. P. (1998) Dimorphism and virulence in Candida albicans. *Curr Opin Microbiol* **1**, 687-692
19. Brown, A. J., and Gow, N. A. (1999) Regulatory networks controlling Candida albicans morphogenesis. *Trends Microbiol* **7**, 333-338
20. Ernst, J. F. (2000) Regulation of dimorphism in Candida albicans. *Contrib Microbiol* **5**, 98-111
21. Zeidler, U., Lettner, T., Lassnig, C., Muller, M., Lajko, R., Hintner, H., Breitenbach, M., and Bito, A. (2009) UME6 is a crucial downstream target of other transcriptional regulators of true hyphal development in Candida albicans. *FEMS yeast research* **9**, 126-142
22. Banerjee, M., Thompson, D. S., Lazzell, A., Carlisle, P. L., Pierce, C., Monteagudo, C., Lopez-Ribot, J. L., and Kadosh, D. (2008) UME6, a novel filament-specific regulator of

- Candida albicans* hyphal extension and virulence. *Molecular biology of the cell* **19**, 1354-1365
23. White, S. J., Rosenbach, A., Lephart, P., Nguyen, D., Benjamin, A., Tzipori, S., Whiteway, M., Meccas, J., and Kumamoto, C. A. (2007) Self-regulation of *Candida albicans* population size during GI colonization. *PLoS pathogens* **3**, e184
 24. Vautier, S., Drummond, R. A., Chen, K., Murray, G. I., Kadosh, D., Brown, A. J., Gow, N. A., MacCallum, D. M., Kolls, J. K., and Brown, G. D. (2015) *Candida albicans* colonization and dissemination from the murine gastrointestinal tract: the influence of morphology and Th17 immunity. *Cellular microbiology* **17**, 445-450
 25. Pande, K., Chen, C., and Noble, S. M. Passage through the mammalian gut triggers a phenotypic switch that promotes *Candida albicans* commensalism. *Nat Genet* **45**, 1088-1091
 26. Pierce, J. V., and Kumamoto, C. A. Variation in *Candida albicans* EFG1 expression enables host-dependent changes in colonizing fungal populations. *mBio* **3**, e00117-00112
 27. Pierce, J. V., Dignard, D., Whiteway, M., and Kumamoto, C. A. Normal adaptation of *Candida albicans* to the murine gastrointestinal tract requires Efg1p-dependent regulation of metabolic and host defense genes. *Eukaryotic cell* **12**, 37-49
 28. Rosenbach, A., Dignard, D., Pierce, J. V., Whiteway, M., and Kumamoto, C. A. (2010) Adaptations of *Candida albicans* for growth in the mammalian intestinal tract. *Eukaryotic cell* **9**, 1075-1086
 29. Noble, S. M., French, S., Kohn, L. A., Chen, V., and Johnson, A. D. Systematic screens of a *Candida albicans* homozygous deletion library decouple morphogenetic switching and pathogenicity. *Nat Genet* **42**, 590-598
 30. Homann, O. R., Dea, J., Noble, S. M., and Johnson, A. D. (2009) A phenotypic profile of the *Candida albicans* regulatory network. *PLoS genetics* **5**, e1000783
 31. Du, H., Guan, G., Xie, J., Sun, Y., Tong, Y., Zhang, L., and Huang, G. (2012) Roles of *Candida albicans* Gat2, a GATA-type zinc finger transcription factor, in biofilm formation, filamentous growth and virulence. *PloS one* **7**, e29707
 32. Schweizer, A., Rupp, S., Taylor, B. N., Rollinghoff, M., and Schroppel, K. (2000) The TEA/ATTS transcription factor CaTec1p regulates hyphal development and virulence in *Candida albicans*. *Molecular microbiology* **38**, 435-445
 33. Nobile, C. J., Fox, E. P., Nett, J. E., Sorrells, T. R., Mitrovich, Q. M., Hernday, A. D., Tuch, B. B., Andes, D. R., and Johnson, A. D. (2012) A recently evolved transcriptional network controls biofilm development in *Candida albicans*. *Cell* **148**, 126-138
 34. Stoldt, V. R., Sonneborn, A., Leuker, C. E., and Ernst, J. F. (1997) Efg1p, an essential regulator of morphogenesis of the human pathogen *Candida albicans*, is a member of a conserved class of bHLH proteins regulating morphogenetic processes in fungi. *The EMBO journal* **16**, 1982-1991
 35. Hnisz, D., Bardet, A. F., Nobile, C. J., Petryshyn, A., Glaser, W., Schock, U., Stark, A., and Kuchler, K. (2012) A histone deacetylase adjusts transcription kinetics at coding sequences during *Candida albicans* morphogenesis. *PLoS genetics* **8**, e1003118
 36. Lu, Y., Su, C., and Liu, H. (2012) A GATA transcription factor recruits Hda1 in response to reduced Tor1 signaling to establish a hyphal chromatin state in *Candida albicans*. *PLoS pathogens* **8**, e1002663

37. Lassak, T., Schneider, E., Bussmann, M., Kurtz, D., Manak, J. R., Srikantha, T., Soll, D. R., and Ernst, J. F. (2011) Target specificity of the *Candida albicans* Efg1 regulator. *Molecular microbiology* **82**, 602-618
38. Earle, K. A., Billings, G., Sigal, M., Lichtman, J. S., Hansson, G. C., Elias, J. E., Amieva, M. R., Huang, K. C., and Sonnenburg, J. L. (2015) Quantitative Imaging of Gut Microbiota Spatial Organization. *Cell host & microbe* **18**, 478-488
39. Johansson, M. E., and Hansson, G. C. (2012) Preservation of mucus in histological sections, immunostaining of mucins in fixed tissue, and localization of bacteria with FISH. *Methods in molecular biology* **842**, 229-235
40. Xu, W., Solis, N. V., Ehrlich, R. L., Woolford, C. A., Filler, S. G., and Mitchell, A. P. (2015) Activation and alliance of regulatory pathways in *C. albicans* during mammalian infection. *PLoS biology* **13**, e1002076
41. Azadmanesh, J., Gowen, A. M., Creger, P. E., Schafer, N. D., and Blankenship, J. R. (2017) Filamentation Involves Two Overlapping, but Distinct, Programs of Filamentation in the Pathogenic Fungus *Candida albicans*. *G3 (Bethesda)*
42. Pietrella, D., Pandey, N., Gabrielli, E., Pericolini, E., Perito, S., Kasper, L., Bistoni, F., Cassone, A., Hube, B., and Vecchiarelli, A. (2013) Secreted aspartic proteases of *Candida albicans* activate the NLRP3 inflammasome. *Eur J Immunol* **43**, 679-692
43. Pietrella, D., Rachini, A., Pandey, N., Schild, L., Netea, M., Bistoni, F., Hube, B., and Vecchiarelli, A. (2010) The Inflammatory response induced by aspartic proteases of *Candida albicans* is independent of proteolytic activity. *Infection and immunity* **78**, 4754-4762
44. Schaller, M., Januschke, E., Schackert, C., Woerle, B., and Korting, H. C. (2001) Different isoforms of secreted aspartyl proteinases (Sap) are expressed by *Candida albicans* during oral and cutaneous candidosis in vivo. *J Med Microbiol* **50**, 743-747
45. Naglik, J., Albrecht, A., Bader, O., and Hube, B. (2004) *Candida albicans* proteinases and host/pathogen interactions. *Cellular microbiology* **6**, 915-926
46. Naglik, J. R., Rodgers, C. A., Shirlaw, P. J., Dobbie, J. L., Fernandes-Naglik, L. L., Greenspan, D., Agabian, N., and Challacombe, S. J. (2003) Differential expression of *Candida albicans* secreted aspartyl proteinase and phospholipase B genes in humans correlates with active oral and vaginal infections. *The Journal of infectious diseases* **188**, 469-479
47. Noble, S. M., and Johnson, A. D. (2005) Strains and strategies for large-scale gene deletion studies of the diploid human fungal pathogen *Candida albicans*. *Eukaryotic cell* **4**, 298-309
48. Chen, C., Pande, K., French, S. D., Tuch, B. B., and Noble, S. M. (2011) An iron homeostasis regulatory circuit with reciprocal roles in *Candida albicans* commensalism and pathogenesis. *Cell host & microbe* **10**, 118-135
49. Carette, J. E., Guimaraes, C. P., Wuethrich, I., Blomen, V. A., Varadarajan, M., Sun, C., Bell, G., Yuan, B., Muellner, M. K., Nijman, S. M., Ploegh, H. L., and Brummelkamp, T. R. (2011) Global gene disruption in human cells to assign genes to phenotypes by deep sequencing. *Nature biotechnology* **29**, 542-546
50. Rohland, N., and Reich, D. (2012) Cost-effective, high-throughput DNA sequencing libraries for multiplexed target capture. *Genome research* **22**, 939-946

51. Langmead, B., Trapnell, C., Pop, M., and Salzberg, S. L. (2009) Ultrafast and memory-efficient alignment of short DNA sequences to the human genome. *Genome Biol* **10**, R25
52. Da Silva, R. M., Jr., Da Silva Neto, J. R., Santos, C. S., Frickmann, H., Poppert, S., Cruz, K. S., Koshikene, D., and De Souza, J. V. (2015) Evaluation of fluorescence in situ hybridisation (FISH) for the detection of fungi directly from blood cultures and cerebrospinal fluid from patients with suspected invasive mycoses. *Ann Clin Microbiol Antimicrob* **14**, 6
53. Amann, R. I., Krumholz, L., and Stahl, D. A. (1990) Fluorescent-oligonucleotide probing of whole cells for determinative, phylogenetic, and environmental studies in microbiology. *Journal of bacteriology* **172**, 762-770
54. Schindelin, J., Arganda-Carreras, I., Frise, E., Kaynig, V., Longair, M., Pietzsch, T., Preibisch, S., Rueden, C., Saalfeld, S., Schmid, B., Tinevez, J. Y., White, D. J., Hartenstein, V., Eliceiri, K., Tomancak, P., and Cardona, A. (2012) Fiji: an open-source platform for biological-image analysis. *Nat Methods* **9**, 676-682
55. Xu, W., Solis, N. V., Filler, S. G., and Mitchell, A. P. (2016) Pathogen Gene Expression Profiling During Infection Using a Nanostring nCounter Platform. *Methods in molecular biology* **1361**, 57-65
56. Turnbaugh, P. J., Ridaura, V. K., Faith, J. J., Rey, F. E., Knight, R., and Gordon, J. I. (2009) The effect of diet on the human gut microbiome: a metagenomic analysis in humanized gnotobiotic mice. *Science translational medicine* **1**, 6ra14
57. Bray, N. L., Pimentel, H., Melsted, P., and Pachter, L. (2016) Near-optimal probabilistic RNA-seq quantification. *Nature biotechnology* **34**, 525-527
58. Ritchie, M. E., Phipson, B., Wu, D., Hu, Y., Law, C. W., Shi, W., and Smyth, G. K. (2015) limma powers differential expression analyses for RNA-sequencing and microarray studies. *Nucleic acids research* **43**, e47
59. Banerjee, M., Uppuluri, P., Zhao, X. R., Carlisle, P. L., Vipulanandan, G., Villar, C. C., Lopez-Ribot, J. L., and Kadosh, D. (2013) Expression of UME6, a key regulator of *Candida albicans* hyphal development, enhances biofilm formation via Hgc1- and Sun41-dependent mechanisms. *Eukaryotic cell* **12**, 224-232
60. Childers, D. S., and Kadosh, D. (2015) Filament condition-specific response elements control the expression of NRG1 and UME6, key transcriptional regulators of morphology and virulence in *Candida albicans*. *PLoS one* **10**, e0122775
61. Perez, J. C., Kumamoto, C. A., and Johnson, A. D. *Candida albicans* commensalism and pathogenicity are intertwined traits directed by a tightly knit transcriptional regulatory circuit. *PLoS biology* **11**, e1001510
62. Iliev, I. D., Funari, V. A., Taylor, K. D., Nguyen, Q., Reyes, C. N., Strom, S. P., Brown, J., Becker, C. A., Fleshner, P. R., Dubinsky, M., Rotter, J. I., Wang, H. L., McGovern, D. P., Brown, G. D., and Underhill, D. M. (2012) Interactions between commensal fungi and the C-type lectin receptor Dectin-1 influence colitis. *Science* **336**, 1314-1317

Chapter 3. Dual role for white-opaque regulators in *C. albicans* GI commensalism

3.1. Introduction

Candida albicans is the major fungal commensal and opportunistic pathogen of humans. Hosts with immune deficits (such as organ transplant recipients), those who have undergone invasive procedures, and those with microbial dysbiosis following antibiotic treatment are vulnerable to life-threatening disseminated candidiasis (1,2). However, the most common niche of this fungus is the mammalian gut, skin, and genitourinary tract since, unlike most other pathogenic fungi, *C. albicans* appears to lack a primary environmental niche apart from the host (3-6). Previous *C. albicans* research has focused primarily on its virulence potential, and it remains to be determined how this commensal-pathogen survives as a ubiquitous component of mammalian gut microbiota and how it transitions between commensal and pathogenic lifestyles.

Multiple transcriptional regulators of commensalism have been identified by means of screens of *C. albicans* mutants in mouse models of stable gastrointestinal colonization. For example, Tye7, Rtg1, Rtg3, Lys144, Hms1 and orf19.3625 were identified as positive regulators in one study (7), and Efg1 and Efh1 were identified as inhibitors in others (8-11). Similarly, Zcf8, Zfu2, and Try4 were identified as commensalism activators and Ume6 and Wor3 as inhibitors in a screen in gnotobiotic animals (12). Finally, we previously showed that the transcription factor Wor1 activates commensal fitness in the mammalian gut by promoting a switch between standard 'white' yeast cells and a morphologically distinct 'GUT' cell type that is optimized for this niche (13). In this study, we independently identified Efg1 as a strong inhibitor of commensal fitness and proposed that at least part of this activity of Efg1 derives from its well-documented activity as a direct transcriptional repressor of *WOR1* (see section 1.2.6. for more detail). Additionally, I identified Brg1, Rob1, Tec1 and Ume6 as inhibitors of commensal fitness in a conventional mouse model of gastrointestinal colonization (Chapter 2).

Efg1 and Wor1 have been extensively characterized for their roles in controlling a different morphological transition that confers sexual competency in this species. As mentioned

above, Efg1 and Wor1 also play mutually antagonistic roles in the regulation of *C. albicans* sexual switching, which is restricted to cells with rare *MTLa* or *MTL α* genotypes. The “white-to-opaque” sexual switch has been intensively studied and, via genetic and biochemical approaches, many additional transcription factors have been shown to coordinate with Efg1 and Wor1 to create a self-reinforcing transcriptional regulatory circuit. It is now known that many transcription factors contribute to the phenotype (14) but at the outset of this study eight core regulators had been identified. In addition to Wor1 and Efg1, those regulators are Wor2, Wor3, Wor4, Czf1, Ahr1 and Ssn6 (15-23). Efg1, Czf1 and Ahr1 have also been shown to play a role in another morphological transition, the yeast-to-hyphal switch (24,25). We hypothesized that the white-to-GUT switch in *C. albicans MTL α* cells is controlled by an analogous circuit that includes additional white-to-opaque regulators. However, because the white-to-GUT switch most likely occurs in a different host niche with different inducing signals and produces a different outcome, there must be differences between the two.

We tested every core white-to-opaque switching regulator for roles in *C. albicans* commensalism. In addition, we profiled RNA expression of *wor1*, *efg1*, *czf1*, *WOR1^{OE}* and *efg1wor1* strains in the mammalian GI tract to determine how the gene expression profile differs from wild type. To define direct regulatory targets of Wor1, Efg1 and Czf1 *in vivo*, we developed a Calling Card-seq method for *C. albicans*. This work sheds light on how the commensal state of this important fungal pathogen is specified, as well as how the transition between the commensal and pathogenic states is regulated.

3.2. Results

3.2.1. Regulators of sexual switching also control commensal fitness

We previously showed that Wor1 is required for *C. albicans* fitness as a commensal in the mammalian gut, whereas Efg1 negatively regulates fitness in this niche (13). To determine whether other canonical regulators of sexual switching also play roles in commensalism, we

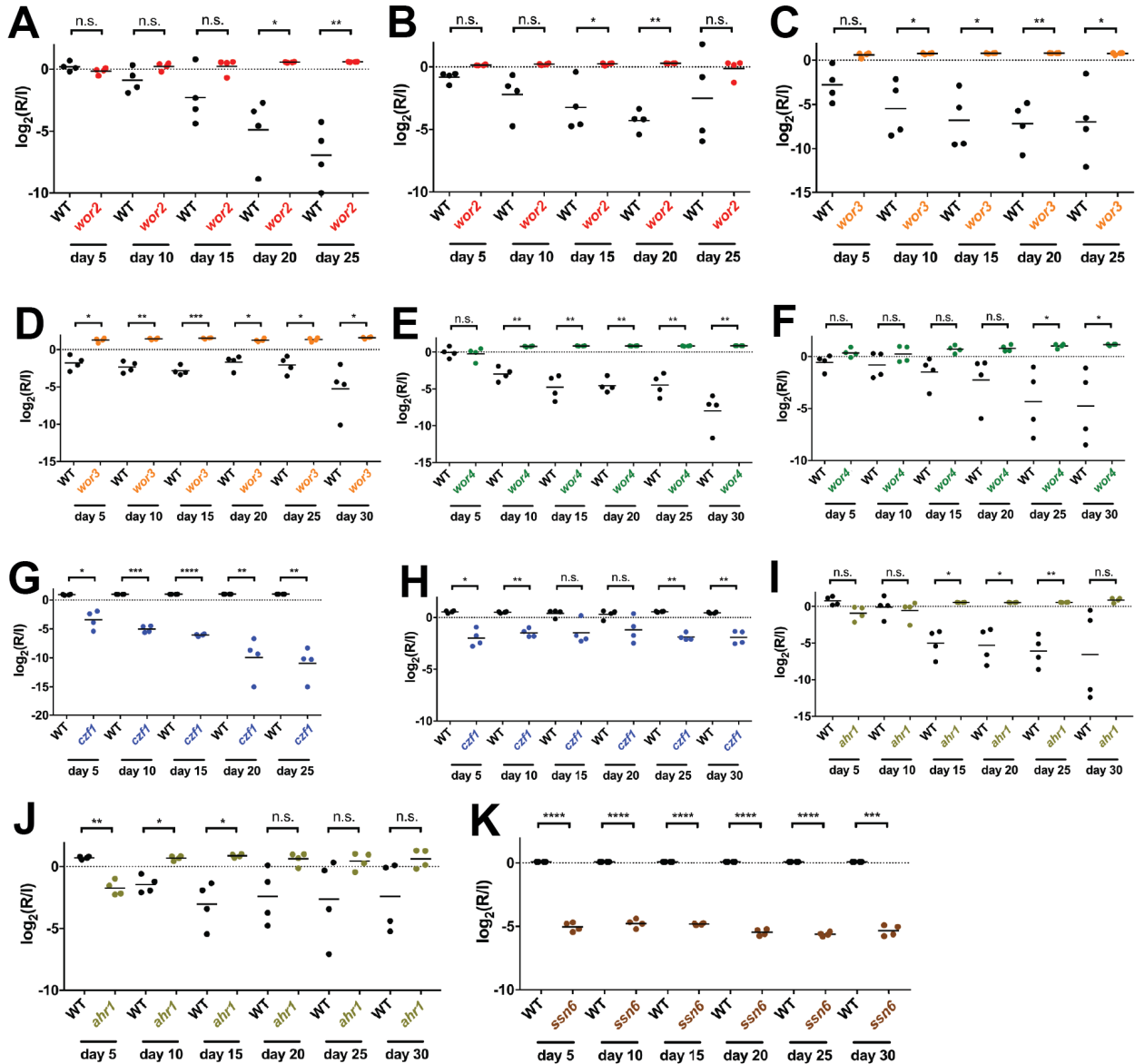


Figure 3.1. One-to-one competitions reveal role for white-opaque regulators in commensalism. A. WT (ySN250) v. *wor2* (ySN1142). B. WT (ySN250) v. *wor2* (ySN1143). C. WT (ySN250) v. *wor3* (ySN1111). D. (ySN250) v. *wor3* (ySN1433). E. WT (ySN250) v. *wor4* (ySN1493). F. WT (ySN250) v. *wor4* (ySN1494). G. WT (ySN250) v. *czf1* (ySN1144). H. WT (ySN250) v. *czf1* (ySN1383). I. WT (ySN250) v. *ahr1* (ySN1187). J. WT (ySN250) v. *ahr1* (ySN1188). K. WT (ySN250) v. *ssn6* (ySN1488). *p<0.05, **p<0.01, ***p<0.001, ****p<0.0001.

generated mutants affecting *CZF1*, *WOR2*, *WOR3*, *WOR3*, *AHR1*, and *SSN6*. Homozygous disruptants of each open reading frame (ORF) were created in the reference strain ySN152, the same genetic background as the *wor1* and *efg1* mutants. To determine the relative fitness of

each strain, competition experiments were performed with a 1:1 mixture of mutant and wild-type (WT) *C. albicans*. qPCR was used to determine strain abundance in the inoculum and in mouse feces over a 25- to 30-day time course, and the results for two independent isolates of each mutant are plotted in Figure 3.1. Surprisingly every tested white-opaque regulator exhibited significant effects on commensal fitness. Specifically, *wor2*, *wor3*, and *wor4* are hypercompetitive compared to WT, suggesting that Wor2, Wor3, and Wor4 function to inhibit commensal fitness in the gut. *Ahr1* may also weakly inhibit commensal fitness but the phenotypes of the mutants are much weaker (**Figure 3.1.I,J**). Conversely, *czf1* and *ssn6* mutants exhibit reduced commensal fitness, implying a positive role for Czf1 and Ssn6 in gut commensalism (**Figure 3.1.G,H,K**). It should be noted that, because the *ssn6* mutant exhibits a substantial growth deficit under *in vitro* conditions, this factor's role in promoting fitness in the GI tract may be nonspecific.

It should be noted that the original *wor1* isolates created for the lab had *in vitro* growth defects not previous seen. To confirm that the *wor1* results were true, we created new *wor1* isolates and performed commensal competitions with wild type (**Figure 3.2A,B**). These isolates overall appear less fit but the defect is not statistically significant. The *WOR1^{OE}* hyperfit phenotype is reproducible using a different strain background and a different overexpression construct (**Figure 3.2.C**). Passage of this strain through the mouse GI tract also resulted in GUT cells (data not shown).

The observation that at least seven of eight key sexual regulators (including Wor1 and Efg1) also control commensal fitness in the gut suggests that there is substantial overlap between the two regulatory circuits. On the other hand, the roles of at least some of these factors appear to differ between sex and commensalism. For example, Wor2, Wor3, and Wor4 all promote the white-to-opaque switch but inhibit fitness in the gut. Regulators with consistent roles in both sexual switching and commensalism include Wor1 and Czf1, which promote both processes, and Efg1, which inhibits both processes.

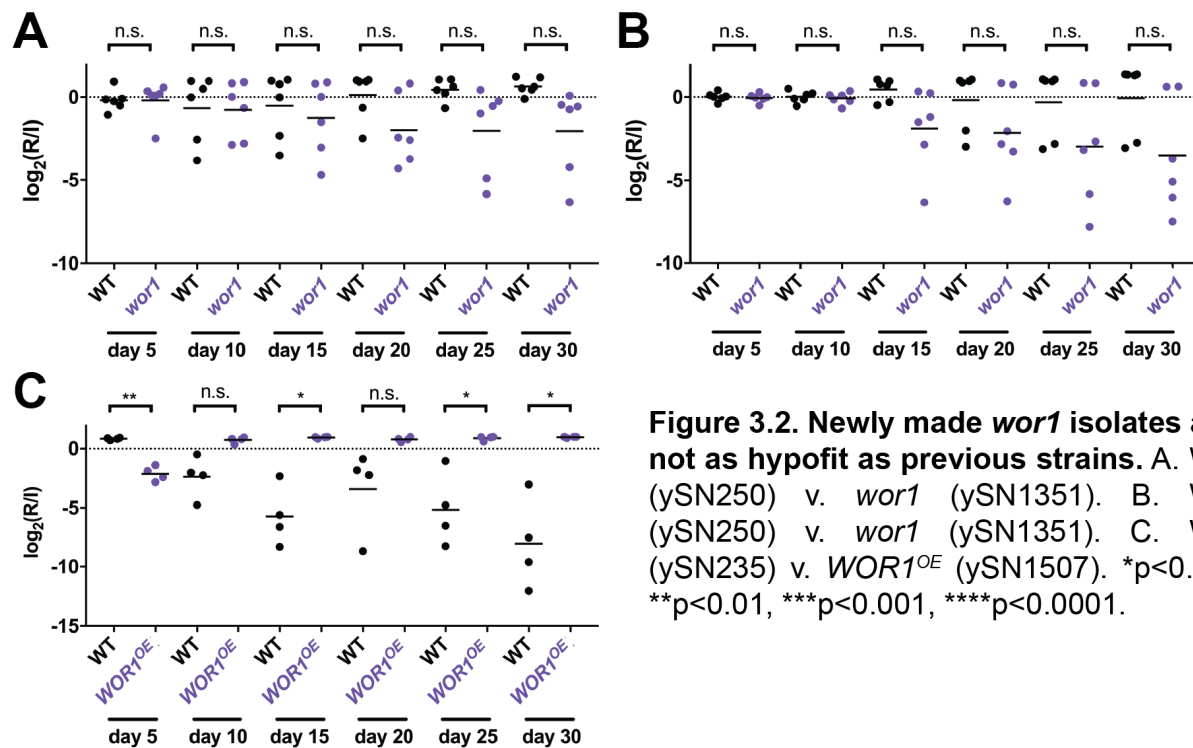


Figure 3.2. Newly made *wor1* isolates are not as hypofit as previous strains. A. WT (ySN250) v. *wor1* (ySN1351). B. WT (ySN250) v. *wor1* (ySN1351). C. WT (ySN235) v. *WOR1^{OE}* (ySN1507). * $p < 0.05$, ** $p < 0.01$, *** $p < 0.001$, **** $p < 0.0001$.

3.2.2. Overexpression of transcription factors leads to commensal phenotypes

As another layer of validation of the transcription factor phenotypes and to prepare for epistasis experiments, we created strains that overexpressed *WOR2*, *WOR3*, *WOR4*, *CZF1* and *AHR1*. Expectedly, *WOR2* and *WOR4* overexpression led to decreased commensal fitness (Figure 3.3.A,C). Overexpression of *CZF1* appeared to have no effect on commensal fitness and did not lead to a change in cell morphology as had been the case with *WOR1^{OE}* (Figure 3.3.D,E, data not shown for morphology). One isolate of *AHR1^{OE}* was hyperfit by day 10 and the other only began to show a statistically significant increase compared to wild type at day 30 (Figure 3.3.F,G). Surprisingly, overexpression of *WOR3* led to hyperfilamentation *in vitro* but decreased filamentation *in vivo* concomitant with enhanced commensal fitness (Figure 3.3.B).

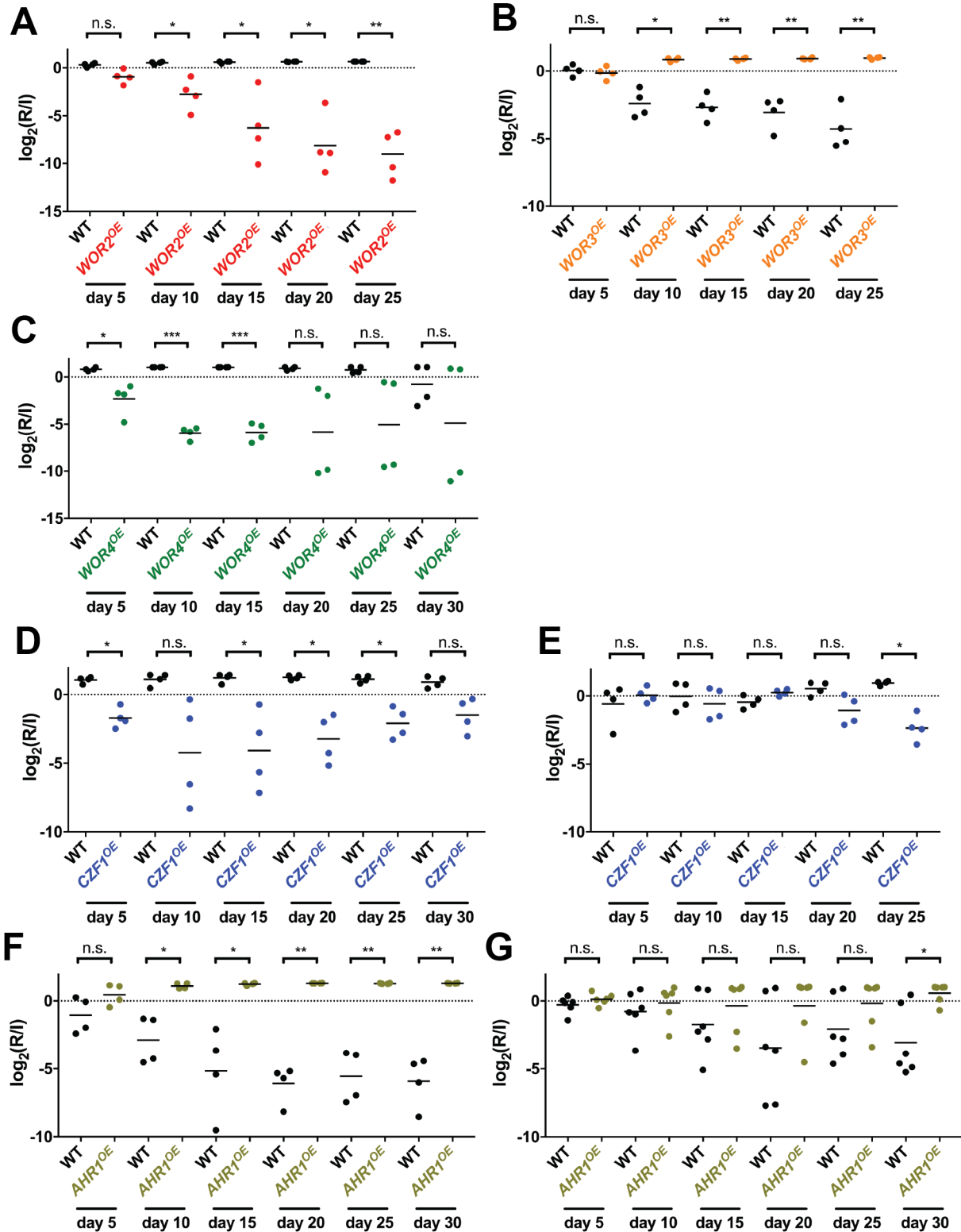
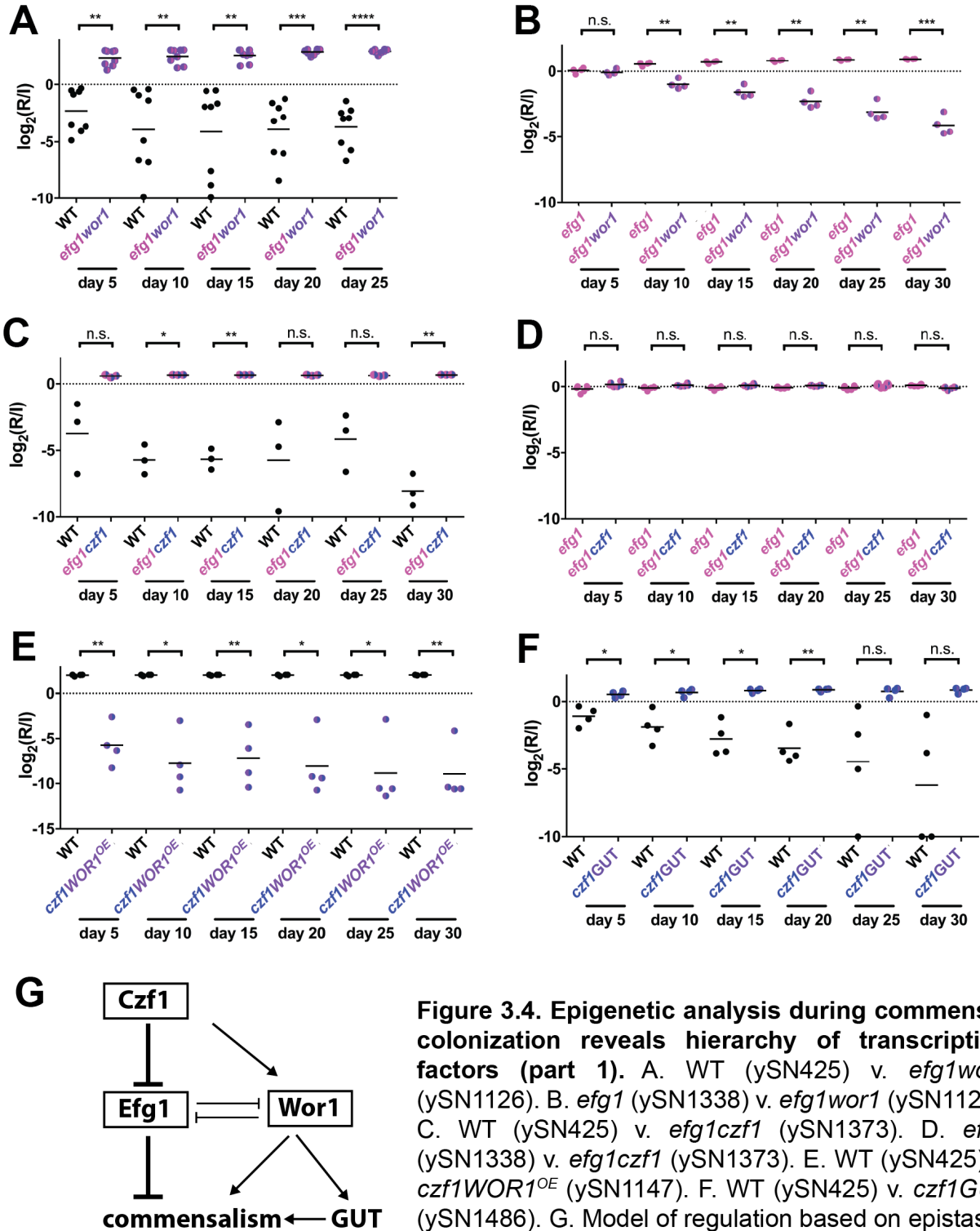


Figure 3.3. Overexpression competitions. A. WT (ySN425) v. *WOR2*^{OE} (ySN1251). B. WT (ySN425) v. *WOR3*^{OE} (ySN1245). C. WT (ySN425) v. *WOR4*^{OE} (ySN1533). D. WT (ySN425) v. *CZF1*^{OE} (ySN1447). E. WT (ySN425) v. *CZF1*^{OE} (ySN1445). F. WT (ySN425) v. *AHR1*^{OE} (ySN1522). G. WT (ySN425) v. *AHR1*^{OE} (ySN1525). *p<0.05, **p<0.01, ***p<0.001, ****p<0.0001.

3.2.3. Genetic epistasis reveals rewiring between the transcriptional circuits controlling sex and commensal fitness

To define the relationship between these different transcription factors and their hierarchy in commensal fitness, we performed epistasis analysis by introducing two mutations with opposite phenotypes into the same strain and determining commensal fitness (e.g. creating an *efg1wor1* strain because *efg1* is hyperfit on its own and *wor1* is hypofit). We first characterized an *efg1wor1* strain in competition with wild type. This strain performed better than wild type at all time points (**Figure 3.4.A**). Clearly the *efg1* phenotype dominates in this strain so we next wanted to know if *Wor1* had any contribution to fitness in an *efg1* background. The *efg1* strain was transformed with a signature-tagged *C.d.ARG4* marker to create an isogenically matched strain to use in competition with the *efg1wor1* strain. Competition between *efg1* and *efg1wor1* resulted in the *efg1* strain dominating (**Figure 3.4.B**). This suggests that *Efg1* has both *Wor1*-dependent and –independent regulatory mechanisms in the gut. To determine the relationship between *Efg1* and *Czf1*, we created an *efg1czf1* double mutant and competed it against either isogenic wild type or *efg1* strains (**Figure 3.4.C,D**). The *efg1czf1* strain outcompeted wild type but had identical fitness to the *efg1* mutant. This suggests *Czf1* is upstream of *Efg1* in regulating commensalism. This would partially explain why a *CZF1^{OE}* strain had no additional fitness advantage over wild type if *Czf1* must work through *Efg1*.

WOR1 overexpression leads to a switch in cell morphology and, subsequently, to increased commensal fitness. To test whether *Czf1* contributes to the GUT cell phenotype in addition to commensalism, we generated a *czf1* strain that overexpressed *WOR1* and competed it against wild type (**Figure 3.4.E**). This strain eventually lost, leading to the conclusion that not even *WOR1* overexpression can compensate for loss of *Czf1*. Because the *czf1WOR1^{OE}* strain decreased abundance quickly, we were unable to determine in competition whether that strain could form GUT cells. In a monotypic infection with the *czf1WOR1^{OE}* strain, GUT cells could eventually be detected if cells were observed microscopically because the gross colony



morphology did not match that seen for *WOR1* overexpression alone in that it still appeared to be the same as the starting strain (data not shown). We had previously generated a *WOR1^{OE}*

strain that had open markers that would allow us to manipulate GUT cells *in vitro*. This strain was passaged through the mouse GI tract and resulted in GUT colonies that were stored for future manipulation (**Figure 3.2.C**). Using this strain we were able to create a GUT strain that lacked *CZF1* (termed *czf1*GUT). In competition with an isogenically matched wild type strain, *czf1*GUT had higher commensal fitness (**Figure 3.4.F**). These data point to the requirement for Czf1 during formation but not maintenance of the GUT phenotype.

In an effort to add *Wor2* and *Wor3* into the regulatory diagram, *WOR1* or *CZF1* were knocked out in a *wor2* or *wor3* background. These strains were competed against wild type in our commensal model. Loss of either *WOR1* or *CZF1* did not affect the hyperfit phenotype of the *wor3* background (**Figure 3.5.A,B**). In the *wor2* background, loss of either *WOR1* or *CZF1* resulted in ambiguity. In both competitions, the two cages behaved differently with wild type and the mutant winning in one of the two (**Figure 3.5.C,D**). These results suggest that these transcription factors act on the same regulatory targets. A *wor3* strain overexpressing *WOR2* is hyperfit like the *wor3* background strain (**Figure 3.5.E**). Overexpressing both *WOR1* and *WOR2* in the same strain resulted in a hyperfit phenotype compared to wild type (**Figure 3.5.F,G**). However, this strain did not take on the elongated GUT phenotype characteristic of *WOR1* overexpression alone. Taken together, these data suggest the gain or loss of *WOR2* expression is secondary to other manipulations in white-opaque regulators.

3.2.4. White-opaque regulators are also regulators of filamentation *in vitro*

There is increasing evidence that certain *C. albicans* transcription factors control multiple morphological transitions, with the outcome of a specific transition dependent upon the local environment. Based on our previous work showing a strong inverse correlation between the filamentation program and commensal fitness, we investigated whether the white-opaque regulators also impact filamentation. Wild-type and mutant strains were propagated filament-inducing media (Lee's glucose pH 6.8 and Spider) and assessed for the ability to generate

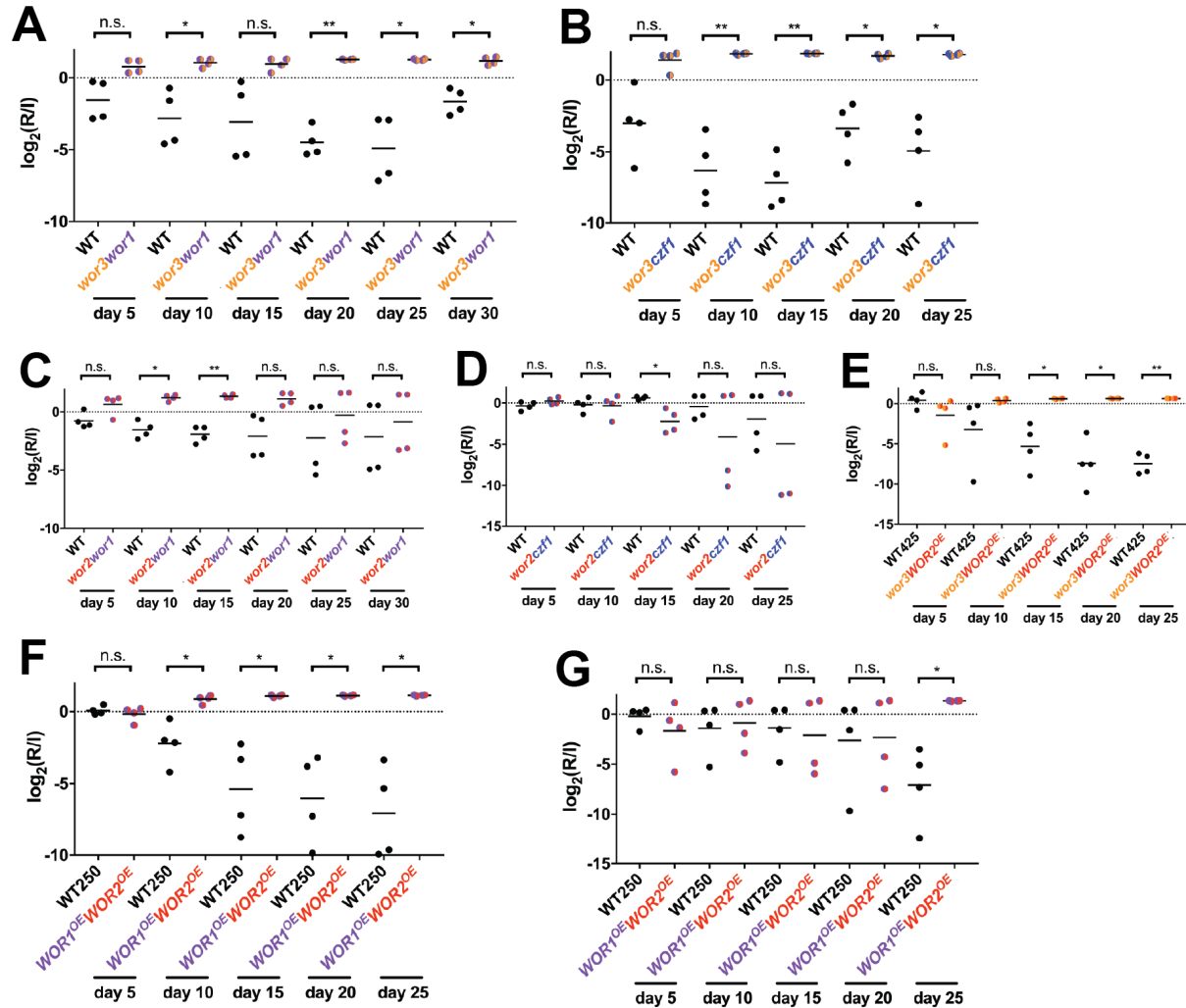


Figure 3.5. Epigenetic analysis during commensal colonization reveals hierarchy of transcription factors (part 2). A. WT (ySN425) v. *wor3wor1* (ySN1341). B. WT (ySN425) v. *wor3czf1* (ySN1377). C. WT (ySN425) v. *wor2wor1* (ySN1340). D. WT (ySN425) v. *wor2czf1* (ySN1375). E. WT (ySN425) v. *wor3WOR2^{OE}* (ySN1245). F. WT (ySN250) v. *WOR1^{OE}WOR2^{OE}* (ySN1656). G. WT (ySN250) v. *WOR1^{OE}WOR2^{OE}* (ySN1657). * $p < 0.05$, ** $p < 0.01$, *** $p < 0.001$, **** $p < 0.0001$.

hyphae and pseudohyphae. As shown in (Figure 3.6), the vast majority of white-opaque regulator mutants do exhibit defects in filamentation (either increased or decreased, compared to wild type). However, unlike the case with canonical regulators of filamentation, mutants affecting the white-opaque regulatory circuit do not exhibit a consistent correlation between the propensity to filament and decreased commensal fitness.

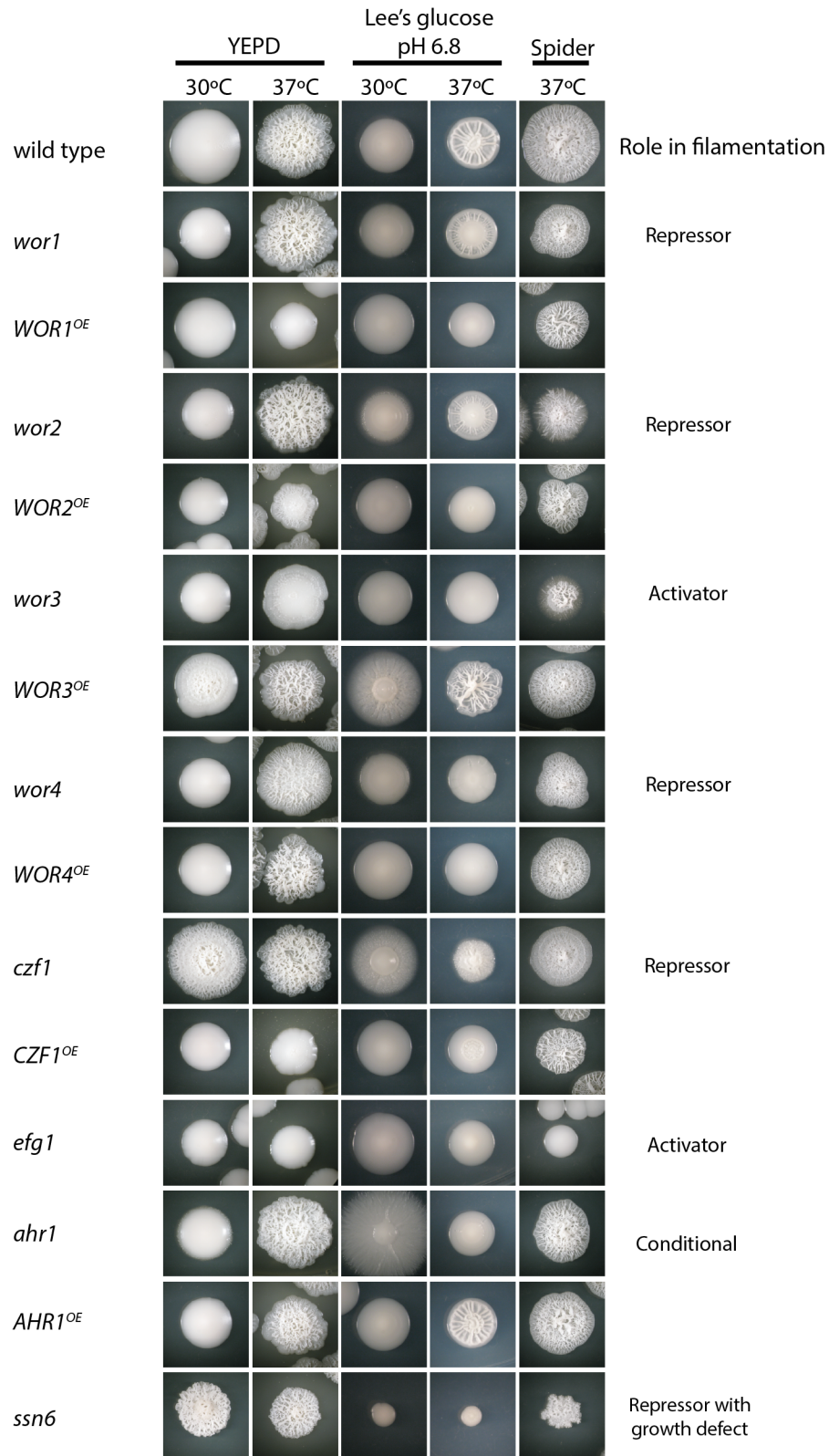


Figure 3.6. Filamentation phenotypes of white-opaque regulators. Single colonies for each strain were plated for 7 days under non-filament inducing (YEPD at 30°C), or filament-inducing (YEPD at 37°C, Lee's glucose pH 6.8 at 30°C, or 37°C, or Spider at 37°C) conditions.

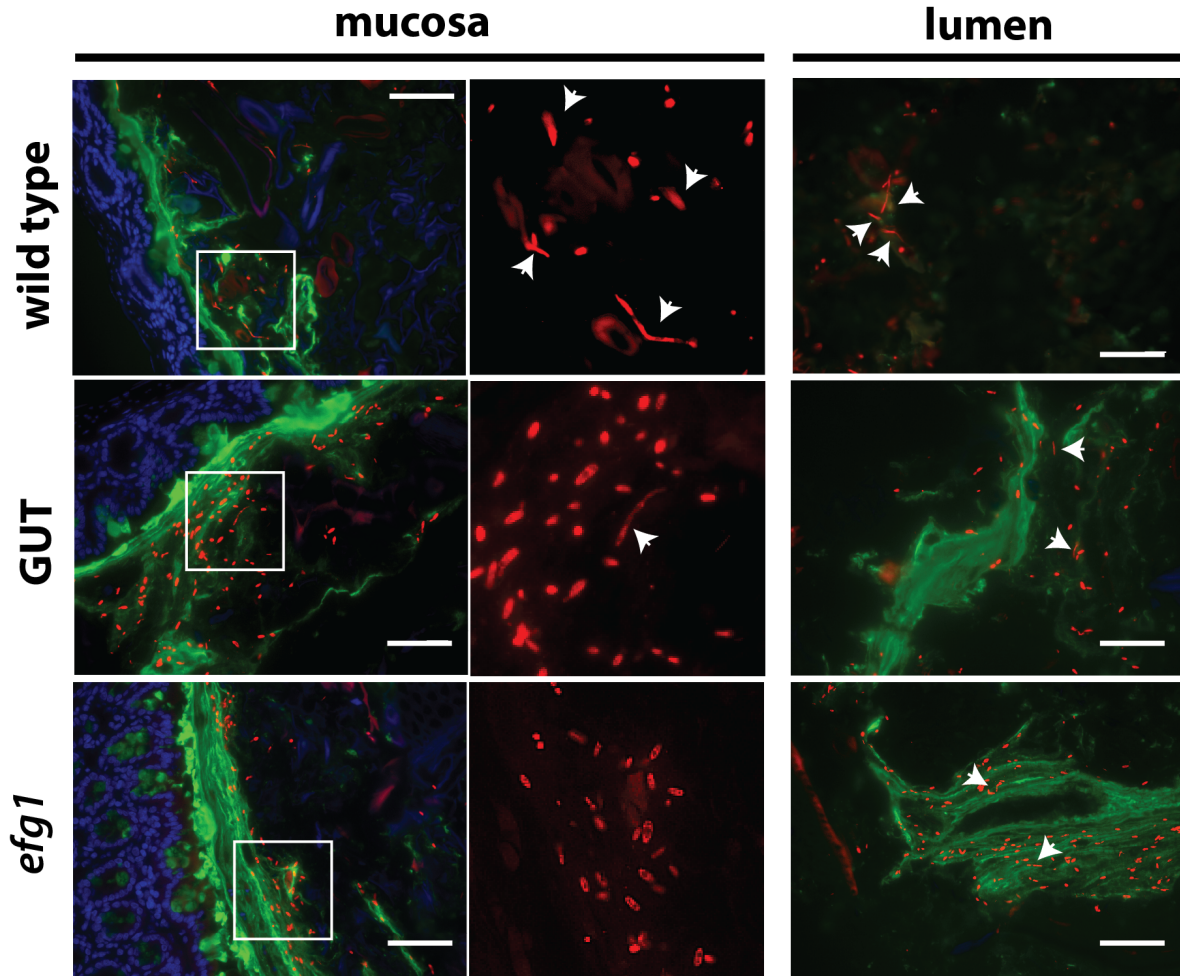


Figure 3.7. GUT cells in the GI tract are hypofilamentous. FISH staining of large intestine mucosa (left) or lumen (right) infected with wild type (ySN425), GUT ($WOR1^{OE}$ post mouse, ySN1045), or *efg1* (ySN1011), respectively. Red = *C. albicans*, green = mucin, blue = nuclei. Scale bar = 20 μ m.

We have previously shown that, in contrast to its *in vitro* phenotype, Ume6 is not required for filamentation within the murine gut. To assess the *in vivo* morphology of white-opaque regulator mutants within the strongest *in vivo* defects, we utilized fluorescent *in situ* hybridization to stain fungal 25S rRNA in the large intestines animals colonized with a single strain. Compared to wild-type *C. albicans*, which exhibits roughly 60% filaments and 40% yeasts in this region of the bowel, GUT cells exhibit far less filamentation (**Figure 3.7**). *efg1* yeasts are slightly elongated but smaller than GUT cells, both *in vitro* and within the host, and this strain

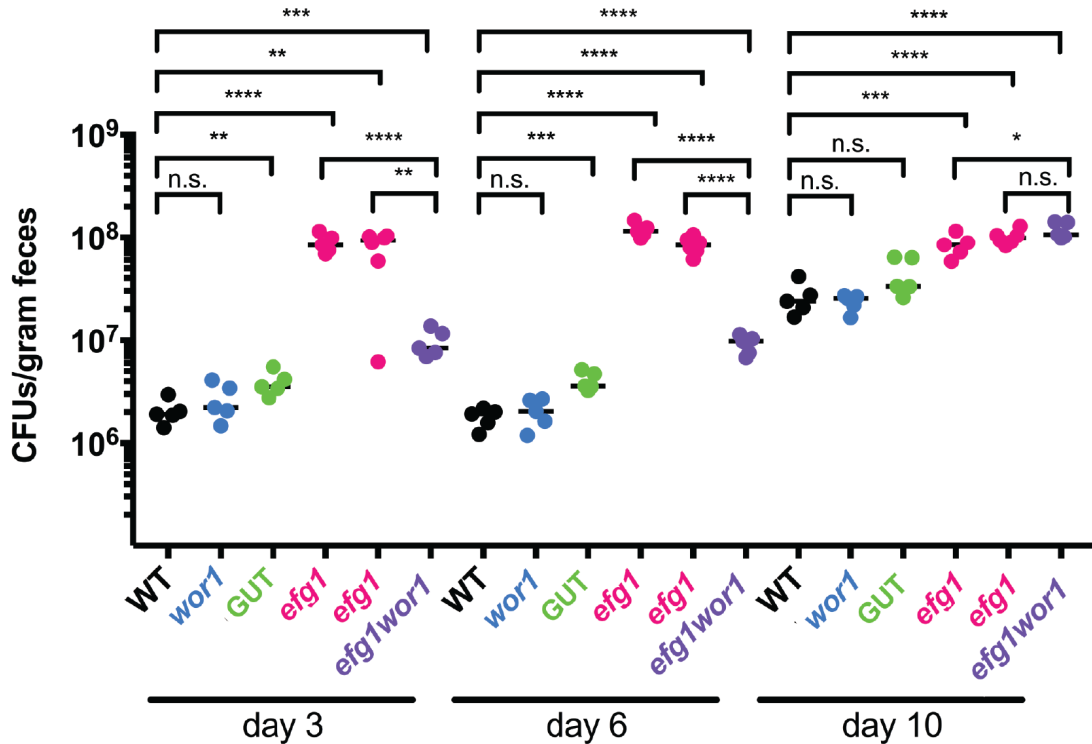


Figure 3.8. Loss of *efg1* or overexpression of *WOR1* confers an early growth advantage in the gut. Colony forming units (CFUs) of wild type (ySN425), *wor1* (ySN1351), GUT (*WOR1*^{OE} post mouse, ySN1045), *efg1* (ySN1011), or *efg1wor1* (ySN1126), respectively. Scale bar = 20 μ m. Unpaired student's t-test * p <0.05, ** p <0.01, *** p <0.001, **** p <0.0001.

colonizes the gut as nearly 100% yeasts (Figure 3.7). Moreover, both GUT cells and *efg1* colonize with a high fungal load, as determined by CFU counts and FISH staining (Figure 3.7, 3.8).

3.2.5. Gene expression changes by mRNA-seq

To determine how white-opaque regulators control commensal fitness, we performed comparative transcriptomics of wild type and mutants recovered directly from murine large intestines. This analysis focused on *Wor1*, *Efg1* and *Czf1*, three core regulators of both the white-opaque switch and commensal fitness that exhibit different genetic relationships in the two processes (Figure 3.9). Mice were monotypically infected with wild-type ySN425, *wor1*, *czf1*, *efg1*, *WOR1*^{OE} GUT, or an *efg1*, *wor1* double mutant, and intestinal contents were extracted at

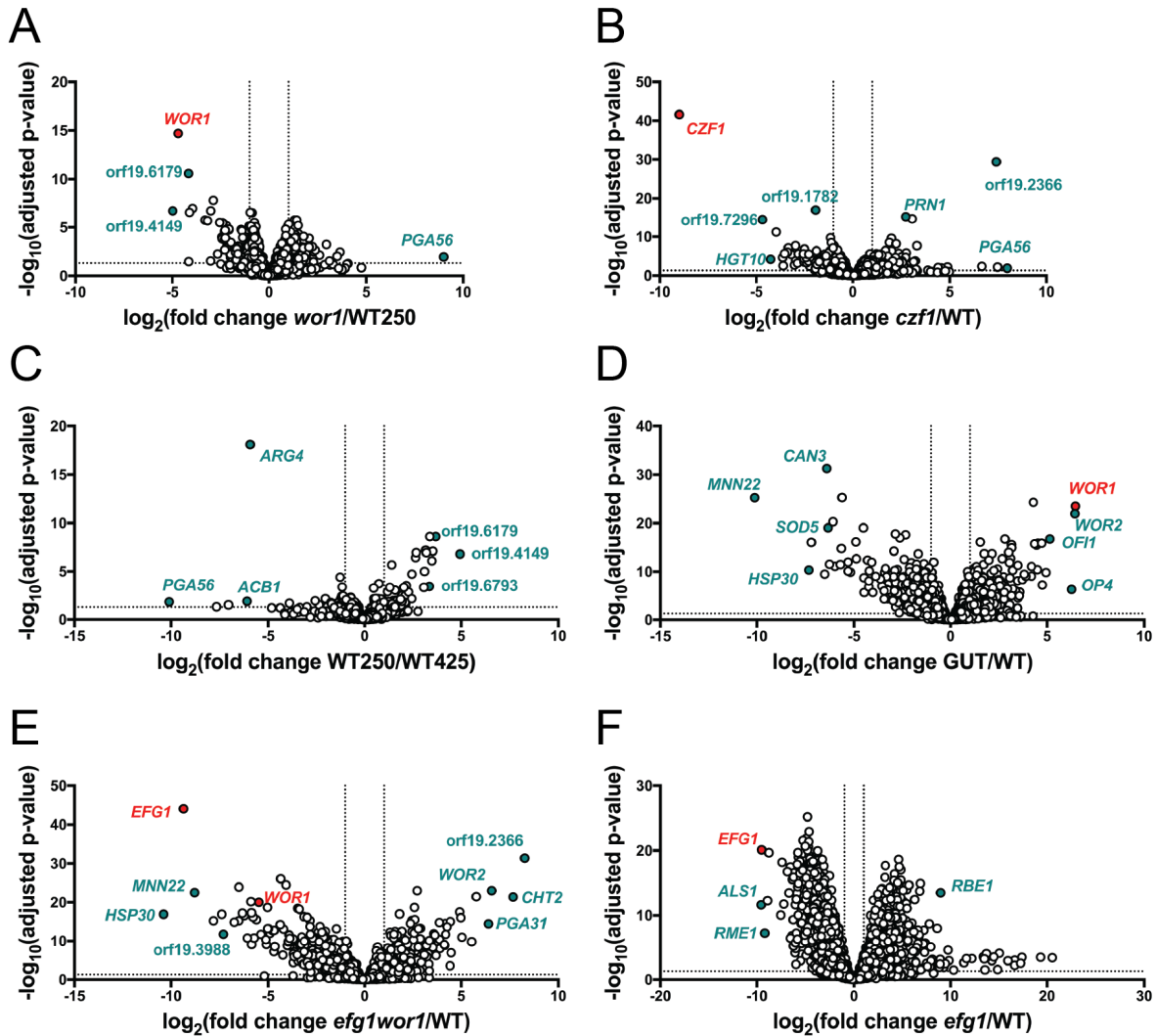


Figure 3.9. Volcano plots of mRNA-seq comparisons in the large intestine. A. WT (ySN250) v. *wor1* (ySN1351). B. WT (ySN250) v. *czf1* (ySN1145). C. WT (ySN250) v. WT (ySN425). D. (ySN425) v. GUT (ySN1045). E. WT (ySN425) v. *efg1wor1* (ySN1126) F. WT (ySN250) v. *efg1* (ySN1011). Vertical dashed lines at 2-fold upregulated or downregulated. Horizontal dashed line at adjusted p-value = 0.05.

day 10. mRNA-seq data for ySN250 from Chapter 2 were used for the wild-type control in comparisons with *wor1* and *czf1*.

Strikingly, all of the strains with hyperfit commensal phenotypes (i.e. *efg1*, GUT, *efg1wor1*) exhibit relative downregulation of hypha-associated genes (**Figure 3.10**). This result is consistent with the increased preponderance of yeasts exhibited by these mutants within the

gut, as detected by FISH.

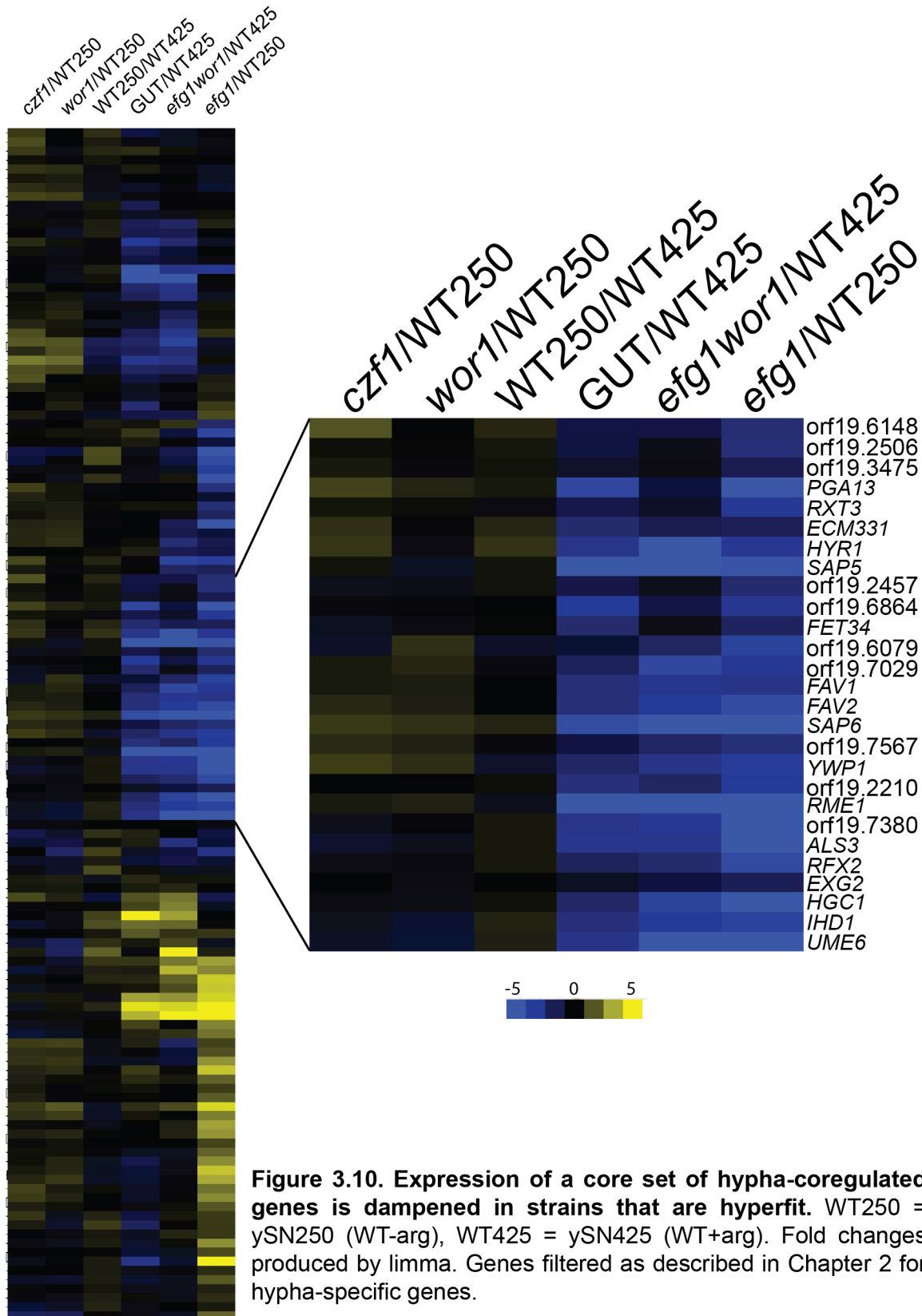


Figure 3.10. Expression of a core set of hypha-coregulated genes is dampened in strains that are hyperfit. WT250 = ySN250 (WT-arg), WT425 = ySN425 (WT+arg). Fold changes produced by limma. Genes filtered as described in Chapter 2 for hypha-specific genes.

In FISH-stained sections of large intestine, *efg1* and GUT strains appear to be enriched in mucin, which is stained with UEA-1. We hypothesized that these cell types may be better at binding to or utilizing mucin as a nutrient source. Reasoning that either type of effector would likely be localized on the *C. albicans* cell surface or secreted into the intestinal lumen, I reviewed a previously generated list of proteins confirmed to be in the *C. albicans* secretome to filter my mRNA-seq data (**Figure 3.11.A**) (26). Within the secretome are a number of enzymes that have been predicted to have activity against a major component of the fungal cell wall, chitin, which is composed of N-acetylglucosamine (GlcNAc) polymers, or serve to break down other external carbohydrates (reviewed in (27)). GlcNAc is also a major component of mucin as well as bacterial membranes. Based on expression patterns of the secretome in the gut, *CHT2*, a predicted chitinase, appears to be the only enzyme with activity against carbohydrates to be highly expressed in all three of the hyperfit mutants, *efg1*, GUT and *efg1wor1*, and downregulated in the hypofit mutant, *czf1* (**Figure 3.11.A**).

Several independent *cht2* isolates were previously generated as part of the Noble deletion collection. A conditional overexpression strain (*tetO-CHT2*) occurs in the *C. albicans* GRACE collection. To test the role of this enzyme in GlcNAc utilization *in vitro*, I plated these strains to synthetic complete (SC) media with glucose (SD) and SC+GlcNAc. Both knockout isolates and the overexpression isolate grew similarly to wild type (ySN250) (**Figure 3.11.B**). However, when plated to a nutrient poor synthetic media, Lee's, with either glucose or GlcNAc, at a neutral (6.8) or acidic pH (5), both *cht2* isolates grew more poorly than wild-type, particularly with GlcNAc as a carbon source. The *tetO-CHT2* strain, which in the presence of doxycycline should behave as another deletion isolate, grew similar to its parent strain CaSS1 with or without doxycycline (**Figure 3.11.B**). The concentration of doxycycline may have needed to be higher than 20 μ g/ml to fully shut off *CHT2* expression. From these observations, we can

conclude that there may be a slight metabolic phenotype on nutrient poor GlcNAc media upon

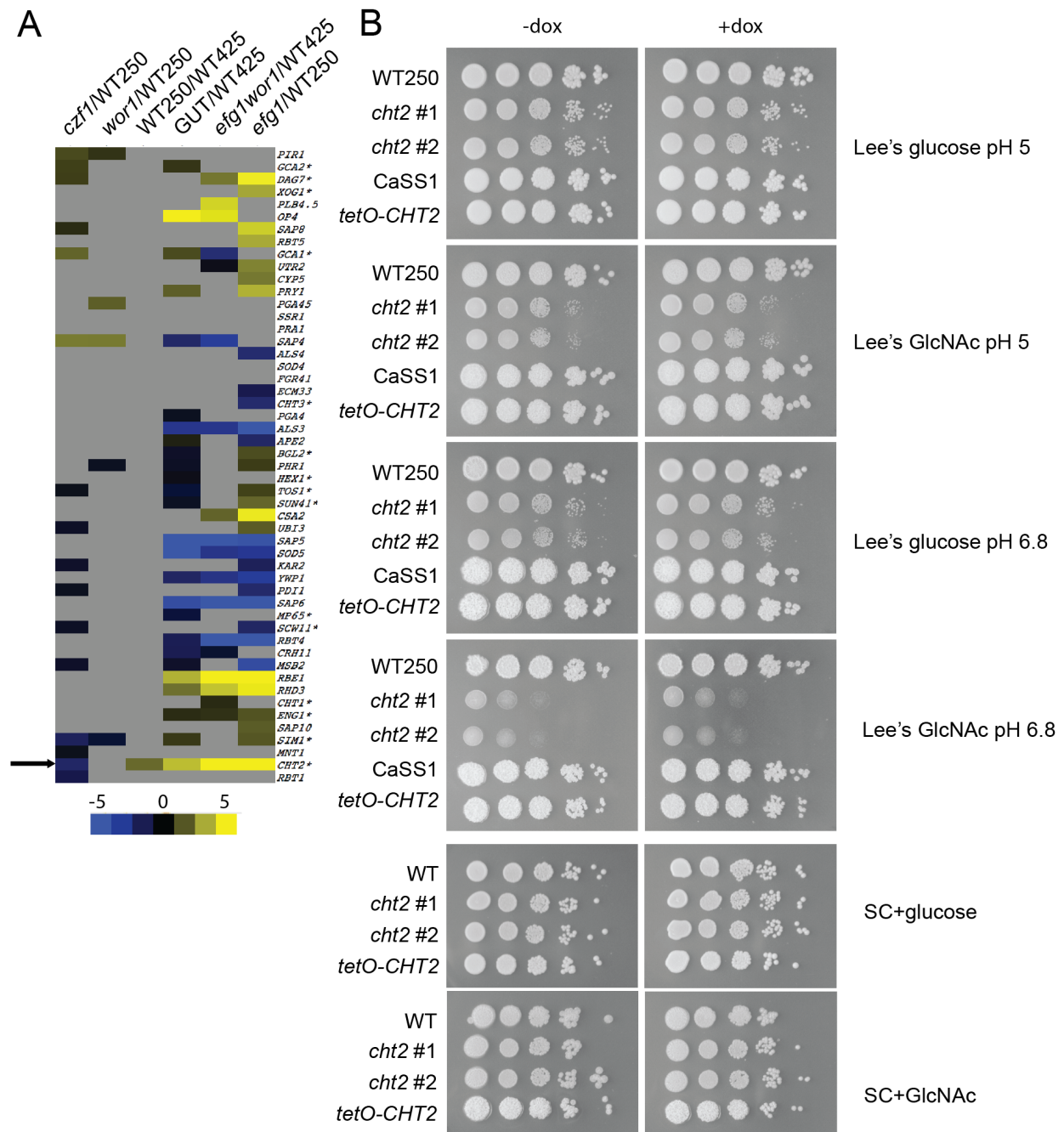


Figure 3.11. Enhanced expression of secreted chitinase may increase fitness of hyperfit strains. A. Fold change of secreted proteins in mutant strains compared to isogenic wild type. WT250 = ySN250 (WT-arg), WT425 = ySN425 (WT+arg). Grey rectangles indicate no significant change in expression. *involved in carbohydrate metabolism based on review of secreted carbohydrate modifying enzymes (27). B. Growth of WT, *cht2* and *tetO-CHT2* mutants on minimal media with different carbon sources. CaSS1 = WT GRACE collection comparator. *tetO-CHT2* is doxycycline-repressible.

deletion of *CHT2* but more characterization will need to be performed to determine its role in *C. albicans* survival in the mammalian gut.

3.2.6. Transcription factors bind upstream of filamentation regulators *in vivo*

To determine the direct regulatory targets of Efg1, Wor1 and Czf1 *in vivo*, we implemented Calling Card-seq, a new technique in *C. albicans*, that had originally been developed for mammalian cells to study transcription factor binding events as an alternative to chromatin immunoprecipitation (28,29). This technique relies on the conservative movement of a transposon by a transcription factor-PiggyBac transposase (TF-PBase) fusion protein from a neutral site in the genome (*LEU2* locus) to a transcription factor binding site upstream of a regulatory target. Efg1-PBase, Wor1-PBase, or Czf1-PBase strains containing two transposons were inoculated into antibiotic-treated mice. Mice were sacrificed after 5, 10, 15, or 20 days, and then the cecum with contents homogenized and plated to SD-histidine-leucine selection media. Sequencing libraries were prepared from recovered cells.

After mapping and selection for high confidence hits, a total of 1542 genes were the target of at least one of the three transcription factors in the mouse gut. As predicted, Wor1, Czf1 and Efg1 bound their own promoters as well as those of the other two transcription factors (depicted in **Figure 3.12**). A total of 86 genes were the target of all three transcription factors (location of tables described in Appendix). These 86 genes included 17 other transcription factors including seven, Wor2, Wor3, Wor4, Ahr1, Tec1, Brg1, and Ume6, that our lab has shown to have roles in commensal fitness (Chapters 2 and 3).

Because of the complex, interlocking nature of these transcription factors in their regulation, combining mRNA-seq results with binding events that occur only in the presence of one of the TF-PBase fusions could yield direct *in vivo* regulatory targets for that transcription factor. As an example, for Efg1 there are only 5 genes, representing 3 intergenic regions, that are not also targets of Wor1 and Czf1. For the two represented intergenic regions, *YCP4*

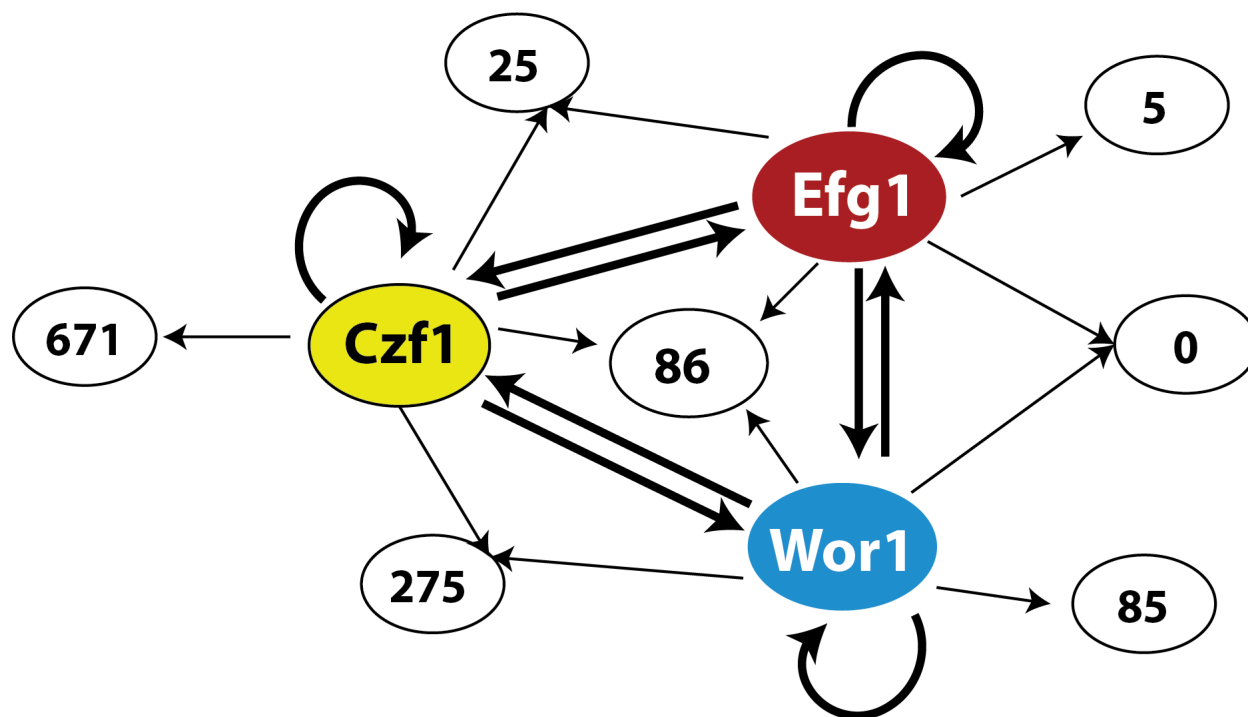


Figure 3.12. Calling card-seq overlap for Efg1-PBase, Czf1-PBase, and Wor1-PBase. Arrows indicate binding events only. White bubble numbers are the number of genes that have overlap between data sets for the transcription factors with arrows pointing to the bubble.

(orf19.5285) and *PST3* (orf19.5286), and orf19.474 and orf19.475, have divergent promoters and sequencing reads were assigned to both genes for each intergenic region. Incorporating the *in vivo* mRNA-seq data for *efg1* compared to wild type, expression in the *efg1* mutant is downregulated for *YCP4* and orf19.474 transcripts, indicating that these genes are the likely targets and are transcriptionally activated by Efg1.

Table 3.1. Efg1-PBase only Calling Card-seq binding events compared to previous ChIP and mRNA-seq data sets.

ORF19 Designation	Common name	Hernday White ChIP	Hernday Opaque ChIP	$\log_2(\text{efg1/WT250})$ mRNA-seq in large intestine	mRNA-seq adjusted p-value	(Efg1-PBase)-(P _{T_{DH3}} -PBase) Calling Card binding events
orf19.2023	<i>HGT7</i>	0.581	0.729	0.8883	0.4072	16
orf19.474		0.796	0.601	-1.3725	0.0009	8
orf19.475		0.796	0.601	-0.3296	0.6400	8
orf19.5286	<i>YCP4</i>	0	0	-2.3483	4.0785E-06	5
orf19.5285	<i>PST3</i>	0	0	0.9990	0.0998	5

Interestingly, *CHT2* is only a direct target of Czf1-PBase. *CHT2* is downregulated in the *czf1* strain, but is upregulated in the *efg1*, *efg1wor1* and GUT strains *in vivo*. These data suggest that perhaps Efg1 or Wor1 is responsible for indirectly regulating Czf1's ability to activate *CHT2*.

3.3 Discussion

Here we present a strong case for the involvement of transcription factors of the white-opaque regulatory network as gastrointestinal commensal regulators. Czf1 and Wor1 act as activators, while Wor2, Wor3, Wor4, Ssn6 and Efg1 are detrimental to commensalism. To tease out a mechanism by which these regulators have an effect, we focused on strains with the strongest phenotypes in our GI competition model by mRNA-seq and Calling card-seq.

Superficially, it would be easy to equate the functions of these regulators with that of the filamentation regulators we have previously described. All white-opaque TFs have at least some mild filamentation phenotype *in vitro*, hyperfit commensal strains have downregulated hypha-coregulated genes, and unlike the *ume6* mutant, which can form hyphae *in vivo* at rates similar to wild type, *efg1* and GUT strains rarely filament *in vivo*. Evidence from our lab as well as others suggests that broadly filamentation is an undesirable commensal characteristic. Therefore, we sought to look beyond the obvious to find something unique to these regulators.

Further digging into the mRNA-seq and Calling card-seq data led up to *CHT2* as a possible downstream effector in the GI tract. As a putative chitinase, the Cht2 enzyme may play an important role in nutrient acquisition during gastrointestinal colonization. The facts that *CHT2* is expressed at lower levels in the GI tract in the hypofit *czf1* strain, high levels in all of the hyperfit mutants we profiled, and is a direct regulatory target of Czf1 *in vivo*, indicated that it is a strong candidate for further characterization in our mouse model of gastrointestinal commensal fitness. The mechanism of action cannot simply be metabolism of GlcNAc containing substrates

as the *cht2* mutants grow more poorly on Lee's minimal media even in the presence of glucose as the carbon source.

Though we did not investigate it here, in the future, the mRNA-seq datasets may also be used to define and investigate a core set of genes that are essential for *C. albicans* survival in the GI tract independent of these transcription factors. The colonization of the *czf1* and *wor1* strains are similar to wild-type in monotypic infections. Thus, the set of genes upregulated in all three strains compared to under standard *in vitro* conditions could yield new insights into the adaptation of *C. albicans* to its host reservoir.

The Calling card-seq method is being continuously improved to limit false positive events and increase transcription factor binding event coverage so that it might be used in host environments where *C. albicans* is not so abundant such as the kidneys. However, these presented data highlight the importance of finding ways to study the molecular mechanisms within the environment of observed phenotype.

Taken together, the results presented here add depth and complexity to the characterization of *C. albicans* commensal interactions with its mammalian host. We have also described several tools that could be widely beneficial to the *Candida albicans* community at large, including *in vivo* transcriptional profiling via mRNA-seq and regulatory binding events via Calling card-seq.

3.4 Materials and Methods

3.4.1. Strains

All yeast strains have been given ySN designations and are described in the Noble Lab yeast strains database. Plasmids are described in the Noble Lab Bacterial strains and plasmids database. All primers are present in the Noble Lab Oligos database and the spreadsheets available on the Noble Lab server and described in the Appendix.

3.4.2. *in vivo mouse studies*

All procedures involving animals were approved by the UCSF Institutional Animal Care and Use Committee. The mouse model of *C. albicans* commensalism was performed essentially as previously described (13,30) with minor modifications. Groups of 8–10-week (18-21 gram) female BALB/c mice were housed 2 per cage, unless otherwise specified, and treated with penicillin 1500 un/ml and streptomycin 2 mg/ml in their drinking water for 7-8 days prior to gavage, and continually throughout the experiment.

For competitions between isogenic wild-type *C. albicans* and mutants of interest, 4-6 mice were gavaged with 10^8 CFUs of a 1:1 mix of wild type and a single mutant in 0.9% saline. Antibiotics were continued, and fecal pellets were collected at specified intervals. *C. albicans* recovery and quantification were performed as described previously (31). Inoculum and fecal pellets from commensal assays were plated on Sabouraud/2% agar (BD) containing ampicillin (50 µg/mL) and gentamicin (15 µg/mL).

3.4.3. *in vivo imaging of Candida albicans*

For FISH experiments, mice were dissected at day 10 post infection, and stomach, small intestine (proximal, medial and distal), cecum and large intestine were placed in tissue cassettes and fixed in methacarn (60% methanol, 30% chloroform, 10% glacial acetic acid) at room temperature from a range of three hours and up to two weeks.

Tissue cassettes were processed post-fixation in the following washes: twice for 35 minutes in 100% methanol, twice for 25 minutes in 100% ethanol, twice for 20 minutes in xylenes (histological grade, Sigma-Aldrich) and then placed in melted paraffin wax for two hours at 70°C. Following processing, sections were embedded by UCSF Cancer Center Immunohistochemistry and Molecular Pathology Core, then sent to Nationwide Histology (Veradale, WA) to be cut into either 4 µm sections.

Fluorescence *in situ* hybridization (FISH) was performed as previously described (32) with the following modifications: hybridization was performed with a pan-fungal DNA probe conjugated to Cy3 (5'-Cy3-CTCTGGCTTCACCCTATTC-3'; Integrated DNA Technologies) (33,34), for three hours at 50°C . Sections were counterstained with DAPI and either FITC conjugated UEA-1 (Sigma) for large intestine sections at 4°C for 45 minutes. Sections were mounted with Vectashield (Vector Laboratories) and imaged on Keyence microscope model BZ-X700.

3.4.4. mRNA-seq library preparation and sequencing

RNA extraction for mRNA-seq was performed as previously described in (35), with modifications. Dow Corning vacuum grease was used for phase separation, instead of phase-lock tubes. Three to five additional acid phenol-chloroform (Ambion) and phenol-chloroform-isoamyl alcohol (Ambion) extractions were added to eliminate endogenous RNases. Following precipitation and resuspension of pellets in RNase-free water, RNA was further cleaned up using the MEGAclear transcription clean-up kit (Ambion) for *wor1* (ySN1351), or Sera-Mag beads for ySN425, *efg1* (ySN1011), *czf1* (ySN1145), *WOR1^{OE}* GUT (ySN1045), and *efg1wor1* (ySN1126). DNase I (NEB) treatment was performed on at least 5 µg RNA for 10 minutes at 37°C. Following DNase treatment, a final acid phenol-chloroform extraction was performed. RNA was then precipitated and resuspended in RNase-free water.

NEBNext Ultra Directional RNA Library Prep Kit for Illumina in combination with NEBNext Poly(A) mRNA Magnetic Isolation Module and NEBNext Multiplex Oligos for Illumina was used to generate mRNA-seq libraries. The protocol provided by NEB was followed using 1 µg total RNA and 14 cycles in the final PCR, with the exception that Ampure XP bead mix was replaced with Sera-Mag Speed Beads (Thermo-Fisher) in a homemade PEG solution (36). Library fragment size was determined using High Sensitivity DNA chips on a 2100 Bioanalyzer (Agilent). Library quantification was performed by qPCR with a library quantification kit from

KAPA Biosystems (KK4824). Sequencing was performed on the UCSF Center for Advanced Technology HiSeq4000.

To determine significant changes in RNA expression between mutants and wild type in the large intestine, reads were mapped to the current haploid *C. albicans* transcriptome (Assembly 21, candidagenome.org) and transcript abundances were then evaluated using kallisto (37). Statistical comparisons of transcript abundances between different samples were performed on estimated counts generated by kallisto using *limma* as previously described (38). Data in heat maps where individual biological replicates are shown were made using transcript per Million mapped reads (tpm) values generated by kallisto. All data files have been deposited on the Noble Lab server and descriptions of location are in the Appendix.

3.4.5. Calling card-seq

From glycerol stocks, Wor1-PBase (ySN1933), Efg1-PBase (ySN1943), and Czf1-PBase (ySN1941) strains were streaked onto YEPD plates and incubated for 16 hours at 30°C. Cells were scraped from these plates, diluted to 5×10^5 CFU/ml and 100 μ l each was spread onto several SD-histidine-leucine plates for 48 hours at 30°C. A disposable yellow loop was used to scrape colonies from the plate into water. From OD measurement, the mixture was resuspended to 5×10^8 CFUs per ml. 200 μ l was gavaged into antibiotic treated mice. One gavage volume was plated to SD-histidine-leucine-arginine plates to select for transposition events that had occurred during inocula preparation that would serve as a background dataset. For subtraction of background transposition events, P_{TDH3}-PBase (ySN1904) was grown in liquid YEPD or YEPD+100 μ M BPS.

After 10, 15, or 20 days animals were sacrificed and each cecum homogenized in 3 ml of PBS pH 7.4. We observed PBS was required to prevent mucus aggregation. 100 μ l was diluted 1:10 in PBS for subsequent plating to determine CFUs/gram cecum. The rest of the

volume was plated 500 μ l per 100 mm SD-histidine-leucine-arginine plate. Cells were allowed to grow for 2 days at 30°C. Colonies that had grown on these plates were collected for subsequent DNA extraction and library preparation. Library preparation and sequencing are described in Section 4.4. All reads from the same strain grown in mice were pooled prior to data analysis. All sequencing file locations are described in the Appendix.

3.5. References

1. Pfaller, M. A., and Diekema, D. J. (2007) Epidemiology of invasive candidiasis: a persistent public health problem. *Clinical microbiology reviews* **20**, 133-163
2. Odds, F. C. (1987) Candida infections: an overview. *Critical reviews in microbiology* **15**, 1-5
3. Diaz, P. I., Hong, B. Y., Dupuy, A. K., and Strausbaugh, L. D. (2017) Mining the oral mycobiome: Methods, components, and meaning. *Virulence* **8**, 313-323
4. Mok, W. Y., and Barreto da Silva, M. S. (1984) Mycoflora of the human dermal surfaces. *Can J Microbiol* **30**, 1205-1209
5. Drell, T., Lillsaar, T., Tummelleht, L., Simm, J., Aaspollu, A., Vain, E., Saarma, I., Salumets, A., Donders, G. G., and Metsis, M. (2013) Characterization of the vaginal micro- and mycobiome in asymptomatic reproductive-age Estonian women. *PloS one* **8**, e54379
6. Nash, A. K., Auchtung, T. A., Wong, M. C., Smith, D. P., Gesell, J. R., Ross, M. C., Stewart, C. J., Metcalf, G. A., Muzny, D. M., Gibbs, R. A., Ajami, N. J., and Petrosino, J. F. (2017) The gut mycobiome of the Human Microbiome Project healthy cohort. *Microbiome* **5**, 153
7. Perez, J. C., Kumamoto, C. A., and Johnson, A. D. Candida albicans commensalism and pathogenicity are intertwined traits directed by a tightly knit transcriptional regulatory circuit. *PLoS biology* **11**, e1001510
8. Pierce, J. V., Dignard, D., Whiteway, M., and Kumamoto, C. A. Normal adaptation of Candida albicans to the murine gastrointestinal tract requires Efg1p-dependent regulation of metabolic and host defense genes. *Eukaryotic cell* **12**, 37-49
9. Rosenbach, A., Dignard, D., Pierce, J. V., Whiteway, M., and Kumamoto, C. A. (2010) Adaptations of Candida albicans for growth in the mammalian intestinal tract. *Eukaryotic cell* **9**, 1075-1086
10. Pierce, J. V., and Kumamoto, C. A. Variation in Candida albicans EFG1 expression enables host-dependent changes in colonizing fungal populations. *mBio* **3**, e00117-00112
11. White, S. J., Rosenbach, A., Lephart, P., Nguyen, D., Benjamin, A., Tzipori, S., Whiteway, M., Meccas, J., and Kumamoto, C. A. (2007) Self-regulation of Candida albicans population size during GI colonization. *PLoS pathogens* **3**, e184

12. Bohm, L., Torsin, S., Tint, S. H., Eckstein, M. T., Ludwig, T., and Perez, J. C. (2017) The yeast form of the fungus *Candida albicans* promotes persistence in the gut of gnotobiotic mice. *PLoS pathogens* **13**, e1006699
13. Pande, K., Chen, C., and Noble, S. M. Passage through the mammalian gut triggers a phenotypic switch that promotes *Candida albicans* commensalism. *Nat Genet* **45**, 1088-1091
14. Lohse, M. B., Ene, I. V., Craik, V. B., Hernday, A. D., Mancera, E., Morschhäuser, J., Bennett, R. J., and Johnson, A. D. (2016) Systematic Genetic Screen for Transcriptional Regulators of the *Candida albicans* White-Opaque Switch. *Genetics* **203**, 1679-1692
15. Hernday, A. D., Lohse, M. B., Fordyce, P. M., Nobile, C. J., DeRisi, J. L., and Johnson, A. D. (2013) Structure of the transcriptional network controlling white-opaque switching in *Candida albicans*. *Molecular microbiology* **90**, 22-35
16. Hernday, A. D., Lohse, M. B., Nobile, C. J., Noiman, L., Laksana, C. N., and Johnson, A. D. (2016) Ssn6 Defines a New Level of Regulation of White-Opaque Switching in *Candida albicans* and Is Required For the Stochasticity of the Switch. *mBio* **7**
17. Lohse, M. B., Hernday, A. D., Fordyce, P. M., Noiman, L., Sorrells, T. R., Hanson-Smith, V., Nobile, C. J., DeRisi, J. L., and Johnson, A. D. Identification and characterization of a previously undescribed family of sequence-specific DNA-binding domains. *Proceedings of the National Academy of Sciences of the United States of America* **110**, 7660-7665
18. Lohse, M. B., and Johnson, A. D. (2016) Identification and Characterization of Wor4, a New Transcriptional Regulator of White-Opaque Switching. *G3 (Bethesda)* **6**, 721-729
19. Lohse, M. B., Zordan, R. E., Cain, C. W., and Johnson, A. D. (2010) Distinct class of DNA-binding domains is exemplified by a master regulator of phenotypic switching in *Candida albicans*. *Proceedings of the National Academy of Sciences of the United States of America* **107**, 14105-14110
20. Zordan, R. E., Galgoczy, D. J., and Johnson, A. D. (2006) Epigenetic properties of white-opaque switching in *Candida albicans* are based on a self-sustaining transcriptional feedback loop. *Proceedings of the National Academy of Sciences of the United States of America* **103**, 12807-12812
21. Zordan, R. E., Miller, M. G., Galgoczy, D. J., Tuch, B. B., and Johnson, A. D. (2007) Interlocking transcriptional feedback loops control white-opaque switching in *Candida albicans*. *PLoS biology* **5**, e256
22. Srikantha, T., Borneman, A. R., Daniels, K. J., Pujol, C., Wu, W., Seringhaus, M. R., Gerstein, M., Yi, S., Snyder, M., and Soll, D. R. (2006) TOS9 regulates white-opaque switching in *Candida albicans*. *Eukaryotic cell* **5**, 1674-1687
23. Wang, H., Song, W., Huang, G., Zhou, Z., Ding, Y., and Chen, J. *Candida albicans* Zcf37, a zinc finger protein, is required for stabilization of the white state. *FEBS Lett* **585**, 797-802
24. Doedt, T., Krishnamurthy, S., Bockmuhl, D. P., Tebarth, B., Stempel, C., Russell, C. L., Brown, A. J., and Ernst, J. F. (2004) APSES proteins regulate morphogenesis and metabolism in *Candida albicans*. *Molecular biology of the cell* **15**, 3167-3180
25. Lo, H. J., Kohler, J. R., DiDomenico, B., Loebenberg, D., Cacciapuoti, A., and Fink, G. R. (1997) Nonfilamentous *C. albicans* mutants are avirulent. *Cell* **90**, 939-949

26. Sorgo, A. G., Heilmann, C. J., Dekker, H. L., Brul, S., de Koster, C. G., and Klis, F. M. (2010) Mass spectrometric analysis of the secretome of *Candida albicans*. *Yeast* **27**, 661-672
27. Klis, F. M., and Brul, S. (2015) Adaptations of the Secretome of *Candida albicans* in Response to Host-Related Environmental Conditions. *Eukaryotic cell* **14**, 1165-1172
28. Wang, H., Mayhew, D., Chen, X., Johnston, M., and Mitra, R. D. (2012) "Calling cards" for DNA-binding proteins in mammalian cells. *Genetics* **190**, 941-949
29. Wang, H., Mayhew, D., Chen, X., Johnston, M., and Mitra, R. D. (2011) Calling Cards enable multiplexed identification of the genomic targets of DNA-binding proteins. *Genome research* **21**, 748-755
30. Chen, C., Pande, K., French, S. D., Tuch, B. B., and Noble, S. M. (2011) An iron homeostasis regulatory circuit with reciprocal roles in *Candida albicans* commensalism and pathogenesis. *Cell host & microbe* **10**, 118-135
31. Noble, S. M., French, S., Kohn, L. A., Chen, V., and Johnson, A. D. Systematic screens of a *Candida albicans* homozygous deletion library decouple morphogenetic switching and pathogenicity. *Nat Genet* **42**, 590-598
32. Johansson, M. E., and Hansson, G. C. (2012) Preservation of mucus in histological sections, immunostaining of mucins in fixed tissue, and localization of bacteria with FISH. *Methods in molecular biology* **842**, 229-235
33. Da Silva, R. M., Jr., Da Silva Neto, J. R., Santos, C. S., Frickmann, H., Poppert, S., Cruz, K. S., Koshikene, D., and De Souza, J. V. (2015) Evaluation of fluorescence in situ hybridisation (FISH) for the detection of fungi directly from blood cultures and cerebrospinal fluid from patients with suspected invasive mycoses. *Ann Clin Microbiol Antimicrob* **14**, 6
34. Amann, R. I., Krumholz, L., and Stahl, D. A. (1990) Fluorescent-oligonucleotide probing of whole cells for determinative, phylogenetic, and environmental studies in microbiology. *Journal of bacteriology* **172**, 762-770
35. Turnbaugh, P. J., Ridaura, V. K., Faith, J. J., Rey, F. E., Knight, R., and Gordon, J. I. (2009) The effect of diet on the human gut microbiome: a metagenomic analysis in humanized gnotobiotic mice. *Science translational medicine* **1**, 6ra14
36. Rohland, N., and Reich, D. (2012) Cost-effective, high-throughput DNA sequencing libraries for multiplexed target capture. *Genome research* **22**, 939-946
37. Bray, N. L., Pimentel, H., Melsted, P., and Pachter, L. (2016) Near-optimal probabilistic RNA-seq quantification. *Nature biotechnology* **34**, 525-527
38. Ritchie, M. E., Phipson, B., Wu, D., Hu, Y., Law, C. W., Shi, W., and Smyth, G. K. (2015) limma powers differential expression analyses for RNA-sequencing and microarray studies. *Nucleic acids research* **43**, e47

Chapter 4. A new method for studying transcription factor dynamics, Calling Card-seq in *C. albicans*

4.1. Introduction

Candida albicans is an opportunistic fungal pathogen that does not have a known environmental niche. Instead this organism normally exists as a commensal of mammals and these colonizing strains are thought to become virulent upon perturbation of the host such as immune deficits. This presents a challenge to developing *in vitro* conditions that could be used to mimic *C. albicans* behavior because it can occupy many different complex host environments, ranging from the gastrointestinal tract to end organs. Previously, to study transcription factor binding events in *C. albicans*, the field was limited to using chromatin immunoprecipitation (ChIP) under *in vitro* conditions that lacked the complexity of the host environment (1).

Reliance on ChIP presents several challenges to study gene expression regulation by transcription factors *in vivo*. For some *C. albicans* transcription factors, such as Efg1, it is known that their regulatory targets change depending on the *in vitro* condition used to grow the cells. For other transcription factors, most notably Wor1, standard FLAG and HA tags interfere with protein function and custom antibodies must be raised to epitopes of these proteins. Custom rabbit polyclonal antibodies that are of high specificity are hard to raise and of finite quantity, limiting the number of assays performed with each antibody.

An alternative technique known as Calling Card-seq was validated to study transcription factor binding events in *Saccharomyces cerevisiae* and human cell culture (2-5). Briefly, this system relies on movement of a transposon by a transcription factor-transposase fusion that results in integration of the transposon near the transcription factor binding site. Next-generation sequencing libraries generated from the sites of integration are analyzed to determine transcription factor regulatory targets.

Here we present a *C. albicans* specific system based on PiggyBac transposase Calling Card-seq developed for mammalian cell culture that can be used to study transcription factor

binding events. Our validation *in vitro* makes using this system to study the dynamics of *C. albicans* transcription factors *in vivo* a possible alternative to CHIP-seq. This technique has limited reagent requirements and the potential to be a powerful system to complement RNA-seq to study molecular regulation in the host.

4.2. Results

4.2.1. Codon optimized PiggyBac transposase is active in *Candida albicans*

In order to determine whether any aspect of the previously described Calling Card methods could be used in *C. albicans*, I first needed to validate transposase activity in *C. albicans*. Genetic manipulation of *C. albicans* must be performed through integration of non-native DNA sequences into the genome. Based on this restriction, I reasoned that the transposon would have to be made so that excision and reintegration events could be selected for using auxotrophic markers. Three such markers, *HIS1*, *LEU2*, and *ARG4* were available to us in the strain ySN152. To select for excision from the integration site, having a split marker that could reproducibly recombine to produce a coding sequence for a functional protein was of paramount importance. The mammalian PiggyBac transposase system was therefore more attractive for this purpose because the transposon is integrated and excised conservatively from any TTAA site leaving no trace of its previous presence.

As part of the CTG clade, *C. albicans* translates CUG codons as serine not leucine (6). A plasmid containing the human PiggyBac transposase (PBase) nucleotide sequence was obtained from Rob Mitra's lab at Washington University, St. Louis but it could not be used directly in *C. albicans* due to non-optimal codon usage. To mitigate mistranslation of ambiguous codons, we contracted GenScript to create a *C. albicans* codon optimized PBase based on the amino acid sequence obtained from the Mitra lab. GenScript synthesized the codon optimized PBase nucleotide sequence on a plasmid.

PBase has its own nuclear localization sequence and thus the untethered PBase is still able to enter the nucleus and interact with its transposon (7). To test whether the codon optimized version had activity in *C. albicans*, I generated a plasmid with *TDH3* homology flanking the PBase sequence to direct the transposase DNA to the *TDH3* gene locus (diagrammed **Figure 4.1.A**). This put PBase under the control of the constitutively active *TDH3* promoter. This construct was transformed into a *C. albicans* strain containing the split *ARG4::tn-HIS1* transposon version 1 (diagrammed **Figure 4.1.B**, construction described in Materials and Methods). After selection for the transformation of this construct, cells were streaked to SD-histidine-arginine. The strain containing the PBase construct grew under selection while the starting transposon only strain did not (**Figure 4.1.C**). This indicated that the untethered PBase was translated and had transposase activity in *C. albicans*.

4.2.2. Iron transcription factors

As part of the validation of this technique, I chose to start by profiling iron utilization regulating transcription factors that had previously been characterized by our lab under *in vitro* conditions by whole genome RNA expression and ChIP-chip (8). Sef1, a $Zn(II)_2Cys_6$ DNA-binding protein, is expressed under low iron conditions and has ~163 regulatory targets (8). Sfu1 is a GATA-type transcription factor for which ChIP-chip identified only 21 regulatory targets but the data were much noisier than for Sef1 so the regulon could be incomplete due to inability to call peaks with confidence (8). Sfu1 acts upstream of Sef1, binding to its promoter and downregulating its expression as well as that of iron uptake genes. Sef1 binds Hap43, the regulatory component of the CCAAT-complex, as well as genes involved in iron uptake, activating their expression.

After 2 days of growth in triplicate on high iron (YEPD) or low iron (YEPD+0.25 mM BPS) plates, Sef1-PBase, Sfu1-PBase, P_{SEF1} -PBase, and P_{SEF1} -PBase strains were replica plated to SD-histidine-arginine plates. After 2 days of selection at 30°C, cells were collected and sequencing libraries prepared. All strains grew as lawns on YEPD while individual colonies were

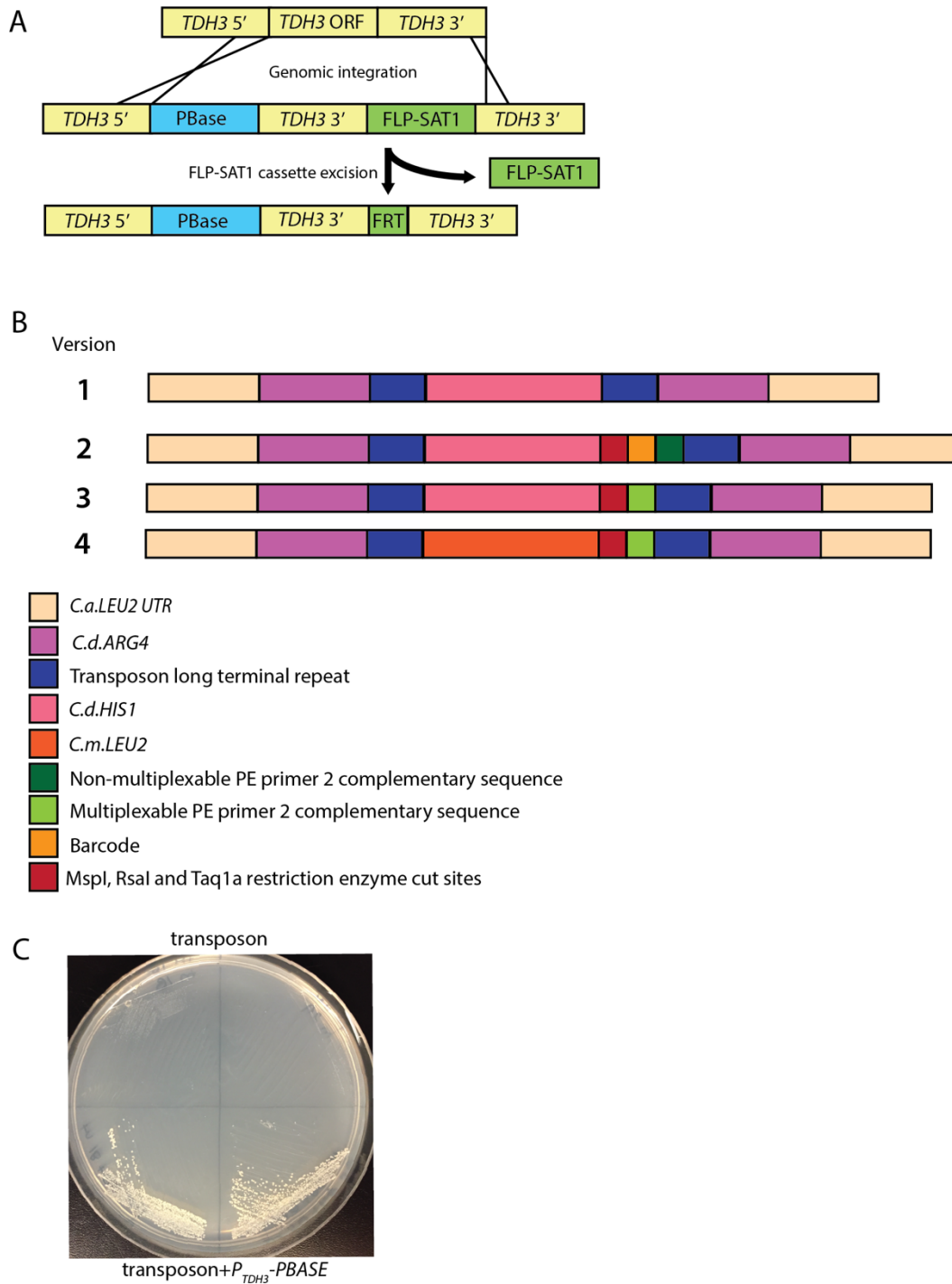


Figure 4.1. PiggyBac transposase validation. A. Steps in construction of the P_{TDH3} -PBASE strains. B. Schematics of every version of the PiggyBac transposon. PE = paired end, *C.a.* = *Candida albicans*, *C.d.* = *Candida dubliniensis*, *C.m.* = *Candida maltosa*. C. Strains with transposon and P_{TDH3} -PBASE integration grew on SD-histidine-arginine media.

distinguishable on YEPD+BPS. After sequencing, none of the strains had enough coverage to assess binding events from individually grown plates, so all reads from each strain were pooled together for further analysis.

In the case of Sef1-PBase, when compared to its P_{SEF1}-PBase background, 38 genes were identified as Sef1 targets. Of these 18 (47%) were also identified by ChIP-chip (**Figure 4.2.B**). Sef1 binds to the promoter of Hap43 and controls its expression (8). An additional 3 Sef1-PBase targets that are not ChIP-chip targets are annotated in the *Candida* Genome Database as Hap43 regulated but not Hap43 ChIP-chip targets suggesting that these may be real previously unidentified Sef1 targets. Only 2 intergenic regions, comprising 4 potential regulatory targets have greater than 10 transposition events above untethered background when all libraries are pooled. Untethered PBase expressed from the *SEF1* locus has much higher activity than the Sef1-PBase fusion protein (2084 fusion insertions to 15131 untethered insertions). Clearly, conditions need to be optimized for *SEF1* expression *in vitro* or modifications made to the fusion construct in order to obtain maximal binding target coverage for this transcription factor.

For Sfu1-PBase, using low stringency filtering with 5 or greater insertions above background, 1700 genes were identified as targets. The number of fusion insertions (38185) and untethered insertions (23384) were much closer in scale than Sef1 data. However, these data appeared to be very noisy and only 12 of 21 (57%) targets called by ChIP-chip were present in this data set (**Figure 4.2.C**). Narrowing to the 20 targets with the highest number of insertion events, which comprised 13 intergenic regions, only 2 intergenic regions (*RBE1-FTR1* and *RPR1-SIT1*) had previously been identified by ChIP-chip as Sfu1 targets (**Figure 4.2.D**). However, an additional 6 of the other 11 intergenic regions were annotated as having a role related to iron or were Hap43 regulated. Expression levels of genes bounding two of these intergenic regions, *FET31* and *FRE10*, which have the highest transposon insertions above background, are also higher in an *sfu1* mutant compared to WT under iron replete conditions. Thus, this Calling Card-seq technique may have identified additional direct regulatory targets of Sfu1.

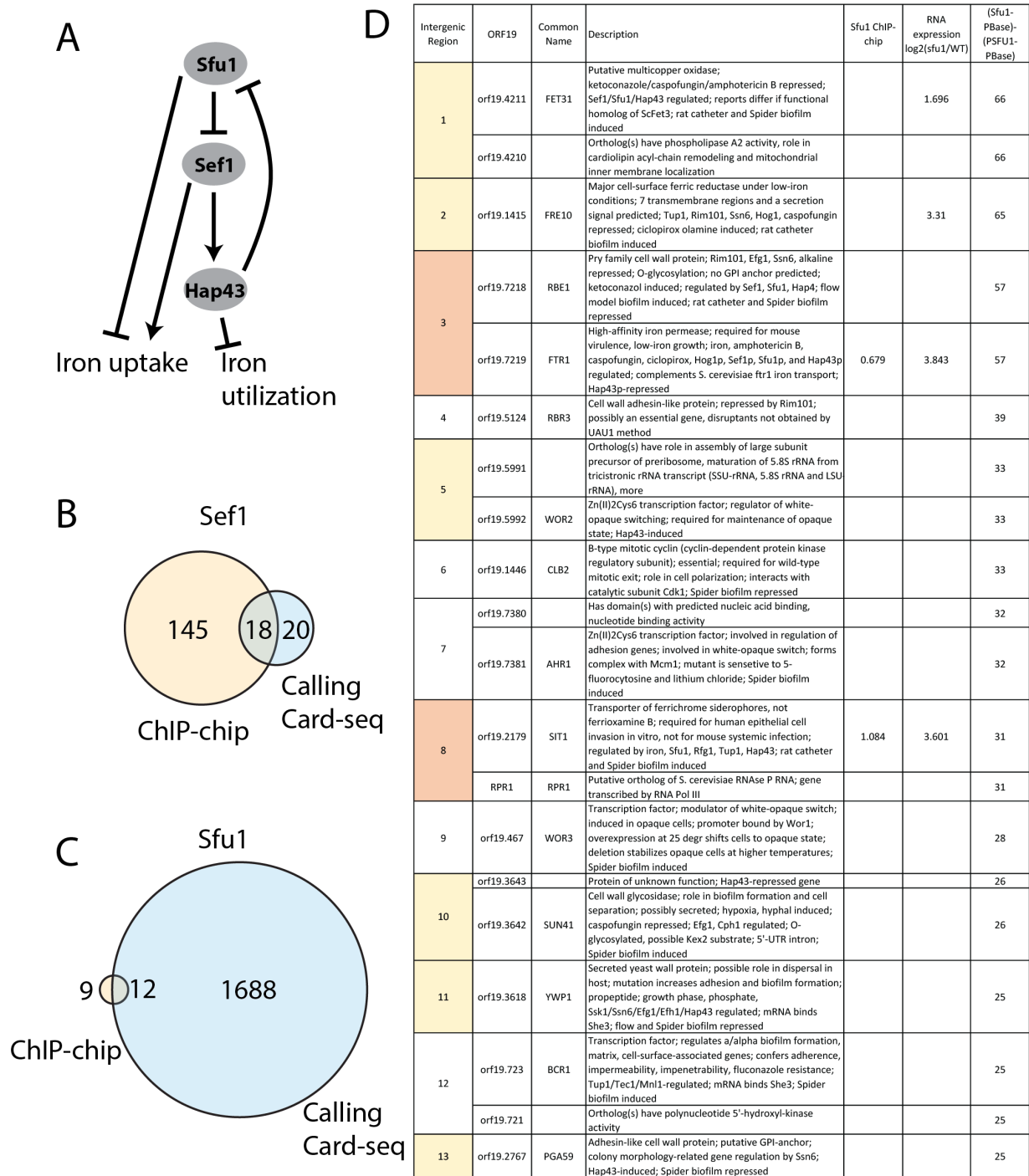


Figure 4.2. Comparison of Calling Card-seq results with ChIP-chip for iron regulated transcription factors. A. Reproduction of proposed iron regulatory network from (8). B. Overlap between Chen ChIP-chip Sef1 peak calls under low iron conditions and my pooled Calling Card-seq under iron replete and limited conditions. C. Overlap between Chen ChIP-chip Sfu1 peak calls under low iron conditions and my pooled Calling Card-seq under iron replete and limited conditions. D. Top 20 Sfu1 binding targets by Calling Card-seq. Orange = called by both ChIP-chip and Calling Card-seq. Yellow = called by Calling Card-seq only but additionally described as Hap43 regulated.

4.2.3. White-opaque regulators

Wor1 and Efg1 are best characterized as transcription factors that act to mutually inhibit each other during the stochastic white^a-opaque^a cell type switch (9-12). Efg1 is an APSES transcription factor with a basic helix loop helix structure, whose deletion has a pleiotropic phenotype in *C. albicans* because it is involved in a number of transcriptional and morphologic changes in response to environmental cues (13). Regulation of Efg1 occurs transcriptionally as well as post-translationally by the PKA pathway (14-16). Recently, Wor1, White-Opaque Regulator 1, has also been shown to play a role in the white^{a/α}-GUT and white^{a/α}-grey^{a/α}-opaque^{a/α} morphological transitions (11,17). Wor1 binds DNA through the recently described WOPR domain (18).

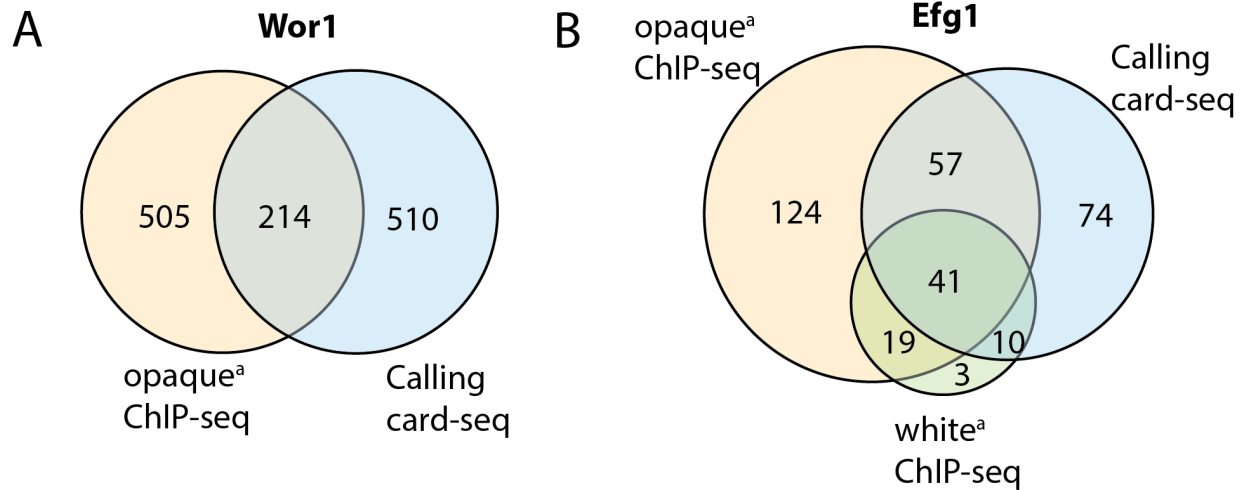
Wor1-PBase *a/α* strains had very low activity when grown on YEPD and then replated to selective media, as expected. To test that the construct was functional, we preliminarily deleted the *MTLa* locus in a Wor1-PBase strain and generated opaque cells. After opaque cell selection, cells were able to grow on the selection medium SD-histidine-arginine. Preparing next-generation sequencing libraries from genomic DNA of the selected cells showed a smear of about 200 bp to 2 kb as opposed to a single distinct band suggesting that the Wor1-PBase fusion was active when expressed under favorable conditions and there was not a stochastic single transposon insertion event that was propagated to all cells (data not shown).

WOR1 is expressed in at about 40-fold higher levels in opaque cells than in white cells (11,19,20), which would make opaque cells a more promising choice for getting high coverage of Wor1 binding sites *in vitro*. The process of generating opaque cells can take several weeks of growth at room temperature and the possibility of a transposition event being propagated over the course of generations made Calling Card-seq in its current version untenable in opaque^{a/α} cells. Previously, the Huang lab showed that low temperature, low pH and Lee's media with GlcNAc as the carbon source favored opaque cell formation (17,21,22). To catch binding events

early, I chose to plate white cells on Lee's GlcNAc pH 5, SC, or YEPD, and grow the colonies for 7 days at 25°C before replica plating. After 7 days, I observed that some colonies were hyperfilamentous but most were yeast in all strains (a/α and a) grown on Lee's GlcNAc pH 5 (data not shown). A similar observation was made during a study of opaque cell filamentation that suggests that these cells would be those that transitioned from white to opaque ^{a/α} or opaque ^{a} (23). Indeed, the highest prevalence of cells that grew after selection on SD-histidine-arginine (i.e. had the highest transposase activity) were those that came from the hyperfilamentous colonies. These observations suggest that on this media, *Wor1* expression occurs at the highest levels in cells that have made a morphological transition. Whether the transition is white yeast to white filaments or, white yeasts to opaque yeasts to opaque filaments, is not clear.

The genome coverage was low for individual *Wor1* samples so all libraries from cells grown on Lee's GlcNAc pH 5, SC, or YEPD were pooled. This resulted in similar numbers of distinct transposon insertions for *Wor1*-PBase fusion (31152) and untethered PBase expressed from the *WOR1* locus (36887). 214 of 504 (42%) of high confidence Calling Card hits are also opaque *Wor1* ChIP-seq hits as defined by Hernday *et al.* 2013 (**Figure 4.3.A**) (9).

Of the four tagged transcription factors, *Efg1*-PBase was the most active. All colonies had at least one transposition event after replica plating on YEPD, Lee's GlcNAc pH 5 and Lee's GlcNAc pH 6.8. However, after sequencing it appeared that the YEPD grown samples were unusable. The Lee's samples had good coverage so I chose to proceed with just those samples. Instead of pooling all conditions, there appeared to be enough coverage to pool just those libraries that were a single strain under a given condition (e.g. 3 biological replicates of Strain 1 *Efg1*-PBase grown on Lee's GlcNAc pH 5 were pooled together). To define high confidence hits, I filtered by presence of 5 insertion events over background of the median of all 8 samples. This resulted in 182 Calling Card-seq peaks of which 41 were also present in both the white and opaque *Efg1* ChIP-seq dataset in (9), 10 were present in the white but not opaque set, and 57



C

ORF19 Assembly	Common Name	Description	Efg1 white ChIP-seq	Efg1 opaque ChIP-seq	(Efg1-PBase)-(PEFG1-PBase) median	Efg1 CCS position	Wor1 opaque ChIP-seq	(Wor1-PBase)-(PWOR1-PBase) median	Wor1 CCS position
orf19.4884	WOR1	Transcription factor ("master switch") of white-opaque phenotypic switching; required to establish and maintain the opaque state; opaque-specific, nuclear; regulates its own expression; suggested role in regulation of adhesion factors	1.002	4.142	20	30	3.992	29	22
orf19.4883		Protein of unknown function; <i>S. cerevisiae</i> ortholog Cos111 confers resistance to the antifungal drug ciclopirox olamine; constitutive expression independent of MTL or white-opaque status; Spider biofilm induced	1.002	4.142	20				
orf19.5992	WOR2	Zn(II)2Cys6 transcription factor; regulator of white-opaque switching; required for maintenance of opaque state; Hap43-induced	0.61	2.248	28	18	2.197	26	31
orf19.5991		Ortholog(s) have role in assembly of large subunit precursor of preribosome, maturation of 5.8S rRNA from tricistronic rRNA transcript (SSU-rRNA, 5.8S rRNA and LSU-rRNA), more	0.61	2.248	28				
orf19.467	WOR3	Transcription factor; modulator of white-opaque switch; induced in opaque cells; promoter bound by Wor1; overexpression at 25 degr shifts cells to opaque state; deletion stabilizes opaque cells at higher temperatures; Spider biofilm induced		4.047	24	23	3.556	31	20
orf19.6713	WOR4	Predicted C2H2 zinc finger protein, involved in transcriptional regulation of white-opaque phenotypic switching; activator of the opaque cell type		1.312	24	24	2.622	14	64
orf19.6715		Ortholog of <i>Candida albicans</i> WO-1 : CAWG_03078		1.312	24		2.622	14	
IG(GCC)1	IG(GCC)1	tRNA-Gly, predicted by tRNAscan-SE; GCC anticodon	1.139	2.996	131.5		2.402	110	
orf19.610	EFG1	bHLH transcription factor; required for white-phase cell type, RPM1 and Spider biofilm formation, hyphal growth, cell-wall gene regulation; roles in adhesion, virulence; Cph1 and Efg1 have role in host cytokine response; binds E-box	1.139	2.996	131.5	1	2.402	110	1
orf19.3127	CZF1	Transcription factor; regulates white-opaque switch; hyphal growth regulator; expression in <i>S. cerevisiae</i> causes dominant-negative inhibition of pheromone response; required for yeast cell adherence to silicone; Spider biofilm induced		2.308	58.5	2	2.52	37	15
orf19.7381	AHR1	Zn(II)2Cys6 transcription factor; involved in regulation of adhesion genes; involved in white-opaque switch; forms complex with Mcm1; mutant is sensitive to 5-fluorocytosine and lithium chloride; Spider biofilm induced			24.5	22	1.891	39	12
orf19.7380		Has domain(s) with predicted nucleic acid binding, nucleotide binding activity			24.5				

Figure 4.3. Comparison of Calling Card-seq results with ChIP-seq for white-opaque transcription factors. A. Overlap between Hernday ChIP-seq Wor1 peak calls for opaque cells from (9) and my pooled Calling Card-seq under opaque favorable conditions. B. Overlap between Hernday ChIP-seq Efg1 peak calls for white and opaque cells and my pooled Calling Card-seq under opaque favorable conditions. C. Core white-opaque transcription factor promoter binding by Hernday ChIP-seq and my Calling Card-seq method. CCS = Calling Card-seq.

were in the opaque but not white, for a combined total of 108 Calling Card-seq targets that were also present in the ChIP-seq datasets (59%) (**Figure 4.3.B**).

Wor1 and Efg1 bind upstream of other white-opaque regulators to inhibit or activate their expression (refer to Chapter 1&3). I looked at whether binding events occurred upstream of these regulators in my Calling Card-seq dataset, and all promoters of core transcription factors, *WOR1*, *WOR2*, *WOR3*, *WOR4*, *EFG1*, *CZF1* and *AHR1* were bound by Wor1 as expected from the ChIP-seq dataset (**Figure 4.3.C**). Efg1 was expected to bind all but the promoter of *AHR1* but in this case, Efg1 also bound upstream of *AHR1*. This indicates that under some circumstances, *AHR1* is also a target of Efg1 though it had not previously been described as such.

4.3. Discussion

Here we present a Calling Card-seq technique that can be used to study *C. albicans* transcription factor binding events both *in vitro* and *in vivo*. We tested transcription factors from four different families of DNA-binding proteins with some level of success in identifying binding events for all four. Interestingly, even the previously untaggable transcription factor, Wor1, showed activity when fused to PBase. This method, with additional optimization, could become a very powerful tool for studying transcription factor regulatory events where ChIP is not viable.

To further develop this technique, the ability to regulate when the transcription factor-PBase fusion is allowed to be active would be the next challenge to tackle. Transcription factor expression control can be achieved already at the transcriptional level using the previously described tet-OFF regulatable system (24). Other potential methods include post-translational control of the protein by incorporation of a regulatable protein degradation signal, potentially from human, FKBP12, that is stabilized by the ligands SFL* or Shld1 (25), or from *E. coli*, DHFR, that is stabilized by the antibiotic, trimethoprim (26). Protein degradation control of PBase has previously been achieved by the Mitra lab (27).

Genome coverage may prove to be a problem for lowly active transcription factor-PBase fusions or for transcription factors with a high number of regulatory targets. Efg1 is an abundant transcription factor for which a single transposon was enough for nearly every cell to have a transposition event. Unfortunately, a single transposon for Sef1 and Wor1 yielded much less reliable data which could be due to their low expression rates. For Wor1, which has >500 transcriptional targets in opaque cells, there may end up being fewer multiple insertions in the same promoter region reducing confidence in the target genes.

For *in vivo* studies, I previously generated strains with 2 transposons. However, due to limited open markers, both transposons had to be made in the same split *ARG4* construct. This greatly increased the background. In the future, use of a tandem transposon array may be required. This tandem construct would have to be integrated into the genome and the problem of high background from the starting genomic location still remains. To limit background, we may be able to use either selective depletion using biotinylated probes to the starting genomic integration site followed by a linear amplification mediated protocol to enrich for transposition targets as we used for screening our *C. albicans* knockout collection (Chapter 2). As an alternative, after libraries are made, we could try using a recently described method for specific depleting unwanted highly abundant transcripts in RNA-seq libraries using Cas9 (28).

Overall, this technique shows promise for expanding our ability to study transcriptional regulation in the mammalian host.

4.4. Materials and Methods

4.4.1. *C. albicans* PiggyBac transposon construction

Version one of the transposon construct consisted of an internal *Candida dubliniensis* *HIS1* marker flanked by PiggyBac transposon long terminal repeats (LTRs) (tn-*C.d.HIS1* v1) amplified from the pBM5211 plasmid received from the Mitra lab as published in (4). This transposon was incorporated into the *Candida dubliniensis* *ARG4* gene at a TTAA site near the

end of the open reading frame, splitting the gene. The final plasmid included *C. albicans* *LEU2* locus homology as flanking sequences to the *C.d.ARG4::tn-C.d.HIS1::C.d.ARG4*. This construct was linearized using PmeI and transformed into the auxotrophic strain, ySN152. Integration at the *C. albicans* *LEU2* locus was confirmed by colony PCR of the left and right junctions. *C. albicans* transformants were initially able to grow on SD-histidine plates but not SD-arginine. This construct was not optimized for high-throughput sequencing. Therefore, a second version of the transposon was created from *tn-C.d.HIS1* v1. This second version additionally contained three restriction enzyme cut sites, one of ten barcodes and 20 bases of homology to non-multiplexable paired-end primer 2 directly adjacent to the 5'LTR. The final libraries produced from this construct could only be sequenced on the HiSeq2500 and, therefore, to bring the construct up to date a third version was created. In version 3 of the transposon, non-multiplexable paired-end primer 2 homology and internal barcode were replaced by the sequence for the multiplexable version of primer 2 that could be used to perform paired end sequencing on the HiSeq4000.

For white-opaque regulators, an *MTL::FLP-SAT1* plasmid was generated that would indiscriminately replace either the *MTLa* or *MTL α* allele (pSN369 and pSN370). *C. albicans* transformants were screened for loss of *MTLa* and/or *MTL α* using primers SNO2358 and SNO2359, and SNO2360 and SNO2361, respectively.

4.4.2. PiggyBac transposase fusion construct generation

The PiggyBac transposase nucleotide sequence was codon optimized for *C. albicans* and synthesized and cloned into pUC19 by GenScript (Piscataway, NJ). To create the linker-PBase-FLP-SAT1 plasmid used to generate transcription factor tagging cassettes, the codon optimized version of the PBase was amplified from the GenScript plasmid by primers with amino acid linker homology at the 5' end and *FLP-SAT1* cassette homology at the 3'. pRS316 was linearized and amplified by PCR with linker homology on one end and *FLP-SAT1* cassette homology on the

other. The FLP-SAT1 fragment was amplified from pSFS2A by primers with homology to PBase at the 5' and pRS316 at the 3'. The three fragments were oligomerized by homologous recombination in *S. cerevisiae*. DNA was prepared from *S. cerevisiae* clones and transformed into *E. coli* DH5 α by electroporation. Restriction digest with PmeI was used to screen colonies and positive clones were sent for sequencing at Sequetech. Primers used are deposited in the Noble Lab Oligos Filemaker Database.

The linker-PBase-*FLP-SAT1* plasmid was cut with PmeI, and then ~300 bp of the 5' UTR or ~300 bp of the 3' end of transcription factor homology added at the 5' and ~300 bp of the 3'UTR added at the 3' by homologous recombination in *S. cerevisiae* as previously described (diagrammed in **Figure 4.4.B**).

C. albicans has limited capacity to propagate plasmids so all constructs had to be incorporated into genome at the original gene locus to persist. After transformation of either the PmeI linearized promoter-PiggyBac transposase or transcription factor-PiggyBac transposase constructs into the strains containing the transposon (ySN1873 and ySN1874), transformants

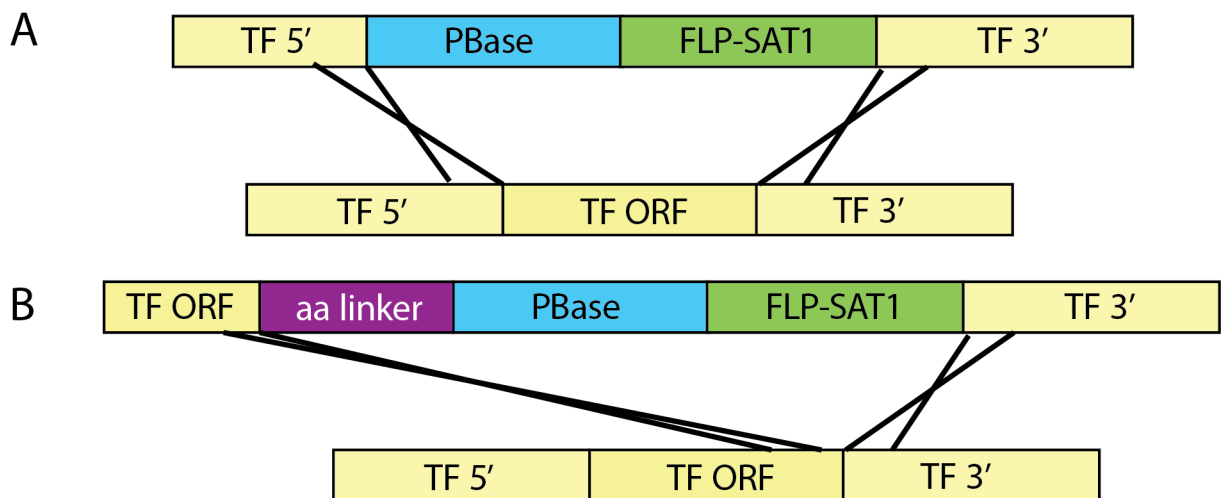


Figure 4.4. Schematic of PiggyBac transposase tagging constructs. A. Untethered PBase replaces open reading frame (ORF) of transcription factor (TF). PBase under control of TF promoter. B. Integrating TF-PBase fusion construct. Construct includes homology to the TF ORF 3' without the stop codon, followed by an 18 amino acid (aa) linker and then PBase nucleotide sequence that ends in a stop codon. FLP-SAT1 was subsequently removed to leave a single FRT site behind.

were selected on YEPD containing 200 ug/ml nourseothricin (YEPD+Nat). Nat-resistant colonies were picked after 1 day at 30C and streaked to fresh YEPD+Nat overnight at 30C. Single colonies were patched to YEPD+Nat, SD-histidine and SD-histidine-arginine. From these patches, correct construct insertion was verified using primers to the left and right junction deposited in the Noble Lab Oligos Filemaker Database. Patches that were still HIS+ but ARG-, i.e. had not already undergone a transposition event, were made into glycerol stocks. The *FLP-SAT1* selection cassette was induced to recombine out of the genome by overnight growth in YEPD+maltose liquid culture at 30C. Overnight cultures were diluted 100,000-fold in water and 100 μ l plated to YEPD. Single colonies were allowed to grow overnight at 30C overnight. This plate was then replica plated to YEPD+Nat, SD-histidine and SD-histidine-arginine. These plates were allowed to grow overnight. Nat-sensitive, HIS+, ARG- colonies from the original YEPD plate were stored as glycerol stocks. This procedure worked to limit transposition prior to experimental procedure.

4.4.3. Strain growth conditions

Strains were streaked from glycerol stocks to YEPD at 30°C for 16 hours. Cells were scraped from plate and resuspended in water. From OD measurements, ~50,000 CFUs were plated to 100 mm plates containing media specific to the assay. For iron transcription factors, Sfu1 and Sef1, strains were plated to YEPD and YEPD+250 μ M bathophenanthrolinedisulfonic acid (BPS) in triplicate for 2 days at 30°C. For white-opaque regulators, Efg1 and Wor1, strains were plated to YEPD, SC plus amino acids, and Lee's media plus N-acetylglucosamine at pH 5 for 7 days at 25°C. Efg1 strains were additionally plated to Lee's media plus N-acetylglucosamine at pH 6.8 for 7 days.

Following growth on conditional media, to isolate colonies that had undergone transposition events, all plates were replica plated to SD-histidine, SD-arginine and SD-histidine-arginine. Colonies from SD-histidine-arginine were washed from plates and collected for DNA isolation.

4.4.4. Sequencing library preparation

After genomic DNA extraction, sequencing libraries were prepared as previously described (4,5) with modifications. DNA was cut with one of three restriction enzymes: MspI, RsaI or TaqI α . DNA from restriction digests was precipitated with isopropanol and 5 M ammonium acetate, washed with 70% ethanol and resuspended in 30 μ l nuclease-free water. Digested DNA was resuspended to 2-3 ng/ μ l in a 400 μ l ligation reaction with T4 ligase. The ligation reaction was incubated at 15°C for greater than 16 hours then precipitated with ethanol and 3 M sodium acetate, washed with 70% ethanol and resuspended in 30 μ l nuclease-free water. 15 μ l of ligated DNA was used in a PCR reaction with Phusion polymerase and custom read one primer SNO2980 and one of 96 barcoded paired end primer 2. The PCR program used was: Step 1: 94°C 2 min, Step 2: 94°C 30 seconds, Step 3: 94°C 30 seconds, go to Step 2 for 30 cycles, hold at 10°C. PCR cleanup was performed using 1.0x homemade SPRI bead mix (29). PCR product quantification was performed using Quant-iT PicoGreen dsDNA assay kit (P11496). After quantification, all reactions were pooled in equal quantities. Size selection was performed on the Center for Advanced Technology (UCSF) Sage Science BluePippin with 2% agarose dye-free cassettes with marker V1 using 250 base pair-500 base pair elution criteria. A subsequent buffer exchange to TE was performed with SPRI bead mix. Libraries were visualized using High Sensitivity DNA chips on the Agilent Bioanalyzer available in the UCSF Diabetes Center. Sequencing was performed at the Center for Advanced Technology, UCSF on the HiSeq4000 with 10% PhiX and using custom read 1 sequencing primer SNO3189.

4.4.5. Data analysis

Sequenced reads were aligned to *C. albicans* haploid genome Assembly 21 using bowtie (30). The Mitra lab Calling Card-seq analysis pipeline was adopted for *C. albicans* based on code

generously provided. Mapped read positions were collapsed to just the starting genomic position of the read. All identical reads were assigned to the same starting position. In order to limit sequencing noise, a cut off of 100 was used to filter the insertions to just the highly abundance read mappings. Transposon insertions were grouped into clusters within 1000 base pair windows. Insertion clusters between fusion and untethered PBase samples for a given transcription factor were compared for significance over background (untethered) by both the Poisson and Hypergeometric distributions. All clusters were annotated with the names of the two closest genes. For quick analysis, I collapsed the data by assigning clusters to the closest promoters and subtracting all untethered PBase transposition events from the TF-PBase insertions. If insertions occurred between two genes transcribed in opposite directions away from each other, both genes were assigned those insertions. In all cases, I arbitrarily chose 5 insertions above background to be the cutoff for considering a promoter as a target of the transcription factor. Typically, anything that was greater than one insertion above background would be significant by Poisson so I considered 5 to be a fair cutoff. Proportional Venn diagrams were created using the online tool at meta-chart.com.

All data files and tables have been uploaded to the Noble Lab server. Code files used to perform data analysis are stored on Noble Lab server and location is described in the Appendix.

4.5. References

1. Hernday, A. D., Noble, S. M., Mitrovich, Q. M., and Johnson, A. D. (2010) Genetics and molecular biology in *Candida albicans*. *Methods in enzymology* **470**, 737-758
2. Mayhew, D., and Mitra, R. D. (2016) Transposon Calling Cards. *Cold Spring Harb Protoc* **2016**, pdb top077776
3. Mayhew, D., and Mitra, R. D. (2016) Calling Card Analysis in Budding Yeast. *Cold Spring Harb Protoc* **2016**, pdb prot086918
4. Wang, H., Mayhew, D., Chen, X., Johnston, M., and Mitra, R. D. (2012) "Calling cards" for DNA-binding proteins in mammalian cells. *Genetics* **190**, 941-949
5. Wang, H., Mayhew, D., Chen, X., Johnston, M., and Mitra, R. D. (2011) Calling Cards enable multiplexed identification of the genomic targets of DNA-binding proteins. *Genome research* **21**, 748-755

6. Santos, M. A., Gomes, A. C., Santos, M. C., Carreto, L. C., and Moura, G. R. (2011) The genetic code of the fungal CTG clade. *C R Biol* **334**, 607-611
7. Keith, J. H., Fraser, T. S., and Fraser, M. J., Jr. (2008) Analysis of the piggyBac transposase reveals a functional nuclear targeting signal in the 94 c-terminal residues. *BMC Mol Biol* **9**, 72
8. Chen, C., Pande, K., French, S. D., Tuch, B. B., and Noble, S. M. (2011) An iron homeostasis regulatory circuit with reciprocal roles in *Candida albicans* commensalism and pathogenesis. *Cell host & microbe* **10**, 118-135
9. Hernday, A. D., Lohse, M. B., Fordyce, P. M., Nobile, C. J., DeRisi, J. L., and Johnson, A. D. (2013) Structure of the transcriptional network controlling white-opaque switching in *Candida albicans*. *Molecular microbiology* **90**, 22-35
10. Sonneborn, A., Tebarth, B., and Ernst, J. F. (1999) Control of white-opaque phenotypic switching in *Candida albicans* by the Efg1p morphogenetic regulator. *Infection and immunity* **67**, 4655-4660
11. Zordan, R. E., Miller, M. G., Galgoczy, D. J., Tuch, B. B., and Johnson, A. D. (2007) Interlocking transcriptional feedback loops control white-opaque switching in *Candida albicans*. *PLoS biology* **5**, e256
12. Zordan, R. E., Galgoczy, D. J., and Johnson, A. D. (2006) Epigenetic properties of white-opaque switching in *Candida albicans* are based on a self-sustaining transcriptional feedback loop. *Proceedings of the National Academy of Sciences of the United States of America* **103**, 12807-12812
13. Doedt, T., Krishnamurthy, S., Bockmuhl, D. P., Tebarth, B., Stempel, C., Russell, C. L., Brown, A. J., and Ernst, J. F. (2004) APSES proteins regulate morphogenesis and metabolism in *Candida albicans*. *Molecular biology of the cell* **15**, 3167-3180
14. Bockmuhl, D. P., and Ernst, J. F. (2001) A potential phosphorylation site for an A-type kinase in the Efg1 regulator protein contributes to hyphal morphogenesis of *Candida albicans*. *Genetics* **157**, 1523-1530
15. Stoldt, V. R., Sonneborn, A., Leuker, C. E., and Ernst, J. F. (1997) Efg1p, an essential regulator of morphogenesis of the human pathogen *Candida albicans*, is a member of a conserved class of bHLH proteins regulating morphogenetic processes in fungi. *The EMBO journal* **16**, 1982-1991
16. Lassak, T., Schneider, E., Bussmann, M., Kurtz, D., Manak, J. R., Srikantha, T., Soll, D. R., and Ernst, J. F. (2011) Target specificity of the *Candida albicans* Efg1 regulator. *Molecular microbiology* **82**, 602-618
17. Xie, J., Tao, L., Nobile, C. J., Tong, Y., Guan, G., Sun, Y., Cao, C., Hernday, A. D., Johnson, A. D., Zhang, L., Bai, F. Y., and Huang, G. (2013) White-opaque switching in natural MTL α /alpha isolates of *Candida albicans*: evolutionary implications for roles in host adaptation, pathogenesis, and sex. *PLoS biology* **11**, e1001525
18. Lohse, M. B., Zordan, R. E., Cain, C. W., and Johnson, A. D. (2010) Distinct class of DNA-binding domains is exemplified by a master regulator of phenotypic switching in *Candida albicans*. *Proceedings of the National Academy of Sciences of the United States of America* **107**, 14105-14110

19. Huang, G., Wang, H., Chou, S., Nie, X., Chen, J., and Liu, H. (2006) Bistable expression of WOR1, a master regulator of white-opaque switching in *Candida albicans*. *Proceedings of the National Academy of Sciences of the United States of America* **103**, 12813-12818
20. Srikantha, T., Borneman, A. R., Daniels, K. J., Pujol, C., Wu, W., Seringhaus, M. R., Gerstein, M., Yi, S., Snyder, M., and Soll, D. R. (2006) TOS9 regulates white-opaque switching in *Candida albicans*. *Eukaryotic cell* **5**, 1674-1687
21. Huang, G., Yi, S., Sahni, N., Daniels, K. J., Srikantha, T., and Soll, D. R. (2010) N-acetylglucosamine induces white to opaque switching, a mating prerequisite in *Candida albicans*. *PLoS pathogens* **6**, e1000806
22. Sun, Y., Cao, C., Jia, W., Tao, L., Guan, G., and Huang, G. (2015) pH Regulates White-Opaque Switching and Sexual Mating in *Candida albicans*. *Eukaryotic cell* **14**, 1127-1134
23. Si, H., Hernday, A. D., Hirakawa, M. P., Johnson, A. D., and Bennett, R. J. (2013) *Candida albicans* white and opaque cells undergo distinct programs of filamentous growth. *PLoS pathogens* **9**, e1003210
24. Shen, J., Cowen, L. E., Griffin, A. M., Chan, L., and Kohler, J. R. (2008) The *Candida albicans* pescadillo homolog is required for normal hypha-to-yeast morphogenesis and yeast proliferation. *Proceedings of the National Academy of Sciences of the United States of America* **105**, 20918-20923
25. Banaszynski, L. A., Chen, L. C., Maynard-Smith, L. A., Ooi, A. G., and Wandless, T. J. (2006) A rapid, reversible, and tunable method to regulate protein function in living cells using synthetic small molecules. *Cell* **126**, 995-1004
26. Iwamoto, M., Bjorklund, T., Lundberg, C., Kirik, D., and Wandless, T. J. (2010) A general chemical method to regulate protein stability in the mammalian central nervous system. *Chem Biol* **17**, 981-988
27. Qi, Z., Wilkinson, M. N., Chen, X., Sankararaman, S., Mayhew, D., and Mitra, R. D. (2017) An optimized, broadly applicable piggyBac transposon induction system. *Nucleic acids research* **45**, e55
28. Gu, W., Crawford, E. D., O'Donovan, B. D., Wilson, M. R., Chow, E. D., Retallack, H., and DeRisi, J. L. (2016) Depletion of Abundant Sequences by Hybridization (DASH): using Cas9 to remove unwanted high-abundance species in sequencing libraries and molecular counting applications. *Genome Biol* **17**, 41
29. Rohland, N., and Reich, D. (2012) Cost-effective, high-throughput DNA sequencing libraries for multiplexed target capture. *Genome research* **22**, 939-946
30. Langmead, B., Trapnell, C., Pop, M., and Salzberg, S. L. (2009) Ultrafast and memory-efficient alignment of short DNA sequences to the human genome. *Genome Biol* **10**, R25

Chapter 5. Host mouse background as well as microbiota can influence white-to-GUT switch and fitness phenotype

5.1. Introduction

The composition of the gastrointestinal microbiota has been shown to play roles in both health and disease of the host (reviewed in (1)). The fungus, *C. albicans* is a common component of a healthy human gut microbiome (2). However, *C. albicans* colonization of the gut has been correlated with exacerbated inflammation if there are perturbations to the microbiome (reviewed in (3)). Despite this potential role in disease, little is known of how the host and bacteria modulate *C. albicans* commensal fitness.

Our lab has previously shown that an elongated yeast cell type termed GUT for Gastrointestinally Induced Transition has increased fitness in a GI colonization model and expresses a metabolic program adapted for this niche (4). GUT cells were identified in a strain that overexpress a transcription factor, *Wor1*. Upon passage of the *WOR1*-overexpression strain through the mouse gut, the fungal strain changed its cell morphology from a standard round or 'white' shape to the elongated GUT shape, and GUT cells rapidly outcompeted residual white cells in this environment. Both *WOR1* overexpression and exposure to the mouse gut were required to produce the GUT phenotype. All of these observations were made in a specific mouse strain (BALB/c) from a specific vendor, and our assumption is that the composition of the bacterial microbiota in these animals is relatively stable.

Here we present data that suggest that both the genetic background of the mouse host and the composition of the bacterial microbiota affect the fitness of white versus GUT cells. These observations include the ability of *WOR1*^{OE} strains to undergo the white-to-GUT transition in germ-free BALB/c but not Swiss Webster animals. In conventionally raised BALB/c mice from different breeding facilities of the same vendor, the outcome of the competition varied. Further investigation of the microbiota in these animals revealed that an increased abundance of *Lactobacillus spp.* may contribute to decreased fitness of the GUT cell phenotype.

5.2. Results

5.2.1. Bacteria are not required for the white-GUT switch

To determine whether bacteria are required for the white-to-GUT switch, we collaborated with Ty Chiaro in June Round's laboratory at University of Utah to perform one-to-one wild-type versus *WOR1^{OE}* competitions in three gnotobiotic BALB/c mice. At the time, it was most convenient to remove animals from the germ-free isolators in order to perform the oral inoculation of *C. albicans*. Once transferred to conventional housing, the animals were caged singly and maintained on penicillin-streptomycin antibiotic water through the course of the experiment.

Based on qPCR of strain-specific genomic differences, the *WOR1^{OE}* strain was initially less fit than wild-type but soon recovered and dominated the gut colonizing population in two of the three mice (**Figure 5.1.A**), whereas the *WOR1^{OE}* remained the minority strain in the third animal. The number of colonies that had the gross colony morphology of GUT cells assessed by plating for single colonies matched what was observed for the abundance of the *WOR1^{OE}* strain by qPCR (**Figure 5.1.B**). To confirm that these smaller, darker colonies were composed of GUT cells, slides of cells from colonies determined to be white and GUT were observed under a light microscope. The cells from the white colonies were round yeasts, whereas the smaller, darker colonies produced elongated yeasts that appeared very similar to previously isolated GUT cells from conventional mice (**Figure 5.1.E**). Of note, GUT cells did appear at a later time point in the mouse, M2, in which the *WOR1^{OE}* strain failed to dominate the commensal population. This mouse had a much lower weight than the other two animals at the beginning of the experiment, suggesting that this animal may have started with an illness, although its weight did catch up to the other two animals by the end of the experiment (**Figure 5.1.C**). Colony forming units (CFUs) for all three animals were similar to those observed in conventional antibiotic-treated experiments (**Figure 5.1.D**). It is possible that a continuation of the experiment beyond 25 days would have resulted in the GUT cell phenotype dominating all three animals.

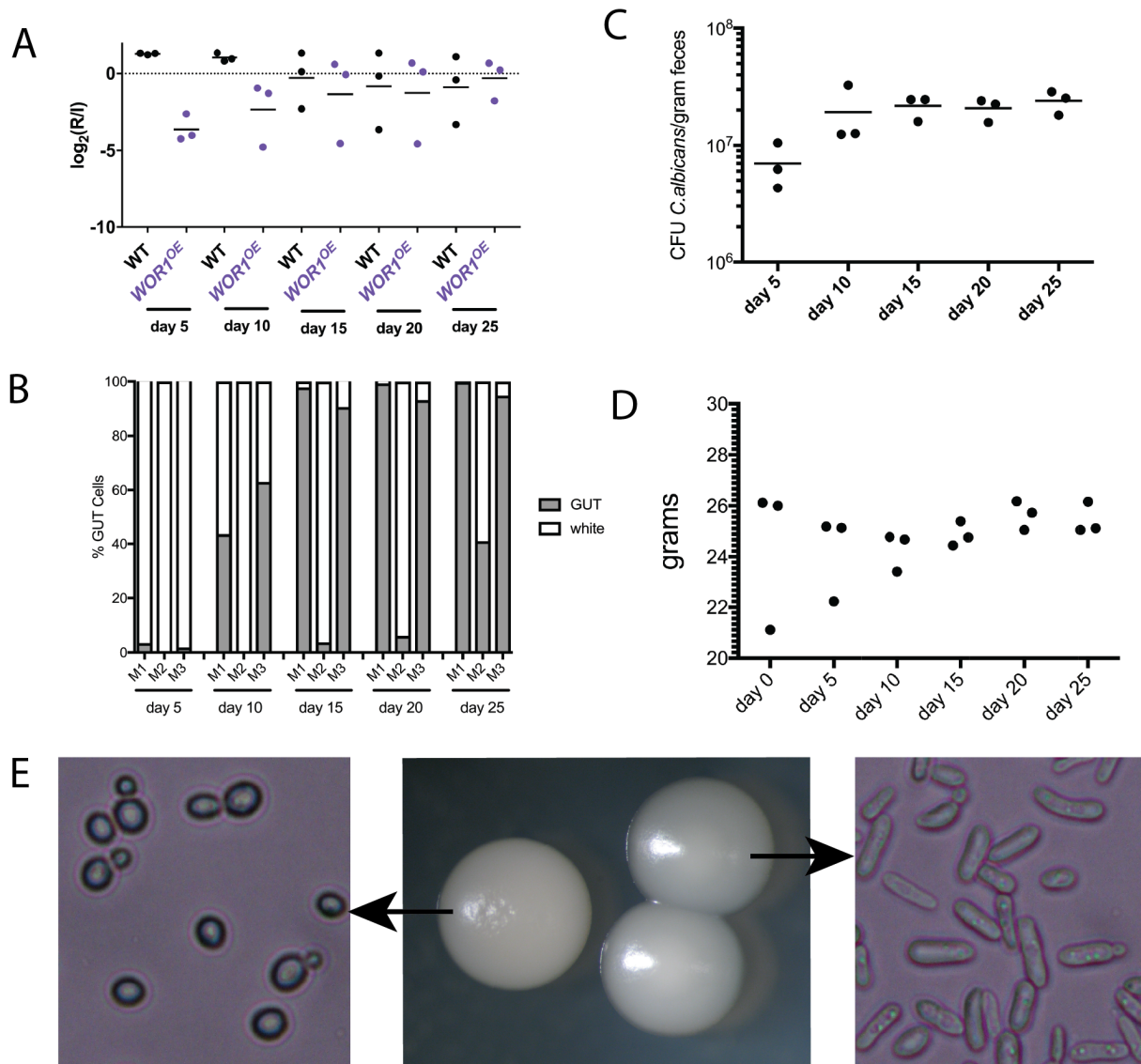


Figure 5.1. GUT phenotype can be observed from gnotobiotic BALB/c mice. A. Strain abundance of a 1:1 WT:WOR1^{OE} competition as determined by qPCR. B. Gross colony phenotype of single colony plating from feces. M1 = mouse 1, M2 = mouse 2, M3 = mouse. 3. C. Examples of white colony cells (left) and GUT colony cells (right) obtained at day 25. D. Colony forming units per gram feces over the course of the experiment. E. Weight of mice over the course of the experiment. Day 0 is day of gavage.

5.2.2. Host background influences timing and fitness of GUT cells

Microbial phenotypes can sometimes be influenced by the mouse background due to factors such as the immune response. To test the influence of mouse background on the GUT cell phenotype, with the Round lab, we inoculated four germ-free Swiss Webster mice (rather than BALB/c animals) with the same wild-type versus *WOR1^{OE}* competition. This time, the mice were maintained in germ-free isolators throughout the experiment. By qPCR, the *WOR1^{OE}* strain eventually dominated the population in all four animals (**Figure 5.2.A**) with the appearance of what looked to be GUT colonies based on gross colony morphology (**Figure 5.2.B**). However, upon microscopic inspection of the cells in these “GUT” colonies, it was revealed that the cells were only slightly elongated (**Figure 5.2.C**). These results suggest that the *WOR1^{OE}* strain had adopted an intermediate phenotype between white and GUT in Swiss Webster animals. It is

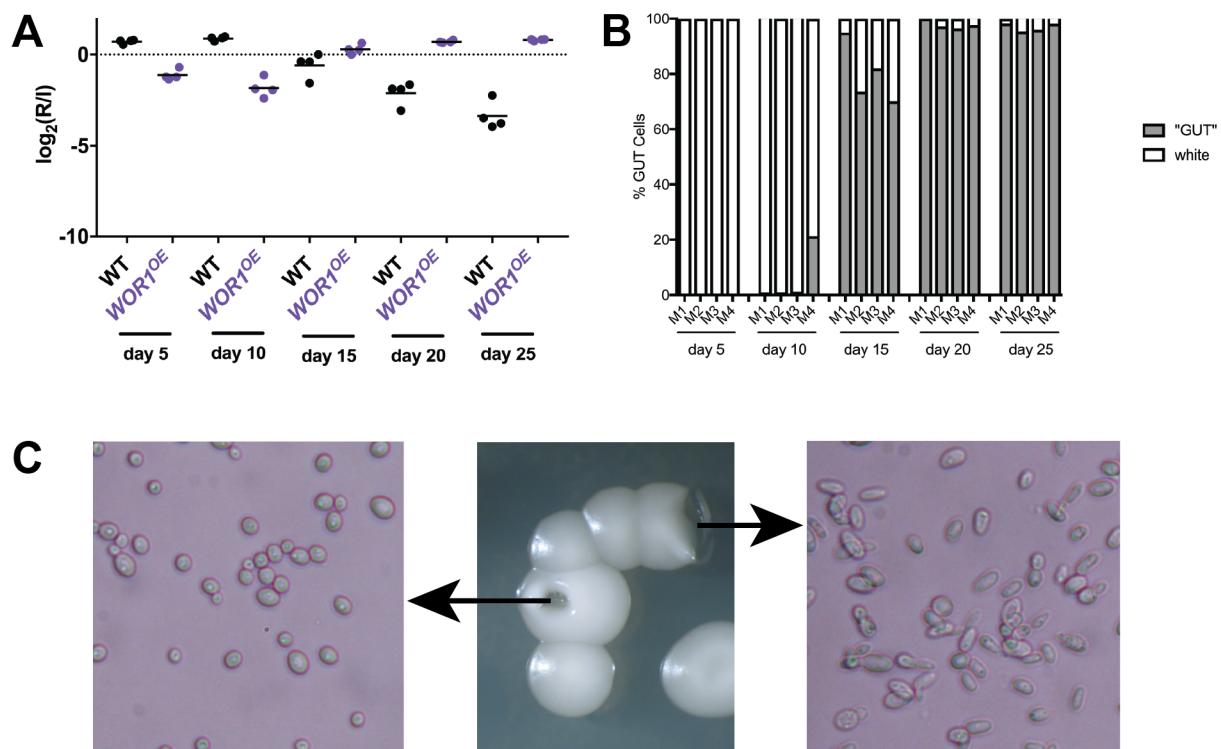


Figure 5.2. Passage through Swiss Webster mice results in intermediate phenotype. A. Strain abundance of a 1:1 WT:*WOR1^{OE}* competition as determined by qPCR. B. Gross colony phenotype of single colony plating from feces. M1 = mouse 1, M2 = mouse 2, M3 = mouse, M4 = mouse 4. C. Examples of white colony cells (left) and intermediate “GUT” colony cells (right) obtained at day 25. Day 0 is day of gavage.

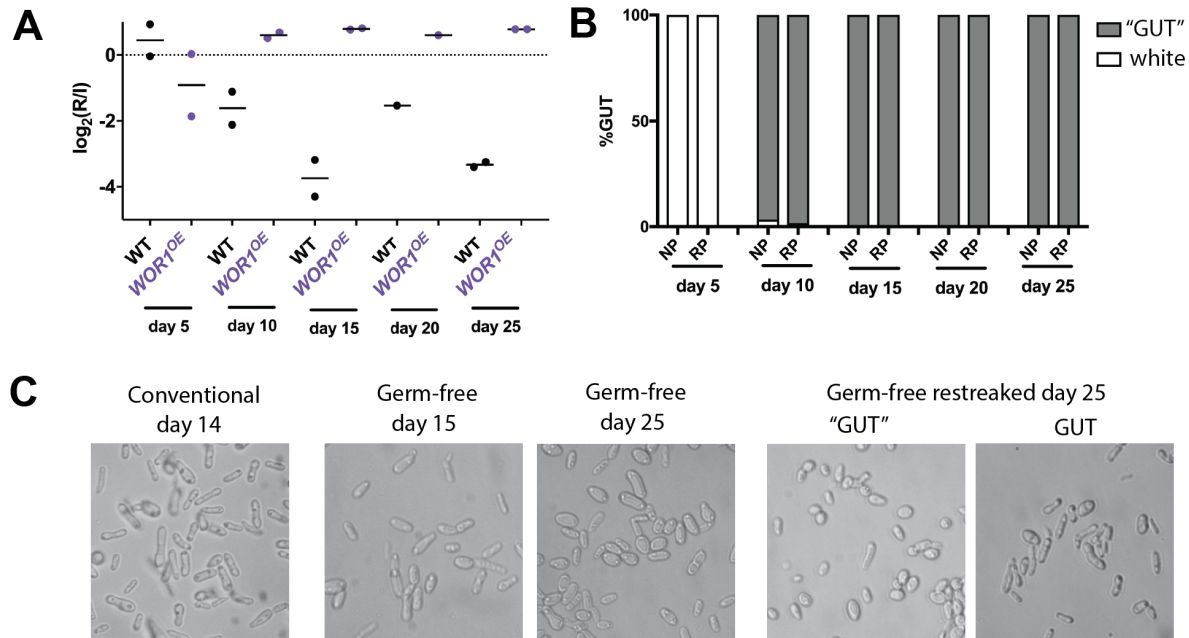


Figure 5.3. Repeat of wild type versus *WOR1^{OE}* competition in gnotobiotic BALB/c animals confirms host-specific role in GUT cell formation. A. Relative abundance measured by qPCR of wild-type and *WOR1^{OE}* strains in competition. B. Percentages of white and GUT appearing colonies. NP = mouse 1, RP = mouse 2. C. Light microscopy of conventionally raised BALB/c GUT cells and germ-free GUT cells. "GUT" = mix of round and elongated yeasts.

formally possible that maintenance of the animals in gnotobiotic isolators rather than the difference in host genotype was responsible for the failure to observe standard GUT cells.

Once we were able to perform gavage in the gnotobiotic isolators, we returned to BALB/c animals to confirm the original phenotype observed was due to mouse background. In the Round lab, we infected 2 germ-free BALB/c animals and they were kept in the germ-free facility for the duration of a 25 day time course. As expected, the *WOR1^{OE}* strain outcompeted wild-type starting at day 10 (**Figure 5.3.A**). At the same time, colonies that appeared to be GUT quickly took over the observed population on Sabouraud plates (**Figure 5.3.B**). Under the microscope, these cells appeared more similar to GUT cells induced in conventionally raised animals than to the intermediate phenotype seen in Swiss Webster animals (**Figures 5.2.C** and **5.3.C**). Colonies that appeared GUT were able to maintain their phenotype after re-streaking to Sabouraud plates (**Figure 5.3.C**).

5.2.3. The co-colonizing bacterial microbiota influences the competitive fitness of GUT cells

Several of my early experiments with wild type versus *WOR1^{OE}* competitions did not produce GUT cells as expected in conventionally raised BALB/c animals. Our lab had to change mouse suppliers after the original hyperfit *WOR1^{OE}* results in our initial vendor because of an outbreak of parvovirus at our standard vendor, Charles River. To test the possibility that the difference in vendors was responsible for this change in experimental outcome, I ordered new mice from Charles River, and once again was able to recover GUT cells.

This result suggested that the microbiota of different mouse facilities might influence the outcome of GUT cell fitness. To investigate this hypothesis, we obtained four animals each from four different Charles River housing facilities; all of these animals are genetically identical, but the bacterial microbiota varies because of differences in the local environments. The facilities included three East Coast Charles River breeding facilities (Raleigh, Kingston and Canada) as well as one West Coast facility (Hollister). Animals obtained from the Raleigh facility were contaminated by antibiotic-resistant bacteria and could not be assessed further (because the bacteria overgrow *C. albicans* on plates and outcompete *C. albicans* within the host). Two of the Kingston animals were also contaminated so only 2 animals could be evaluated further. In the West Coast facility from which we typically obtain animals, the competition behaved as expected with GUT cells appearing by day 10 and taking over the population (**Figure 5.4.A,B**). In mice obtained from the Canada facility, the fitness between wild type and the *WOR1^{OE}* strain were similar with GUT cells appearing in 3 of 4 animals (**Figure 5.4.C,D**). In Kingston animals, the *WOR1^{OE}* strain switched from white-to-GUT and took over the population by day 15 (**Figure 5.4.E,F**). However, surprisingly, the GUT cells subsequently disappeared and simultaneously CFUs per gram feces dropped by two orders of magnitude in the Kingston animals (**Figure 5.4.F,G**). This suggested that the bacteria inhabiting the Kingston animals could be actively detrimental to the GUT cells.

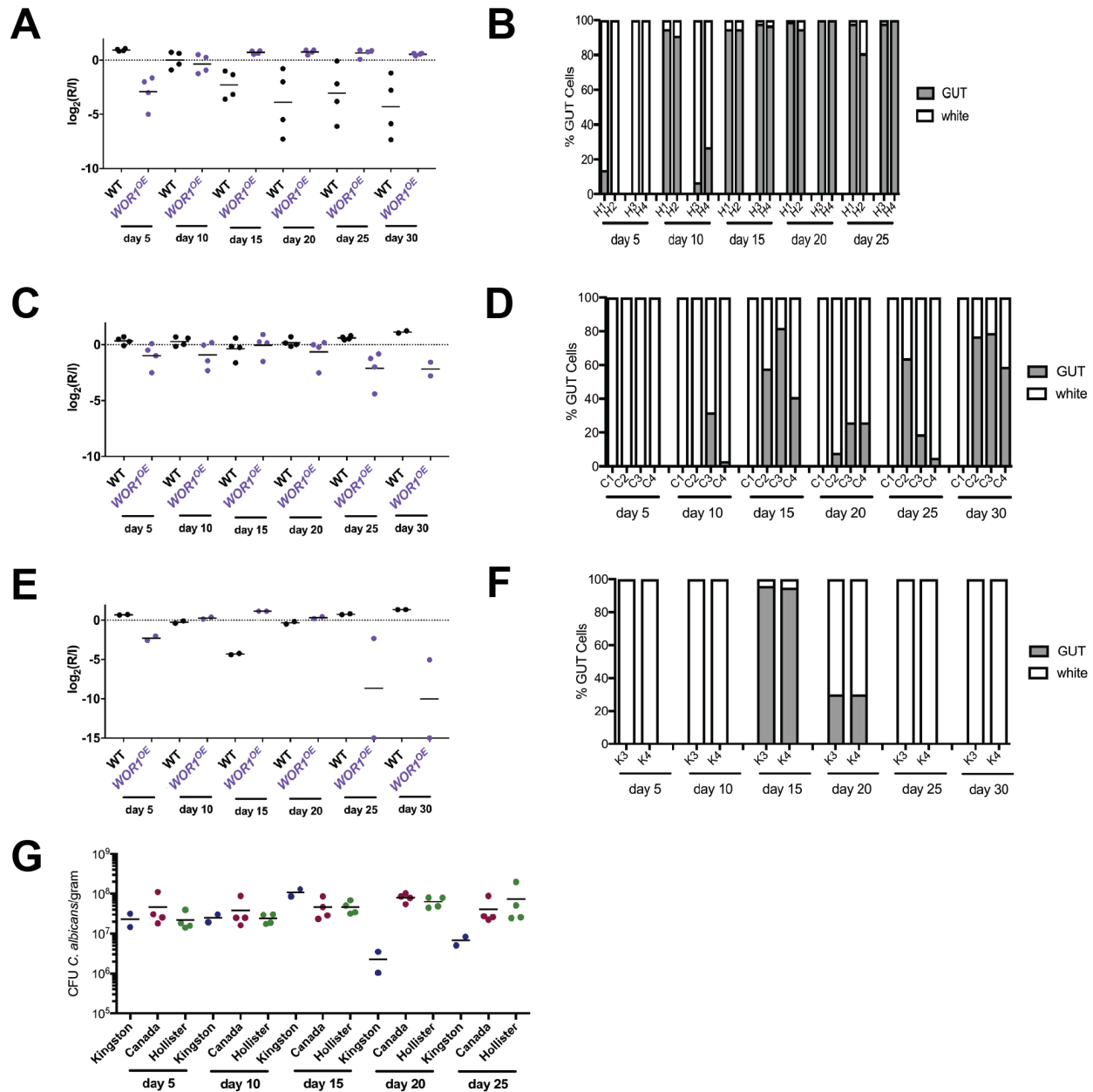


Figure 5.4. Facility specific microbiota in BALB/c mice can modulate GUT phenotype. Relative abundance of wild-type and *WOR1^{OE}* strains and GUT cell appearance in Hollister (A,B), Canada (C,D), and Kingston (E,F). G. Colony forming units (CFUs) of *C. albicans* per gram feces in mice from all three facilities.

To determine whether the loss of GUT cell fitness was transferrable, after 30 days Hollister animals were cohoused with either Kingston or Canada animals in pairs. In all animals, the *WOR1^{OE}* strain was outcompeted by wild type eventually (**Figure 5.5.A**), thus confirming that the phenotype was transferrable, most likely via bacterial transfer during coprophagy. In

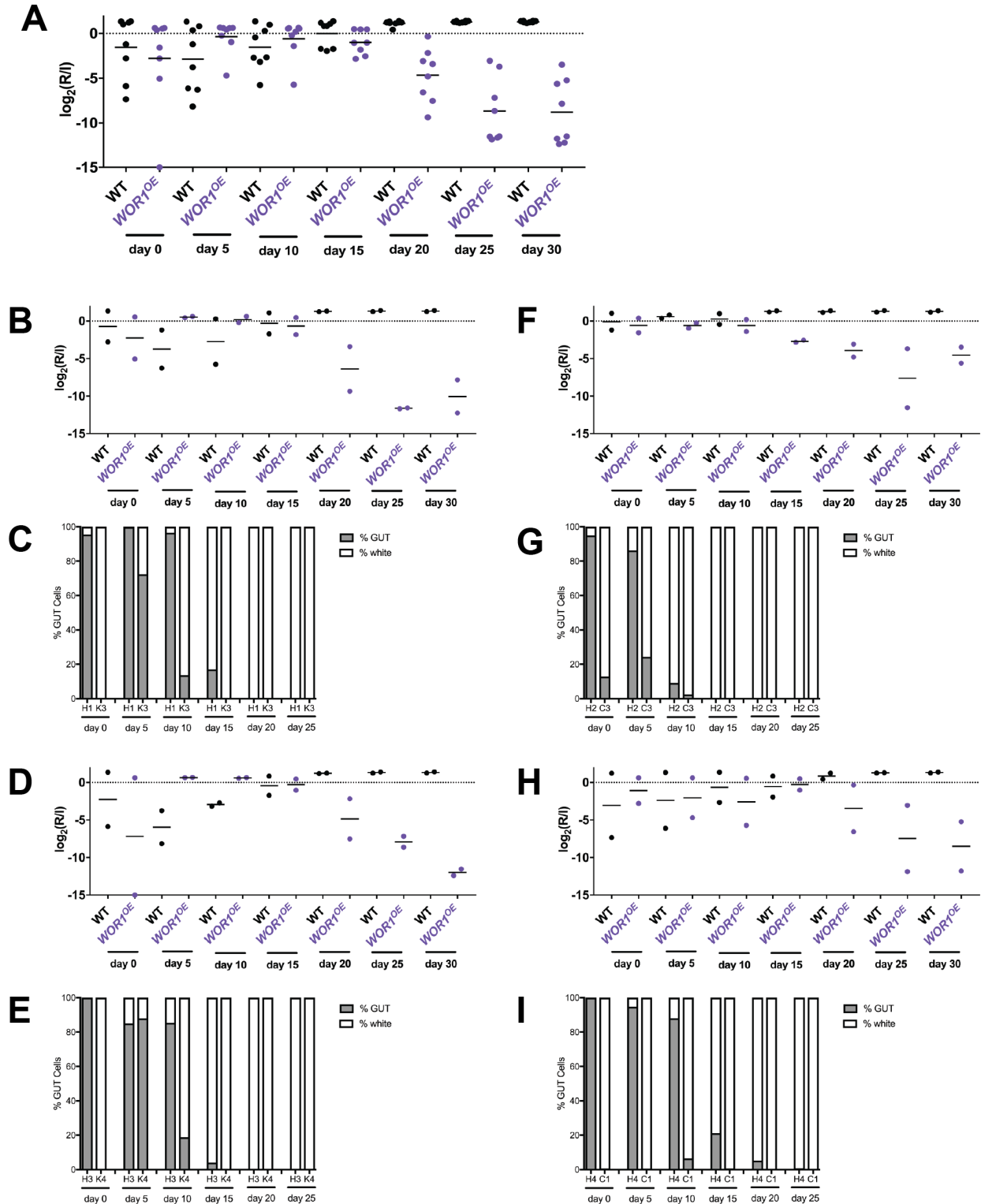


Figure 5.5. Post cohousing animals, GUT cell phenotype is lost. A. Relative abundance of wild type and *WOR1^{OE}* in all co-housed animals. B,D. Relative abundance of wild type and *WOR1^{OE}* in Hollister-Canada cohousing cages. C,E. GUT cell populations in Hollister-Canada cohousing cages. F,H. Relative abundance of wild type and *WOR1^{OE}* in Hollister-Kingston cohousing cages. G,I. GUT cell populations in Hollister-Kingston cohousing cages.

one of the Hollister-Canada cages, the Canada animal picked up GUT cells from the Hollister animal but eventually both animals lost GUT cells (**Figure 5.5.B,C**). In the second cage, the Canada animal had resisted development of GUT cells prior to cohousing and did not pick them up from the Hollister mouse (**Figure 5.5.D,E**). By the end, both animals had lost the GUT cell phenotype. In cages with Hollister-Kingston pairings, the Kingston animals became populated by GUT cells again but eventually GUT cells were lost from all animals (**Figure 5.5.F-I**).

5.2.4. *Increased abundance of Lactobacillus species is coincident with decreased GUT cell fitness*

To gain insight into which bacterial species could be having this detrimental effect on the GUT cell phenotype, we sent mouse feces collected at day 0 and each 5-day time point to Andrew Koh's laboratory at University of Texas Southwest to determine the relative abundance of different bacterial groups. Laura Coughlin isolated DNA from the fecal pellets and assessed the abundance of different bacteria using primers specific for all bacteria (EUBAC), Clostridial cluster IV (CLEPT), mouse intestinal bacteroides (MIB), Enterobacteraciae (ENTERO), and *Lactobacillus* species (LACTO). The greatest difference was observed between the Hollister and Kingston animals at day 20 for the abundance of *Lactobacillus*, which was 8 orders of magnitude less in the Hollister animals (**Figure 5.6**). These results suggest that *Lactobacillus spp.* in Kingston animals may inhibit the commensal fitness advantage of GUT cells.

5.3. Discussion

In this work, we set out to determine if mouse background or bacterial microbiome could contribute to the fitness of a specialized cell type, GUT, discovered by our lab. We observed that, in the absence of bacteria, the white-to-GUT transition occurs in our standard mouse background, BALB/c. However, in a Swiss Webster background only an intermediate slightly elongated phenotype could be achieved despite colony appearance being similar to GUT. The

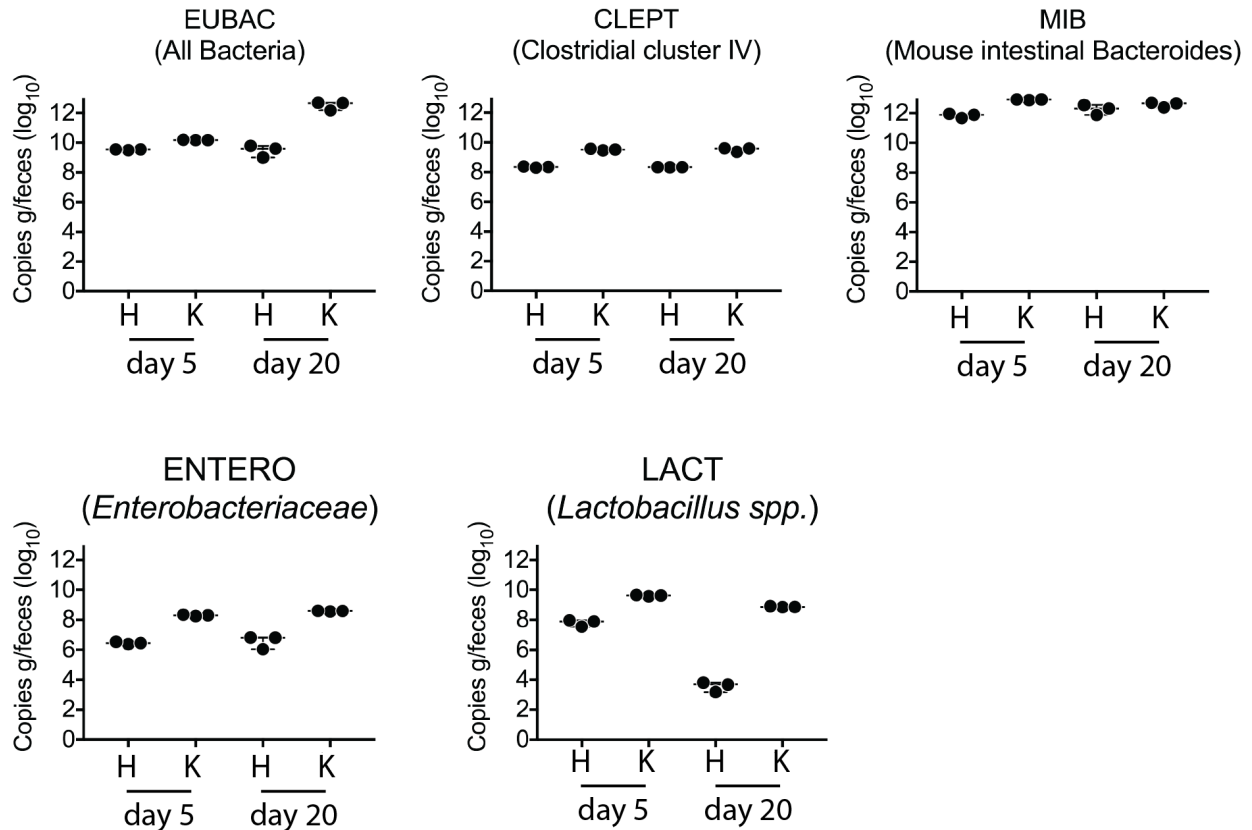


Figure 5.6. *Lactobacillus spp.* abundance is higher in Kingston animal. qPCR of DNA extracted from one Kingston and one Hollister animal at days 5 and 20. Primers for specific bacterial groups are described in (7).

original germ-free BALB/c animals had to be removed from the germ-free isolators and kept in a conventional mouse room. When we were able to perform the competition in BALB/c animals in the germ-free isolators, the *WOR1^{OE}* fitness advantage was maintained as well as the ability to switch to the GUT cell phenotype suggesting that mouse background plays a role in *C. albicans* commensal fitness.

With animals obtained from different breeding facilities, we observed variation in GUT cell fitness. The microbial composition of the feces in these animals revealed a much higher abundance of *Lactobacillus spp.* in Kingston animals compared to Hollister animals. There is recent evidence to suggest that *Lactobacillus spp.* can induce filamentous growth of opaque cells in co-culture (5). We have previously seen that hypha-coregulated genes can negatively

impact commensal fitness. GUT cells are resistant to filamentation in the mouse gut (see White-Opaque story). However, GUT cells behave like opaque cells in many ways so we predict that *Lactobacillus* species may induce filamentation of GUT cells *in vivo* thus leading to expression of detrimental hypha-coregulated genes that decrease the fitness of GUT cells.

To determine the exact species of *Lactobacillus* in the Kingston animals, we will use *in vitro* selection to attempt to culture it from feces. We will also perform shotgun sequencing in collaboration with the Koh lab of feces from the Kingston and Hollister animals, in which relative abundance of bacterial groups was examined, to confirm that the *Lactobacillus* that natively inhabits Kingston animals is stable over time.

The data presented here suggests that both mouse background in a germ-free environment and the differences in microbiota of conventionally raised animals contribute to *C. albicans* behavior *in vivo*. Due to the complex nature of the *C. albicans*-microbiota-host relationship, follow-up studies will be required to determine the mechanism by which the host immune response and microbes modulate *C. albicans* commensal fitness.

5.4. Materials and Methods

5.4.1. Yeast strains

Genotypes for strains used in this study were described in Pande *et al.* 2013 (4). Wild-type strain was prototroph ySN425 and the *WOR1*^{OE} strain was ySN928.

5.4.2. Mouse lines

Gnotobiotic female mice, BALB/c and Swiss Webster, were bred and maintained at the University of Utah under the supervision of the Round lab. Adult female SPF BALB/c were obtained from Charles River Laboratories Hollister facility room H44 unless otherwise noted in Results.

5.4.3. *in vivo* competitions

Gastrointestinal competition setup and analysis for conventional mice are described in Chapter 2. Primers used in qPCR were SNO1342 and SNO1343 for wild type and SNO1355 and SNO1361 for *WOR1^{OE}*.

For the gnotobiotic experiments, the inocula was prepared as previously described with several additional steps. Instead of inoculating animals right away, the inocula was resuspended in 17% (v/v) glycerol in YEPD and stored at -80C until it could be sent to the Round lab on dry ice. We typically observe about a four-fold loss in viability after thawing and washing the inocula in saline and therefore inocula was resuspended post-thaw with this assumption to achieve $\sim 5 \times 10^8$ CFUs/ml. Feces were collected from germ-free animals and resuspended in 17% glycerol and stored at -80C until they could be shipped to our lab on dry ice. Feces were allowed to thaw for >30 minutes before creating dilutions. No loss of viability of *C. albicans* recovered from feces was observed using this technique.

5.4.4. *Bacteria abundance analysis*

DNA isolation from fecal pellets and qPCR was performed as previously described by the Koh lab (6). Primer sequences for qPCR can be found in (7).

5.5. References

1. Marchesi, J. R., Adams, D. H., Fava, F., Hermes, G. D., Hirschfield, G. M., Hold, G., Quraishi, M. N., Kinross, J., Smidt, H., Tuohy, K. M., Thomas, L. V., Zoetendal, E. G., and Hart, A. (2016) The gut microbiota and host health: a new clinical frontier. *Gut* **65**, 330-339
2. Nash, A. K., Auchtung, T. A., Wong, M. C., Smith, D. P., Gesell, J. R., Ross, M. C., Stewart, C. J., Metcalf, G. A., Muzny, D. M., Gibbs, R. A., Ajami, N. J., and Petrosino, J. F. (2017) The gut mycobiome of the Human Microbiome Project healthy cohort. *Microbiome* **5**, 153
3. Kumamoto, C. A. (2011) Inflammation and gastrointestinal *Candida* colonization. *Curr Opin Microbiol* **14**, 386-391
4. Pande, K., Chen, C., and Noble, S. M. Passage through the mammalian gut triggers a phenotypic switch that promotes *Candida albicans* commensalism. *Nat Genet* **45**, 1088-1091

5. Liang, W., Guan, G., Dai, Y., Cao, C., Tao, L., Du, H., Nobile, C. J., Zhong, J., and Huang, G. (2016) Lactic acid bacteria differentially regulate filamentation in two heritable cell types of the human fungal pathogen *Candida albicans*. *Molecular microbiology* **102**, 506-519
6. Fan, D., Coughlin, L. A., Neubauer, M. M., Kim, J., Kim, M. S., Zhan, X., Simms-Waldrip, T. R., Xie, Y., Hooper, L. V., and Koh, A. Y. (2015) Activation of HIF-1alpha and LL-37 by commensal bacteria inhibits *Candida albicans* colonization. *Nat Med* **21**, 808-814
7. Barman, M., Unold, D., Shifley, K., Amir, E., Hung, K., Bos, N., and Salzman, N. (2008) Enteric salmonellosis disrupts the microbial ecology of the murine gastrointestinal tract. *Infection and immunity* **76**, 907-915

Chapter 6. Hgc1, a hypha-specific G1 cyclin-like protein, plays an inhibitory role in GI commensal fitness

6.1. Introduction

Like many fungal species, *Candida albicans* can adopt different cell morphologies. Given that *C. albicans* is primarily associated with mammalian hosts, we and others have hypothesized that these different cell types may be specialized for particular *in vivo* niches (reviewed in (1)). The best characterized morphological change is the yeast to hypha transition. Round-to-oval yeasts are the default cell type of *C. albicans* when grown *in vitro*. Upon exposure to environmental signals that would be found in a mammalian host such as serum or mammalian body temperature (37°C), *C. albicans* can adopt a multicellular elongated structure called a filament or hypha. Hyphae have upregulated expression of genes that could possibly be used to damage the host, such as secreted aspartyl proteases and the pore-forming toxin Candidalysin, so these cells were thought to be the virulent form of *C. albicans*. However, using yeast-locked and hypha-locked strains it was found that both cell types contribute to virulence in a mouse model of systemic infection (2-4). Our lab has been working to characterize the role of yeasts and hyphae in commensal colonization of the gastrointestinal (GI) tract and have observed that hypha-coregulated gene expression decreases commensal fitness.

C. albicans Hgc1 has previously been described as a hypha-specific G1 cyclin-related protein that affects the ability to switch from round yeasts to elongated hyphal cells but does not affect gene expression (3). The assertion that Hgc1 does not affect the hyphal gene expression program is based almost entirely on Northern analysis of three genes that are highly upregulated in hyphae *in vitro* (3). Under hypha-inducing conditions (YEPD+10% serum, 37°C), the *hgc1* strain still expresses high levels of *HWP1*, *HYR1* and *ECE1* (3). Given that an *hgc1* deletion mutant exhibits attenuated virulence in a mouse bloodstream infection model, these data were used to assert that the morphological transition from yeast to hyphae is required for *C. albicans* virulence, independent of any changes in hypha-specific gene expression. However,

a recent report has implicated Hgc1 in negatively regulating hypha-specific gene expression via post-translational repression of the transcription factor Ume6 (5). This would suggest that Hgc1 also plays a previously uncharacterized role in the control of hypha-coregulated transcripts. We have observed that a *ume6* knockout mutant exhibits enhanced commensal fitness in a mouse model of gastrointestinal colonization (Chapter 2). If Hgc1 negatively regulates Ume6 within the host, as it does under *in vitro* conditions, then one would expect an *hgc1* knockout mutant to have reduced fitness in the murine GI colonization model.

Here we present evidence that, rather than enhancing commensal fitness as predicted, Hgc1 inhibits competitive fitness within the GI colonization model. In commensal competitions, independent isolates of *hgc1* exhibit a hypercompetitive phenotype. Unlike *ume6* strains, *hgc1* strains do not adopt normal hyphal morphology within the murine GI tract. Finally, in contrast to the published literature, we show that Hgc1 does affect the expression of many genes under hypha-inducing conditions *in vitro* as well as within the mammalian gut. These results support an inhibitory role for either hyphal morphology per se or, more likely, of Hgc1-dependent genes on commensal fitness in the host GI tract.

6.2. Results

6.2.1. Loss of *Hgc1* confers increased commensal fitness

We have previously described the role of Ume6 as a negative regulator of GI commensalism. The hyperfit phenotype of the *ume6* knockout mutant could not be attributed to changes in morphology as *ume6* form hyphae at a similar frequency to wild-type *C. albicans* within our animal model (see Chapter 2). We initially hypothesized that deletion of *HGC1* would have no effect on the fitness of *C. albicans* due to its reported lack of effect on gene expression (3). However, two out of three independent isolates of *hgc1* strongly outcompeted wild type in one-to-one competition experiments; the third isolate showed no fitness phenotype (**Figure 6.1A,C,B**). Although we cannot fully account for the lack of reproducibility in the third *hgc1*

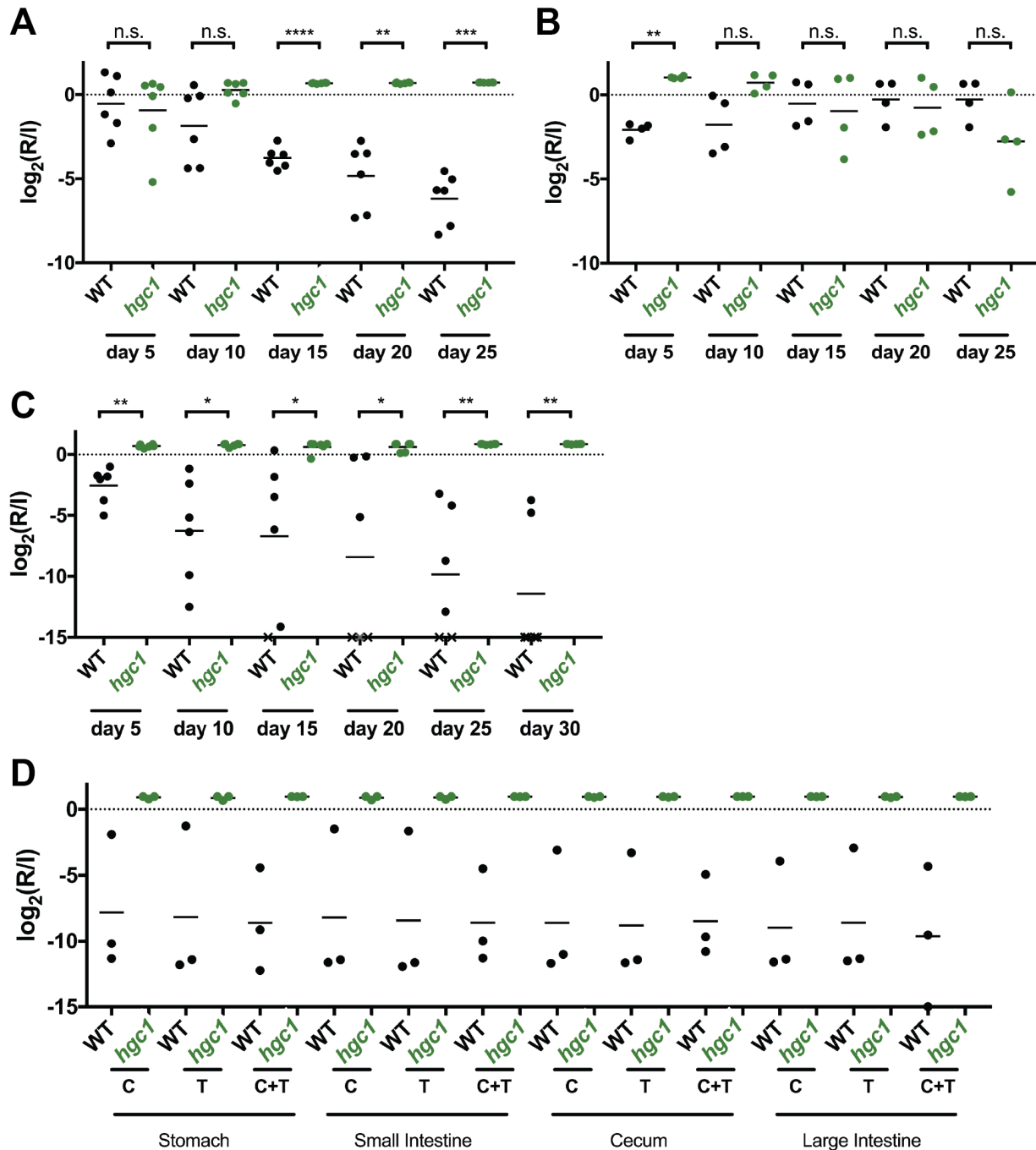


Figure 6.1. Loss of Hgc1 enhances gastrointestinal commensal fitness. A. Relative abundance of wild type versus *hgc1* (ySN1353) in commensal competition. B. Relative abundance of wild type versus *hgc1* (ySN1354) in commensal competition. C. Relative abundance of wild type versus *hgc1* (ySN1489) in commensal competition. D. Tissue plating of competition in panel C for GI compartments. From 3 animals, tissue was separated from luminal contents and each was plated separately. The tissue and contents was plated together from the other 3 animals. T=tissue separate from contents; C=contents separate from tissue; C+T=tissue and contents plated together. * $p < 0.05$, ** $p < 0.01$, *** $p < 0.001$, **** $p < 0.0001$.

isolate, two possibilities are the presence of an unlinked mutant that affects fitness in this strain or stochastic variation in the biological assay. To confirm that the fitness effects deduced from analysis of feces are relevant to commensally growing organisms within the host, we repeated the analysis with GI contents recovered directly from murine stomach, small intestines, the cecum, and large intestines after 37 days. As shown in **Figure 6.1D**, the results obtained from GI contents were almost identical to those obtained from feces, supporting our reliance on fecal specimens for the majority of our experiments.

6.2.2. *Hgc1* mutant does not form hyphae in the mammalian GI tract

Because we previously observed that filamentation occurs normally in a *ume6* mutant propagated within the host, unlike the behavior of this mutant under *in vitro* filamentation conditions, we next asked whether Hgc1 is required for normal filamentation *in vivo*. Mice were monotypically infected with *hgc1* and sacrificed after 10 days. The gastrointestinal compartments were fixed and stained with a fluorescent probe specific to *C. albicans*. Unlike the *ume6* mutant, which forms normal hyphae in this environment, the *hgc1* strain forms stunted hyphae that appear similar to pseudohyphae or elongated yeast cells (**Figure 6.2**).

6.2.3. *Hgc1* contributes to gene expression in different environments

As described above, Hgc1 is thought to control hyphal cell morphology but not hypha-specific gene expression based on analysis of three hypha-associated genes in the *hgc1* mutant. To determine whether other genes might be affected in the *hgc1* mutant under *in vitro* or *in vivo* conditions, we performed RNA-seq on the *hgc1* strain under standard *in vitro* conditions (YEPA, 30°C), hypha-inducing conditions (YEPA plus 10% serum, 37°C) and during commensal infection (monotypic murine large intestine colonization, 10 days). We compared the data for *hgc1* with data previously obtained for a wild-type strain propagated under the same conditions; of note, because these *in vitro* cultures were obtained on different days, some

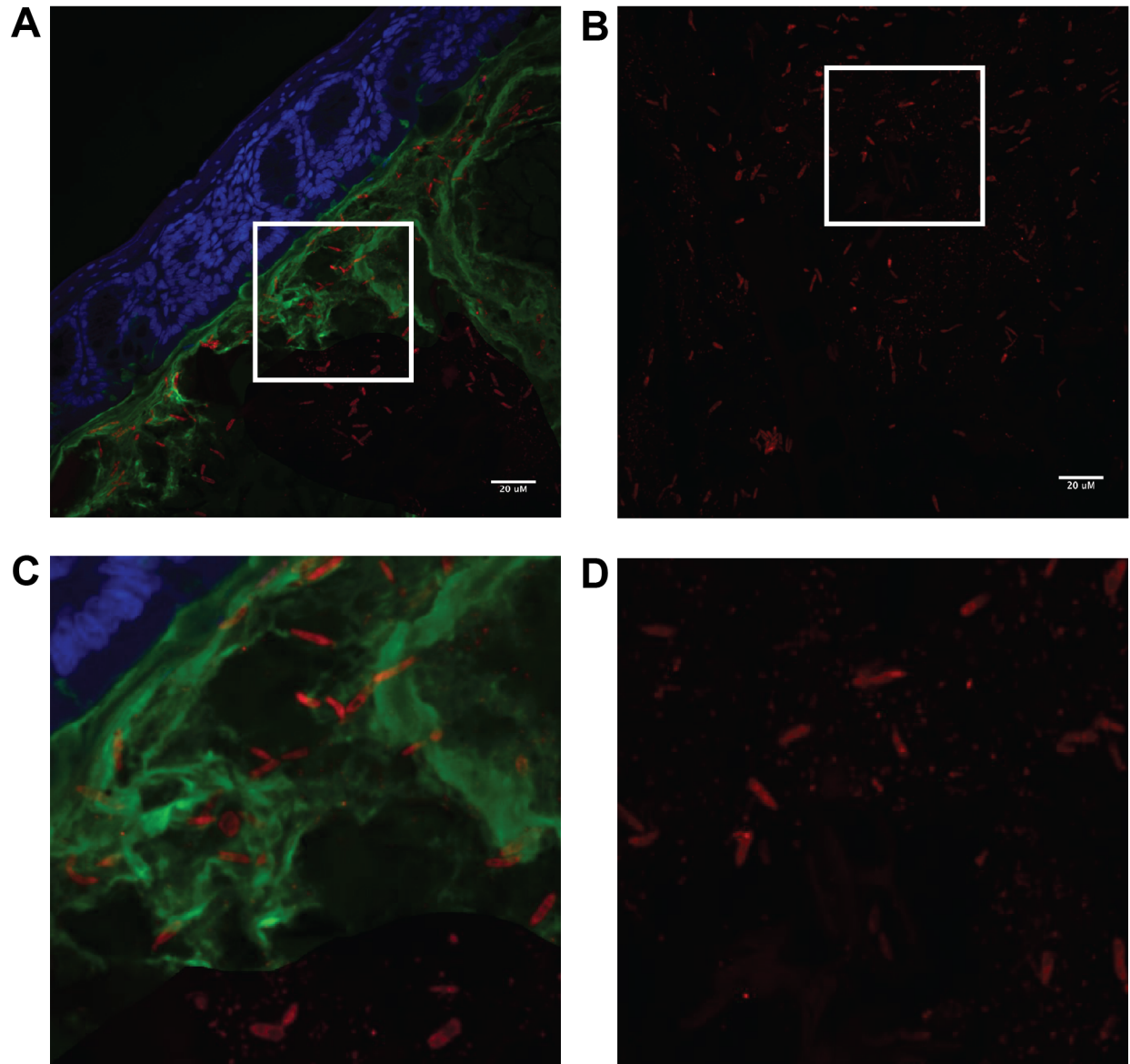


Figure 6.2. *hgc1* mutant does not form hyphae *in vivo*. FISH staining of *hgc1* (ySN1353) colonized large intestine imaged (A) near the mucosa or (B) in the lumen. C. Zoomed in view of white box area from A. D. Zoomed in view of white box area from B. Scale bars on A and B are 20 μ m. Red=*C.albicans*; green= mucin; blue=nuclei. Images courtesy of Pallavi Penumetcha.

differences in gene expression may derive from exogenous factors (media, humidity, etc.) that are unrelated to the genetic difference between the strains. Consistent with previous reports, comparison of the *hgc1* mutant with wild-type propagated under *in vitro* hypha-inducing conditions (YEPD+10% serum at 37°C) revealed no significant differences in levels of *ECE1*, *HWP1*, or *HYR1*. However, 510 genes were significantly ($p < 0.05$) upregulated and 321 were

downregulated by 2-fold or more in *hgc1* compared to wild type. By contrast, a *ume6* mutant profiled on the same day as the wild-type strain exhibited no upregulated genes and 13 downregulated genes by 2-fold at a p-value less than 0.05. If the stringency of the cutoff is increased to 4-fold with a p-value less than 0.01, 135 genes were upregulated and 41 downregulated in the *hgc1* mutant.

In the gastrointestinal tract, an even larger set of genes is differentially expressed between wild-type and the *hgc1* strain. In the large intestine, 1064 genes are upregulated and 1176 genes are downregulated two-fold with a p-value less than 0.05 in the *hgc1* mutant compared to wild type. The most highly upregulated gene was *PGA56*, which is a regulator of sorbose utilization (**Figure 6.3A**) (6). This was followed by many unannotated genes that give no indication of functional relevance. Of the ten most highly downregulated genes, four are involved in cell wall biogenesis (*MNN22*, *BMT4*, *MNN4*, and *MNN1*). The most highly downregulated gene (orf19.3988; >20-fold) codes for a putative adhesin-like protein (7). This gene is not expressed under the *in vitro* conditions we tested but may be induced in the gut due to the acidic environment as it has previously been reported to be induced under weak acid stress (8). It is interesting to note though that this transcript is still one of the most highly upregulated if the *hgc1* strain in the large intestine is compared to the strain grown at 30°C in YEPD (**Figure 6.3.D**).

6.3. Discussion

Our *in vitro* and *in vivo* analysis of *hgc1* has revealed that, in contrast to previous reports, Hgc1 does affect the expression of many *C. albicans* genes. Further, Hgc1 is required for normal filamentation in the host, as well as under *in vitro* conditions. Finally, contrary to our original expectation, Hgc1 inhibits the fitness of *C. albicans* within the mammalian gastrointestinal tract.

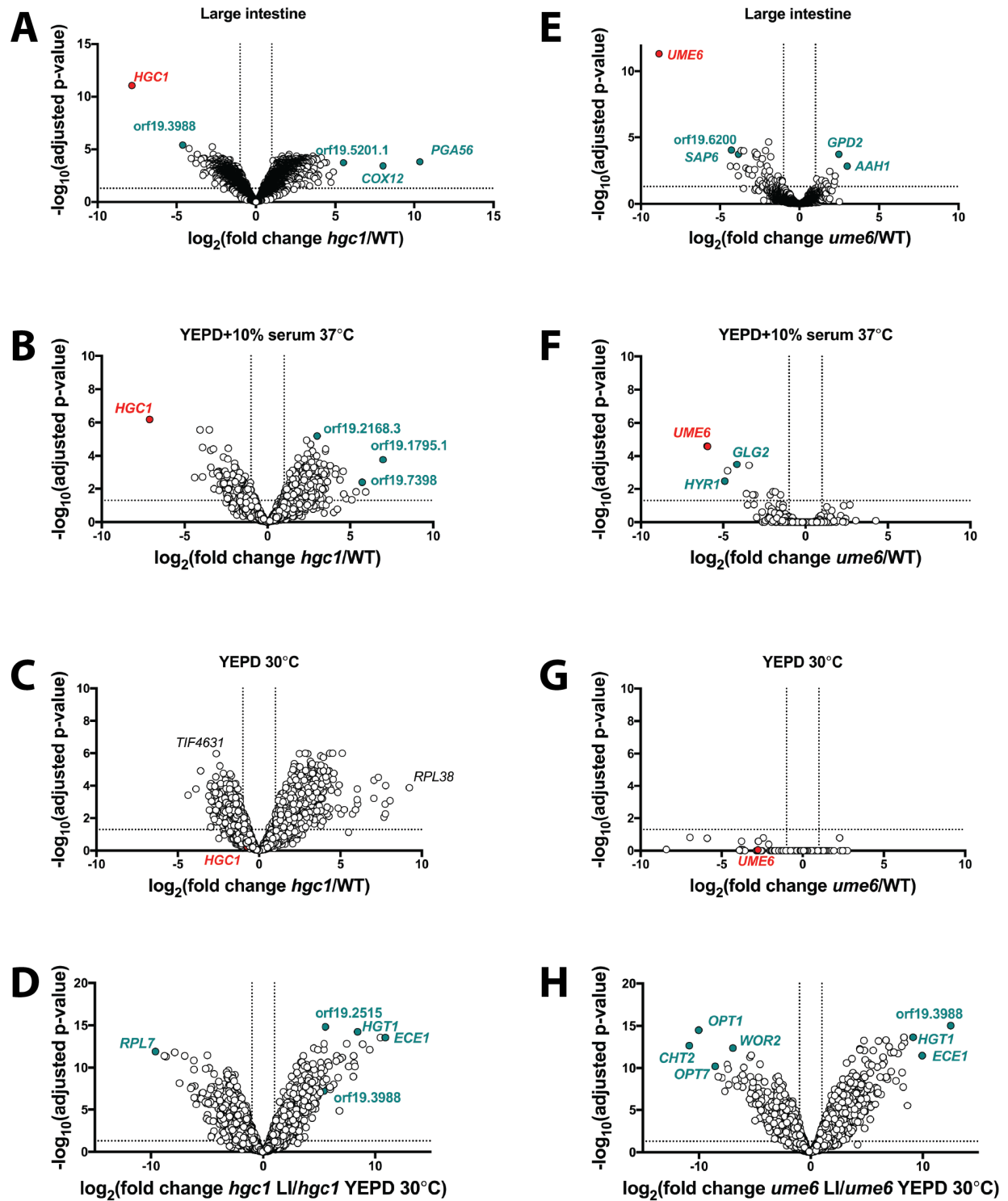


Figure 6.3. Volcano plots of RNA expression data from large intestine and under *in vitro* conditions. A. *hgc1* versus wild type in large intestine. B. *hgc1* versus wild type in YEPD+10% serum at 37°C. C. *hgc1* versus wild type in YEPD at 30°C. D. *hgc1* from large intestine versus *hgc1* in YEPD at 30°C. E. *ume6* versus wild type in large intestine. F. *ume6* versus wild type in YEPD+10% serum at 37°C. G. *ume6* versus wild type in YEPD at 30°C. H. *ume6* from large intestine versus *ume6* in YEPD at 30°C.

Although it remains unclear why the *hgc1* mutant might survive the GI tract better than wild-type, we favor the possibility that an Hgc1-regulated gene is required for normal commensal fitness. For example, the *in vivo* RNA-seq data reveal that a transcript for an adhesin-like protein is highly downregulated in the *hgc1* mutant compared to wild-type. Cell surface proteins can serve as anchoring molecules to substrates in the gut to allow persistence or as proteins that are targeted for clearance by the host immune system. In this case, because it has reduced expression in the hypercompetitive strain, the latter is more likely.

These data present a more complicated interplay of the yeast and hypha morphologies and co-regulated gene expression that will require further study to tease apart.

6.4. Materials and Methods

6.4.1. Yeast strains

Wild-type strain used was ySN250. *hgc1* strains were ySN1353, ySN1354 and ySN1489 derived from ySN152 using auxotrophic markers as previously described (9).

6.4.2. Gastrointestinal mouse competitions

All mouse infections were performed as previously described (10). Briefly, 8-10 week old BALB/c mice were housed two per cage. Animals began drinking water that contained penicillin and streptomycin 7 days before gavage. Each animal was given an inoculum of 1×10^8 CFUs of *C. albicans*. Feces were collected every 5 days, plated for 2 days on Sabouraud agar containing ampicillin and gentamicin, and *C. albicans* DNA was recovered for qPCR analysis of relative abundance. Primers used for wild type were SNO509 and SNO322. Primers used for *hgc1* strains were ST4 and SNO322.

6.4.3. Fluorescent in situ hybridization (FISH)

FISH was performed as previously described in Chapter 2.

6.4.4. Gene expression analysis

All gene expression analyses were performed as previously described in Chapter 2. However, the linear fit model generated by *limma* incorporated WT (ySN250), *ume6* (ySN1479), and *hgc1* (ySN1353) data so the statistics changed slightly for WT and *ume6* compared to Chapter 2. All data files are on the Noble Lab server and file names are described in the Appendix.

6.5. References

1. Noble, S. M., Gianetti, B. A., and Witchley, J. N. (2017) *Candida albicans* cell-type switching and functional plasticity in the mammalian host. *Nat Rev Microbiol* **15**, 96-108
2. Saville, S. P., Lazzell, A. L., Monteagudo, C., and Lopez-Ribot, J. L. (2003) Engineered control of cell morphology in vivo reveals distinct roles for yeast and filamentous forms of *Candida albicans* during infection. *Eukaryotic cell* **2**, 1053-1060
3. Zheng, X., Wang, Y., and Wang, Y. (2004) Hgc1, a novel hypha-specific G1 cyclin-related protein regulates *Candida albicans* hyphal morphogenesis. *The EMBO journal* **23**, 1845-1856
4. Lo, H. J., Kohler, J. R., DiDomenico, B., Loebenberg, D., Cacciapuoti, A., and Fink, G. R. (1997) Nonfilamentous *C. albicans* mutants are avirulent. *Cell* **90**, 939-949
5. Mendelsohn, S., Pinsky, M., Weissman, Z., and Kornitzer, D. (2017) Regulation of the *Candida albicans* Hypha-Inducing Transcription Factor Ume6 by the CDK1 Cyclins Cln3 and Hgc1. *mSphere* **2**
6. Kabir, M. A., Ahmad, A., Greenberg, J. R., Wang, Y. K., and Rustchenko, E. (2005) Loss and gain of chromosome 5 controls growth of *Candida albicans* on sorbose due to dispersed redundant negative regulators. *Proceedings of the National Academy of Sciences of the United States of America* **102**, 12147-12152
7. Chaudhuri, R., Ansari, F. A., Raghunandan, M. V., and Ramachandran, S. (2011) FungalRV: adhesin prediction and immunoinformatics portal for human fungal pathogens. *BMC Genomics* **12**, 192
8. Ramsdale, M., Selway, L., Stead, D., Walker, J., Yin, Z., Nicholls, S. M., Crowe, J., Sheils, E. M., and Brown, A. J. (2008) MNL1 regulates weak acid-induced stress responses of the fungal pathogen *Candida albicans*. *Molecular biology of the cell* **19**, 4393-4403
9. Hernday, A. D., Noble, S. M., Mitrovich, Q. M., and Johnson, A. D. (2010) Genetics and molecular biology in *Candida albicans*. *Methods in enzymology* **470**, 737-758
10. Pande, K., Chen, C., and Noble, S. M. Passage through the mammalian gut triggers a phenotypic switch that promotes *Candida albicans* commensalism. *Nat Genet* **45**, 1088-1091

Appendix

Table A.1. Screen details for Chapter 2

Screen	Mouse background, facility	Time points analyzed
1	female BALB/c, Hollister	3,10,25 days
2 – <i>efg1</i> -depleted	female BALB/c, Raleigh	5,10,14 days
3 – <i>brg1,rob1</i> -depleted	female BALB/c, Hollister	3,10,25 days

A.1. File locations

Chapter 2 files are hosted on the secure micro-bigcat server at the following path:

/shared1\$/Noble Lab/Labshare/Shared Folders/Witchley Thesis Supplemental Data/Chapter 2

Chapter 3 files are hosted on the secure micro-bigcat server at the following path:

/shared1\$/Noble Lab/Labshare/Shared Folders/Witchley Thesis Supplemental Data/Chapter 3

Chapter 4 files are hosted on the secure micro-bigcat server at the following path:

/shared1\$/Noble Lab/Labshare/Shared Folders/Witchley Thesis Supplemental Data/Chapter 4

Chapter 6 files are hosted on the secure micro-bigcat server at the following path:

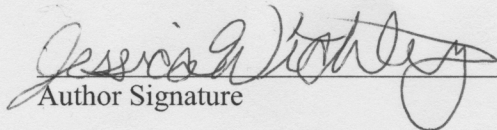
/shared1\$/Noble Lab/Labshare/Shared Folders/Witchley Thesis Supplemental Data/Chapter 6

Publishing Agreement

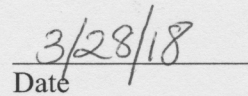
It is the policy of the University to encourage the distribution of all theses, dissertations, and manuscripts. Copies of all UCSF theses, dissertations, and manuscripts will be routed to the library via the Graduate Division. The library will make all theses, dissertations, and manuscripts accessible to the public and will preserve these to the best of their abilities, in perpetuity.

Please sign the following statement:

I hereby grant permission to the Graduate Division of the University of California, San Francisco to release copies of my thesis, dissertation, or manuscript to the Campus Library to provide access and preservation, in whole or in part, in perpetuity.



Author Signature



Date